MODELING FIRE OBSERVATIONS, IGNITION SOURCES, AND NOVEL FUELS TO UNDERSTAND HUMAN IMPACTS ON FIRE REGIMES ACROSS THE U.S.

MODELING FIRE OBSERVATIONS, IGNITION SOURCES, AND NOVEL FUELS TO UNDERSTAND HUMAN IMPACTS ON FIRE REGIMES ACROSS THE U.S.

A Dissertation Presented

by

EMILY J. FUSCO

Submitted to the Graduate School of the
University of Massachusetts Amherst in partial fulfillment
of the requirements for the degree of

DOCTOR OF PHILOSOPHY

MAY 2019

Organismic and Evolutionary Biology

MODELING FIRE OBSERVATIONS, IGNITION SOURCES, AND NOVEL FUELS TO UNDERSTAND HUMAN IMPACTS ON FIRE REGIMES ACROSS THE U.S.

A Dissertation Presented

by

EMILY J. FUSCO

Approved as to style and content by:

_____
Bethany A. Bradley, Chair

_____
Jesse Bellemare, Member

_____
John Finn, Member

_____
Paige Warren, Member

_____
Paige Warren, Graduate Program Director
Organismic and Evolutionary Biology

DEDICATION

for the green spaces and wild places

ACKNOWLEDGMENTS

First, I would like to thank my advisor, Bethany Bradley, for her guidance, support and mentorship. Without her, none of this work would have been possible. I would also like to thank Jack Finn, for serving on my committee as well as for sharing his vast statistical wisdom. In addition, I would like to acknowledge my committee members, Jesse Bellemare and Paige Warren, for their guidance and helpful comments along the way. I would also like to acknowledge my collaborators on this work, John Abatzoglou, Jennifer Balch, Sepideh Dadashi, Michael Falkowski, Steven Filippelli, Adam Mahood, Nathan Mietkiewicz, Chelsea Nagy, and Benjamin Rau. I sincerely thank all of the Bradley lab members, Jenica Allen, Eve Beaury, Tyler Cross, Caroline Curtis, Brittany Laginhas, and Valerie Pasquarella, and undergraduate research assistants, Anthony Accavallo, Devon Dunajski, Brigid Ryan, Amira Soltani, and Gabriella Soloio, for their assistance and feedback over the years. Thank you to the Organismic and Evolutionary Biology Program, and my friends and family for their constant support.

This research was supported by NASA's Terrestrial Ecology Program [grant number NNX14AJ14G], Joint Fire Sciences Program [grant number 15-2-03-6], the National Science Foundation [grant number 1740267], the Sagebrush Steppe Treatment Evaluation Project (SageSTEP; US Joint Fire Science Program, the Bureau of Land Management, the National Interagency Fire Center, and the Great Northern Landscape Conservation Cooperative), and a summer research fellowship from the Massachusetts Space Grant Consortium.

ABSTRACT

MODELING FIRE OBSERVATIONS, IGNITION SOURCES, AND NOVEL FUELS TO UNDERSTAND HUMAN IMPACTS ON FIRE REGIMES ACROSS THE UNITED STATES

MAY 2019

EMILY J. FUSCO, B.A., UNIVERSITY OF NORTH CAROLINA WILMINGTON

Ph.D., UNIVERSITY OF MASSACHUSETTS AMHERST

Directed by: Professor Bethany A. Bradley

Fire is a natural, and necessary, component of many ecosystems. However, people are changing the spatial and temporal distribution of wildfires in the U.S. at great economic and ecological costs. My dissertation addresses the impacts of humans on U.S. fires both through the introduction of ignition sources and flammable grasses. Further, I evaluate fire datasets that are widely used to investigate these phenomena over large spatial and temporal scales. Finally, I create an aboveground carbon map that can be used to estimate the potential carbon loss consequences in western U.S. ecosystems most at risk to fire.

My work shows that humans ignited more than 77% of fires in seven western U.S. ecoregions, and when modeling human ignited fires, I found that the importance of ignition proxies varied considerably among ecoregions. In 21 ecoregions across the U.S., I found that eight species of non-native invasive grasses increased rates of fire occurrence by 27%-230%, and six species increased rates of fire frequency by 24%-150%. I also quantified differences in commonly used satellite derived and agency recorded fire records and found they were disparate across the U.S., suggesting that great care should be taken when deciding which fire database to use when analyzing human impacts on fire regimes. Finally, the new estimates I provide for aboveground carbon in semi-arid western U.S. ecosystems are roughly double that

of previous estimates; indicating that potential carbon losses from fire in these ecosystems are much larger than originally thought.

I conclude that fire ignitions from human sources, and the alteration of fuels through the introduction of non-native, invasive grasses, have already dramatically impacted fire regimes across the U.S. These impacts are presently and will continue to be compounded by climate change. My dissertation suggests that we must consider human impacts on ignitions, vegetation, and their interaction with climate to most effectively manage, predict, and live with fire.

TABLE OF CONTENTS

Page

ACKNOWLEDGMENTS v

ABSTRACT vi

LIST OF TABLES xi

LIST OF FIGURES xiii

CHAPTER

1. DETECTION RATES AND BIASES OF FIRE OBSERVATIONS FROM MODIS AND AGENCY REPORTS IN THE CONTERMINUOUS UNITED STATES 1

1.1 Abstract 1
1.2 Introduction 2
1.3 Methods 6

1.3.1 Satellite Fire Data 6
1.3.2 Agency Fire Data 7
1.3.3 Detections 8
1.3.4 Understanding limitations of MODIS fire data 9
1.3.5 Understanding limitations of agency fire data 10
1.3.6 Modeling 11

1.4 Results 14

1.4.1 Overall product agreement 14
1.4.2 Satellite detection of agency fires 15
1.4.3 Agency detection of satellite fires 17

1.5 Discussion 24

1.5.1 Overall product agreement 24
1.5.2 Satellite detection of agency fires 24
1.5.3 Agency detection of satellite fires 28

1.6 Conclusion 29

2. QUANTIFYING THE HUMAN INFLUENCE ON FIRE IGNITION ACROSS THE WESTERN USA 31

2.1 Abstract 31
2.2 Introduction 32
2.3 Methods 35

2.3.1 Fire data 35
2.3.2 Response variables 35
2.3.3 Validation of ignition sources 37
2.3.4 Predictor variables 38
2.3.5 Modeling 39

2.4 Results 40
2.5 Discussion 50

3. INVASIVE GRASSES INCREASE FIRE OCCURRENCE AND FREQUENCY ACROSS U.S. ECOREGIONS 54

3.1 Abstract 54
3.2 Introduction 55
3.3 Methods 57

3.3.1 Invasive grass data 57
3.3.2 Fire data 58
3.3.3 Modeling 59

3.4 Results 60
3.5 Discussion 67

4. ACCOUNTING FOR ABOVEGROUND CARBON STORAGE IN SHRUBLAND AND WOODLAND ECOSYSTEMS INCREASES TOTAL CARBON ESTIMATES IN THE GREAT BASIN REGION 70

4.1 Abstract 70
4.2 Introduction 71
4.3 Methods 74

4.3.1 Study region 74
4.3.2 Land cover classification 74
4.3.3 Pinyon-juniper percent cover product and validation 76
4.3.4 Carbon estimation for pinyon-juniper 78
4.3.5 Carbon estimation in three shrubland landcover types 80
4.3.6 Carbon estimation for forest, non-forest, and other 81
4.3.7 Comparison to the National Biomass and Carbon Dataset 82

4.4 Results 82

4.4.1 Land cover classifications in the Great Basin 82
4.4.2 Validation of the pinyon-juniper percent cover product 83
4.4.3 Carbon estimates for land cover classes 83
4.4.4 Total Great Basin carbon estimates 84
4.4.5 Comparison to the National Biomass and Carbon Dataset 84

4.5 Discussion 90

4.5.1 Land cover classifications in the Great Basin 91
4.5.2 Pinyon-juniper carbon 91
4.5.3 Carbon in other land cover 93
4.5.4 Total Great Basin carbon estimates 94
4.5.5 Product applications and management implications 94

BIBLIOGRAPHY 96

LIST OF TABLES

Table Page

Table 1.1: The total number of fire events in each dataset >1ha that were included in the analysis with the percent of those fires detected by the indicated fire database. Positive detection rates ranged from 3.5–48%. 18

Table 1.2: There are eight generalized linear models (GLMs) for fire detections. Each GLM consists of a conditional and zero inflated part which together comprise the full model. For each model type, we list all potential model variables for both the conditional and zero inflated model parts. Then for each region and product, we show the variables used, their significance in the model, and the total deviance explained (pseudo r2; Zuur et al., 2009)..... 19

Table 1.3: Detection probability for fire sizes 10ha, 100ha, and 500ha as well as the fire size required for a 50% probability of detection were determined for each product/region based on the high detection scenarios. The fire size for 50% detection probability includes a 95% confidence interval (CI) for the detection probabilities associated with that fire size. The active fire performs best in the eastern U.S. where it has a 50% detection probability of wildfires with a final size of 10ha. 20

Table 2.1: Predictor data layers used in this analysis are associated with one or more of the wildfire causes listed in the National wildfire coordinating group origin and cause determination handbook. 43

Table 2.2: The total number of lightning and anthropogenic ignitions in each of the seven western US ecoregions. Ecoregion 43

Table 2.3: MODIS Burned Area Product (MCD445A1) ignitions that overlapped with the Fire Program Analysis fire- occurrence database (FPA FOD) data set were used to validate attribution of lightning as an ignition source. 44

Table 2.4: The deviance explained by the best generalized linear model (GLM) varied by ecoregion but was comparable to the deviance explained by the general additive model (GAM) with the same variables for each region. 44

Table 2.5: After testing for multicollinearity, the remaining predictor variables were used to create ecoregion GLMs. 45

Table 3.1: Invasive grass species in the U.S. and reported impacts on fire regimes. 62

Table 3.2: Available spatial data and affected ecoregions for each grass species. The extents of invaded points within affected Level III Ecoregions (U.S. Environmental Protection Agency, 2013) were used to define each study area..... 63

Table 3.3: Generalized linear models (GLMs) show significant relationships between invaded areas and fire occurrence and frequency. 64

Table 4.1: Carbon per pixel calculated for each land cover type. pinyon-juniper is calculated as a function of canopy cover per pixel (x). The three shrubland categories (low sagebrush, salt desert, and sagebrush steppe) have a mean carbon estimate followed by a low and high estimate based on the standard error. 85

Table 4.2: Total area and teragrams (Tg) of carbon by land cover type using mean estimates for the shrubland categories. 85

LIST OF FIGURES

Figure Page

Figure 1.1: There are clear spatial disparities between A) the MODIS burned area product, B) the MODIS active fire product, and C) the agency fire records>1 ha. Agency fire product points and MODIS burned and active fire product pixels from 2003 to 2013 are shown in gray and a black line separates the eastern and western U.S. states. All agency fire point locations are the same size regardless of final fire size. Maps are in an Albers equal area conic projection. 21

Figure 1.2: An illustration of the 2007 Zaca fire as seen by MODIS burned area (above) and active fire (below) products. Included are points associated with all fires>1ha near the Zaca fire as recorded by the agency database. Each point location for an agency fire is named, with the Julian date of discovery below the fire point. For example, the agency record of the Zaca fire is located in the northwest corner and was discovered on Julian day 185. The Zaca fire is counted as "detected" by both MODIS products because they are within 10km and±7days of at least one burned area and one active fire pixel. The Sedgewick fire, which burned on Julian day 294 is counted as detected because of the nearby MODIS pixels outside the range of the Zaca fire perimeter (burn dates outside Julian dates 180–245 have pixels shown in black). The Rancho fire, while within 10km of the overall perimeter, is not considered detected because its discovery date was not within±7days of the MODIS pixels within 10km. 22

Figure 1.3: The ability of MODIS products to detect agency fire records was strongly dependent on fire size. As expected, likelihood of detected increased with fire size for each of the products and regions (such that the top left plot is for active fire in the west). Under best-case scenarios, the active fire product detected 50% of agency fires if fire size was >78ha in the west and 10ha in the east. The burned area product detected 50% of agency fires under best-case scenarios if fire size was >234ha in the west, and 169ha in the east. 23

Figure 1.4: Agency fire data has the highest percent detection in the western U.S. for the MODIS burned area product. However, the likelihood that agency fire records correctly identified fire perimeters from the MODIS burned area product in the western U.S. varied markedly by state. For example, agency records from Washington were least likely to detect MODIS burned area events, whereas agency records from Nevada and Utah had a>75% likelihood of detection. 23

Figure 2.1: The study area is composed of the eleven westernmost contiguous US states. (a) Burned and (b) ignition pixels were determined using the MODIS Burned Area Product (MCD45A1). 46

Figure 2.2: Fire ignitions are distributed throughout the western USA. For all ignitions that occurred from May to October 2000– 2012, we determined whether the ignition had an (a) anthropogenic or (b) lightning source using data from Vaisala National Lightning Detection Network. (c) The distribution of anthropogenic ignitions varied between ecoregions. The ecoregions are abbreviated as follows: MWF, Marine West Coast Forest; NAD, North American Desert; MC, Mediterranean California; TS, Temperate Sierras; SSH, Southern Semiarid Highlands; GP, Great Plains; NFM, Northwest Forested Mountains. 46

Figure 2.3: The percent of MODIS (MCD45A1) lightning ignitions that were confirmed by the Fire Program Analysis fire- occurrence database (FPA FOD) data varied among ecoregions, but averaged 83%. The average number of confirmed anthropogenic ignitions per region was 48%. We correctly identified lightning ignitions above a rate of 75% for five out of the seven ecoregions, with the lowest accuracy in the Marine West Coast Forest and Mediterranean California. 47

Figure 2.4: The top anthropogenic predictors of anthropogenic ignition varied widely between ecoregions. Pie charts show the independent model contribution of each predictor variable for the best ecoregion model. Negative values show that the variable acts as a suppressor of other model variables, meaning that it is not a great predictor itself, but suppresses the residual error of the model. 48

Figure 2.5: The relationship of the two best model predictors and anthropogenic ignition are shown for each ecoregion. These relationships are in (a–d) the expected direction in the four ecoregions with the highest explanatory power, but (e–g) are counter intuitive in the three ecoregions with poor explanatory power. The black line denotes a linear relationship, while the gray line shows the loess smoother. 49

Figure 3.1: The grass species analyzed span U.S. ecoregions. A) Twenty-nine EPA level III ecoregions were included in the analysis. Ecoregion names are listed in Table 3.2. B) Study areas for the target invasive grass species based on convex hull polygons of invaded pixels located in fire-prone ecoregion(s). Both maps are displayed in U.S. Albers Equal Area Conic projection). 65

Figure 3.2: Invasive grasses are significantly related to changes in fire regimes. A) Of the twelve species tested, eight showed significant increases in fire occurrence, B) two showed a significant increase in mean fire size and C) six showed significant increases in fire frequency. Six species were not tested for changes in fire frequency because it was rare for invaded pixels to burn more than once. Significance: ***p<0.001, **p<0.01, *p<0.05, ^p<0.1. 66

Figure 4.1: Schematic of land cover classification. All pinyon-juniper pixels were classified first. The remaining pixels were reclassified based on their LandFire EVT vegetation group (LF EVT_GP_N) classifications. Non-

woodland, non-shrubland pixels were classified based the dominant life form (LF EVT_LF) of that pixel. The vegetation groups within each final classification are listed in order of prevalence within the group, with the percent total in parentheses. 86

Figure 4.2: Land cover classification for the Great Basin based on a combination of woodland cover from Falkowski et al. 2017a,b and other land cover from LandFire (Rollins, 2009; LANDFIRE, 2014a). 87

Figure 4.3: Modeled pinyon-juniper canopy cover showed a strong, positive relationship (R2 = 0.62) with SageSTEP field measurements of pinyon-juniper percent cover. Canopy cover estimates were aggregated to a 30 m pixel size, which corresponds to the SageSTEP plot size..... 88

Figure 4.4: Total aboveground carbon in pinyon-juniper is strongly related to canopy cover. 88

Figure 4.5: Estimated aboveground biomass carbon storage in the Great Basin (kg/ha) using mean estimates for the three shrubland categories. 89

Figure 4.6: Regression of carbon estimates compared to the carbon estimates in the National Biomass and Carbon Dataset for the pinyon-juniper land cover type. There was a weak but significant positive relationship (R2=.147, p<0.01). 89

Figure 4.7: For six land cover classes, we provided static carbon estimates (stars; values in Table 4.1). The boxplots show a mean estimate of carbon in the NBCD dataset. Most of the pixels in the associated NBCD dataset for these land cover types had values of 0, with means ranging from 94-20,989 kg/ha. All means (denoted by a line in each boxplot) in the NBCD dataset were lower than the static estimates with the exception of the “other/ excluded” classification. The stars represent the modeled mean for each landcover type. The modeled mean for pinyon-juniper is 12,222 kg/ha and refers to the mean of the 855 pinyon-juniper designated points included in the comparison analysis. 90

CHAPTER 1

DETECTION RATES AND BIASES OF FIRE OBSERVATIONS FROM MODIS AND AGENCY REPORTS IN THE CONTERMINUOUS UNITED STATES

1.1 Abstract

With growing concern about the impacts of fires on ecosystems and economies, satellite products are increasingly being used to understand fire regimes. Concurrently, where available, agency records of fires have also been used to assess fire regimes. Yet, it remains unclear if these independent datasets measure the same fires, which raises concerns about the interpretation and benchmarking of models derived from these products. Here, we present a novel product intercomparison of the MODIS burned area and active fire products across the conterminous United States using nearly 250,000 agency reported wildfires as reference data to model consistencies and inconsistencies between all three datasets. We compared agency reported wildfires from the Fire Program Analysis fire occurrence database to the MODIS products to identify which fires were detected vs. omitted by MODIS products relative to agency fire records, and by agency fire records relative to MODIS. We created generalized linear models as a function of fire attributes (e.g. size) and environmental variables (e.g. cloud cover) to predict MODIS detection of agency wildfires, and anthropogenic variables (e.g. agriculture) to predict agency detection of MODIS fires. We modeled fire detection probability separately for MODIS burned area and active fire products, and for the eastern and western U.S. Overall, we found that MODIS product detection rates ranged from 3.5% to 23.4% of all documented agency wildfires>1ha, and that likelihood of detection increased with fire size. Agency detection rates ranged from 23.5% to 48% of MODIS burned area and active fires. Under ideal conditions, the MODIS active fire product had a 50% probability of detecting a wildfire that grew to at least

10ha (eastern U.S.) – 78ha (western U.S.), while the burned area product had a 50% probability of detecting a wildfire that grew to at least 169ha (eastern U.S.) –234ha (western U.S.). Cloud cover and leaf area index were significant predictors of MODIS fire detection, while state boundaries were significant predictors of agency fire detection. This analysis presents an important assessment of the fire attributes and ground conditions that influence MODIS fire detection relative to extensive and increasingly used ground-based wildfire records. The large discrepancy in records of fire occurrence between MODIS and agency fire datasets highlights the need for this type of analysis into the types of fires likely to be included in each database.

1.2 Introduction

Current understanding of modern fire regimes relies heavily on fire data derived from remotely sensed satellite images. The Moderate Resolution Imaging Spectrometer (MODIS) active fire and burned area products are widely used to assess the interplay between fire and climate (e.g. Krawchuk et al.,2009; Langmann et al., 2009; Hantson et al., 2015), human land use (e.g. Archibald et al., 2008; Syphard et al., 2009), and ecosystems (e.g. Giglio et al., 2006; Archibald et al., 2010) in order to predict fire risk (Gillespie et al., 2007), and quantify emissions (van der Werf et al., 2010). However, estimates by different satellite fire products of fire counts and area burned vary by thousands of hectares (e.g. Chang and Song, 2009; Loepfe et al., 2012), suggesting these sensors are detecting different types of fire events, or providing different representations of the same events due to omission and commission errors. Attempts have been made to validate MODIS fire products primarily using other remotely sensed data (e.g. Korontzi et al., 2004; Schroeder et al., 2008; Padilla et al., 2015), however, a lack of consistent ground-based data has made independent assessment from ground-based fire observations difficult (e.g. Hawbaker et al., 2008; Boschetti et al., 2016). With wildfires increasing over large

portions of the conterminous U.S. (Westerling et al., 2006; Westerling, 2016), a better understanding of the limitations of satellite fire products is needed.

Moderate resolution satellite data, including the MODIS burned area and active fire products, are typically validated using data from finer resolution sensors such as the Advanced Spaceborne Thermal Emission and Reflection Radiometer (ASTER) or Landsat. Satellite-based validation is used both to compare number of fires (fire occurrence) as well as area burned. However, because ASTER and MODIS are on the same platform (Justice et al., 2002), they are both more likely to detect fire events occurring during the satellite overpass time, while possibly both missing fires burning at different times of day (Cardoso et al., 2005; Hawbaker et al., 2008). The potential for both sensors to miss fires that do not match the overpass time could inflate accuracy estimates (Cardoso et al., 2005). While Landsat satellites do not have the same overpass time as MODIS, the long interval between images (8–16days) limits Landsat detection to only those fires that are large enough to leave a burn scar (Hawbaker et al., 2008). Even validation with daily satellites (e.g. TRMM) faces similar detection limitations due to different overpass times (van der Werf et al., 2003). Moreover, reliance on satellite to satellite validation potentially introduces other unknown biases by only focusing on the subset of fires detectable remotely (Cardoso et al., 2005; Csiszar et al., 2006).

Despite these limitations, satellite validation of satellite fire products remains a standard approach for evaluating records of fire occurrence because independent fire records collected on the ground are lacking. When evaluating detection rates for fire occurrence, one global analysis reported MODIS active fire detection rates ranging from 100% in South Africa to 80% in Kazakhstan using Landsat reference fires> 500ha (Hantson et al., 2013). However, when fires as small as 10ha were included, detection rates decreased and ranged from 76% in Canada to 14% in South Africa (Hantson et al., 2013). In the U.S., the MODIS active fire product detected

82% of Landsat reference fires ranging from roughly 20 to 50,000ha (Hawbaker et al., 2008). While the MODIS burned area product is typically evaluated in terms of overall burned area agreement (e.g. Padilla et al., 2015; Zhu et al., 2017), one validation based on fire occurrence found detection rates ranging from 10 to 62% using Landsat reference fire perimeters across study sites in South Africa (Tsela et al., 2014). The wide range of detection accuracies for fire occurrence revealed in these studies for both MODIS products highlights the need for continued work to understand when, where, and what type of fires MODIS is most likely to identify.

Validation of satellite data using ground observations is less common because ground validation is both time consuming and costly, particularly at extensive spatial scales (Boschetti et al., 2016). Notable exceptions have included MODIS active fire validation using a combination of agency fire data and remotely sensed observations in Portugal, Greece, Alaska, California, and Australia (Benali et al., 2016), passive ground observation in Brazil (Cardoso et al., 2005), and with national fire statistics in Europe (Loepfe et al., 2012). These studies matched satellite fire records to ground observations and reported MODIS detection rates that ranged from 1% (Cardoso et al., 2005) to 17% (Benali et al., 2016). The broad range of accuracy estimates reported in these studies coupled with relatively modest numbers of ground-based validation points underscores the additional need for large-scale comparison between satellite and ground-based fire data.

Not surprisingly, given the paucity of ground-based validation of satellite fire products, very little is also known about the accuracy and spatial biases of ground-based fire records. One exception compared primarily local agency fire data from California with the MODIS active fire product and found that the 68% of the fires recorded by MODIS within local jurisdictions were not in the agency database (Butry and Thomas, 2017). Because this comparison focused on local lands within the state of California, it is unclear whether the lack of ground-based fire records

relative to MODIS is a more widespread problem. Until Short (2014, 2015a), no comprehensive national scale database of fire records across land agencies existed for the U.S. This database of agency records is the most comprehensive available for the U.S., but it is known to suffer from reporting biases at the state level as well as potentially missing records on local and non-federal lands (Short, 2014; 2015b). Given that the agency records are increasingly being used to assess temporal trends in fire regimes (e.g., Balch et al., 2017; Nagy et al., 2018), it is critical to understand potential spatial biases at a national scale.

Here, we compared records of fire occurrence from the MODIS active fire and burned area products with agency fire reports in the most extensive satellite to ground intercomparison to date. We also provide a first model assessment encompassing the conterminous U.S. and assessing spatial and temporal conditions that influence fire detection probability. We identified positive and negative detections for the MODIS active fire and burned area products relative to the agency data to ask why fires identified on the ground might go undetected by MODIS. Conversely, we identified positive and negative detections for the agency fire data relative to the MODIS active fire and burned area products to ask why fires identified by MODIS might go undetected or unreported on the ground. We modeled positive detections for each product to examine how environmental factors, anthropogenic land use, and political boundaries contributed to geographic variability in detection efficacy. This analysis provides new insight into discrepancies in records of fire occurrence existing in fire data products for the conterminous U.S.

1.3 Methods

1.3.1 Satellite Fire Data

We used data from the Moderate Resolution Imaging Spectrometer (MODIS) active fire collection 5.1 (MCD14ML; Giglio et al., 2003) and burned area collection 5.1 (MCD64A1; Giglio et al., 2009) products from 2003 to 2013, which at the time of analysis, spanned the time period in which all MODIS sensors were running (Figure 1.1; Hawbaker et al., 2008) and agency fire data were collected. The MODIS products are derived from NASA's Aqua and Terra satellites, which each have twice daily overpasses (crossing the equator locally at 1:30/13:30 for Aqua and 10:30/22:30 for Terra; Giglio et al., 2006) and therefore generate daily fire products. The MODIS burned area product (Giglio et al., 2009) detects burned areas using a hybrid algorithm based on MODIS surface reflectance changes and the MODIS active fire product (Giglio et al., 2009). The MODIS active fire product (Giglio et al., 2003) uses thermal anomalies to detect active fires at the time of satellite overpass at a 1km pixel resolution. The MCD14ML data is a point product that refers to the MODIS active fire hotspots. We converted these points to a gridded format (similar to the gridding approach by Oom et al., 2016) snapped to the MODIS MCD64 burned area pixels and extents such that each MCD14 active fire pixel is made up of four MCD64 pixels. We used all points designated as active fire regardless of the level of confidence because low confidence pixels tend to be grouped with high confidence pixels (Hawbaker et al., 2008), suggesting that adding low confidence pixels will make fire perimeters larger rather than increasing the number of fire events. In instances where there was more than one active fire hotspot within a pixel, the maximum value was taken. Based on 2007 data, 77% of pixels contained a single active fire detection. Active fire detections in pixels typically occurred within 7days of one another (94% of pixels), suggesting that multiple burns should not influence our identification of overlapping fire events between MODIS active fire and the agency fire

database. The final gridded formats of the MCD64 and MCD14 products are 463m and 926m resolution, respectively. All analyses of MODIS product detection of agency fires were performed using these gridded products.

In contrast, correctly identifying omission of agency fires required combining the MODIS pixels into fire perimeters. To identify unique fire events detected by MODIS, we compiled daily active fire or burned area pixels into fire events based on spatial and temporal proximity. This type of flood-fill approach has been previously used to identify fire events (e.g. Archibald and Roy, 2009; Fornacca et al., 2017). Here, a MODIS burned area event is defined as a cluster of pixels within a 5pixel and 9day distance (Dadashi et al., 2017). The active fire perimeters were clustered based on a 3pixel, 9day criteria to account for the larger size of the active fire pixel. This spatial and temporal aggregation was found by Dadashi (2018) to create burned area perimeters that best matched those identified by the Monitoring Trends in Burn Severity (MTBS; Eidenshink et al., 2007) in the U.S. The resulting fire event perimeters were generated as single band raster grids where each perimeter has a unique identification number and a minimum and maximum Julian date associated with the first and last pixel that burned within the cluster (Dadashi et al., 2017).

1.3.2 Agency Fire Data

The Fire Program Analysis fire occurrence database (FPA fod; Short, 2015a), hereafter referred to as agency fire data, is the most complete record of agency reported wildfire events available that covers the entire U.S. (Short, 2014; 2015b). In this database, each record represents one fire event. The database contains records for over 800,000 wildfire events during the study period (2003–2013; Figure 1.1), and only includes fire events that required an agency response (i.e., excluding agricultural or prescribed burns). Agency fire events are derived from

federal (e.g., U.S. Forest Service), state (e.g., Maine Forest Service, New Mexico State Forestry), and interagency records that include local reports (e.g., ICS 209) and include a point location for the origin of each fire event that is accurate within 1.6km (one mile; Short, 2014). The record for each event contains attribute information such as discovery date, final fire size, and fire name, and roughly half of the records also list a containment date (Short, 2014).

1.3.3 Detections

We compared the two types of fire products (MODIS vs. agency) to identify where the two datasets overlap and where fires were undetected by MODIS or by the agency database. MODIS successfully detected an agency fire if the agency's point location was within 10km of any MODIS pixel and the agency's discovery date was within 7days before or after the burn date associated with that MODIS pixel. The agency database successfully detected a MODIS fire event if the fire event perimeter was within 10km of any agency point and the fire event's minimum or maximum burn dates were within 7days of the discovery date associated with the agency point (Figure 1.2). Using this method, multiple agency fire events could be matched with MODIS pixels within the same MODIS fire event perimeter. Similarly, multiple MODIS fire events could be matched with a single agency fire event. We set a large spatial window to account for potential discrepancies in local, state, and federal reporting of fire location as well as differences in fire size in the agency data (e.g. Short, 2014; 2015b). A10kmradius around the fire points encompasses 99.9% of agency reported fire events based on reported fire size if we assume the ignition point is at the center. We set a large temporal window because sensor limitations and cloud cover could delay satellite detection of fire events (Giglio et al., 2009). Both of these windows were broad to encompass as much overlap between datasets as possible. We identified positive and negative detections individually for each comparison. Positive detections

included agency fires detected by MODIS burned area, agency fires detected by MODIS active fire, MODIS burned area perimeters detected by agency, and MODIS active fire perimeters detected by agency. We identified negative detections as the fires that the MODIS product or agency product failed to detect. Thus, there were also four relevant negative detections (agency fires missed by MODIS burned area, agency fires missed by MODIS active fire, MODIS burned area perimeters missed by agency, and MODIS active fire perimeters missed by agency), and therefore four unique spatial databases of negative detections. We used these positive and negative detections to model what influences detection probability for the two MODIS fire products as well as the agency fire database. We also calculated positive detection rates for each of the products. A positive detection rate for a MODIS product is calculated as the number of fires in the agency database detected by a MODIS product divided by the total number of fires in the agency database. A positive detection rate for the agency database is calculated as the number of fire event perimeters in the MODIS database detected by the agency database divided by the total number of fire event perimeters in a MODIS database.

1.3.4 Understanding limitations of MODIS fire data

Fires that appear in the agency database may not be detected by MODIS because they are too small to be detected or because atmospheric or landscape conditions interfere with satellite detection. Therefore, our analysis of fires missed by MODIS focused on agency reported fire size, regional cloudiness, and land cover. Final fire size of each event is reported in the agency fire database. To account for potentially obstructed satellite views of ground fires due to canopy cover, we used the GLASS leaf area index (LAI) product which is an 8day composite at 1km resolution (Liang and Xiao, 2012; Xiao et al., 2014). Because there is seasonal variation in canopy cover, we extracted LAI values based on four timesteps during 2007 using the middle

month of the meteorological seasons. For example, fires with a discovery date in December, January, or February received the LAI value associated with the January 1, 2007 time step, while fires in March, April, or May received the LAI value associatedwithApril7, 2007. LAI values from July 4thtoSeptember8thwereusedforrecordsassociatedwithsummerand fall months, respectively. We used 2007 values for all events because it was near the middle of our study period. These 2007 LAI values were highly correlated (r=0.91–0.97) with the same timesteps in 2004 and 2011, suggesting that 2007 LAI values are representative. We used the MODIS mean annual cloud cover (MCD09 1–12; Wilson and Jetz, 2016) as a metric of overall cloudiness. The LAI and cloud cover data are both available at 1km resolution, and values were extracted to each agency fire record. We also included vegetation information using the LANDFIRE database (LANDFIRE, 2012a; Rollins, 2009). LANDFIRE is a suite of U.S. national scale data products that include vegetation, fuel, and disturbance information at 30m resolution. These data products are derived from a combination of satellite observations, field data, and decision tree analyses (Rollins, 2009). To determine current landcover types, we used Existing Vegetation Type (LANDFIRE.US_130EVT) to classify landcover at each positive and negative detection of an agency fire point as tree, shrub, herb, or other.

1.3.5 Understanding limitations of agency fire data

Fires identified by the MODIS satellites may not appear in the agency database due to a lack of reporting. Fires may not be reported if they are agricultural or prescribed fires (which are excluded from the agency database), they are detected but not reported by federal, state, or local agencies, or they remain undetected. Therefore, our analysis of fires missed by the agency database focuses on correlates based on land use, prescribed fire, land ownership, and U.S. political state designations, hereafter referred to as state.

Because the agency database should not include intentional fires from agriculture or prescribed burns (unless they escape and become a wildfire that requires agency action), we included percent agriculture and percent prescribed burn within each MODIS event perimeter. Percent agriculture was derived using Existing Vegetation Type (LANDFIRE.US_130EVT; EVT_LF) from LANDFIRE (Rollins, 2009; LANDFIRE, 2012a). Percent prescribed burn within each MODIS fire perimeter was derived using disturbance data from LANDFIRE (LANDFIRE.US_DIST2003–2013; Rollins, 2009; LANDFIRE, 2012b). Agency reporting biases may also be due to differences in land ownership. To test for reporting inconsistencies based on land ownership, we associated presence of public land (federal, state, local vs. private) with each MODIS fire event based on the U.S. Public Areas Database (U.S. Geological Survey, 2015).

In addition to lack of reporting, the agency database also excludes fires that were not detected. Fires may go undetected due to their remoteness from human activity. As a metric for fire remoteness, we calculated the Euclidean distance to nearest developed landcover from the centroid of each MODIS fire perimeter using Existing Vegetation Type (LANDFIRE.US_130EVT; EVT_PHYS) from LANDFIRE (Rollins, 2009; LANDFIRE, 2012a). We also calculated Euclidean distance to roads (TIGER/Line Shapefiles, 2016).

1.3.6 Modeling

We identified fires missed by each of the two MODIS fire products, but present in the agency fire data. We also identified fires missed by the agency fire database, but present in each of the two MODIS fire product. We modeled these four comparisons for both the eastern and western U.S. (11 westernmost states; Figure 1.1). We chose this grouping because detection by the MODIS active fire product may be limited by the combustion patterns characteristic of the surface fires most common in the central and eastern U.S. as compared to those in the western

U.S. which typically has more high intensity crown fires (Hawbaker et al., 2008). This regional split resulted in a total of eight models. We used zero inflated binomial generalized linear models (ZIB GLMs) to account for "false zeros" which caused overdispersion in the response variable (Zuur and Ieno, 2016). "False zeros" include those caused by design error, in this case meaning zeros recorded under conditions in which a detection would not be possible. For example, a satellite cannot detect an agency fire if it is too cloudy or if there was no overpass during the fire, and agency data do not include agricultural fires. We limited our dataset of agency fires to include only those fires with a final area above 1ha. A preliminary analysis revealed that positive detection rates for fires under 1ha were 1.7% for burned area and 9.6% for active fire across the U.S., suggesting that these small fires are difficult to detect. In addition, theoretical calculations suggest the MODIS active fire product can detect fire hotspots larger than 100m2 (Giglio et al., 2003), and comparisons to ASTER fire data suggest MODIS can detect instantaneous hotspots on the order of 2–7ha (Morisette et al., 2005; Csiszar et al., 2006; Schroeder et al., 2008). Therefore, a 1ha agency fire size was a plausible minimum size to evaluate MODIS detection rates which would also allow us to model detection across a range of fire sizes. Although theoretical calculations report the burned area product reliably detects fires over 40–120ha (Giglio et al., 2009; Giglio et al., 2013), we chose to use the 1ha threshold for the burned area comparisons as well for consistency across models. All modeling was conducted in R version 3.3.2 (R Studio Team, 2015) using the glmmTMB package (Brooks et al., 2017; Magnusson et al., 2017).

We tested for variable collinearity using the correlation variation inflation factor (corvif) function from Zuur Highstats Library 10 (Zuur et al., 2009; Zuur and Ieno, 2016; http://highstat.com), and did not use any combination of variables that produced a vif value>7. The resulting eight ZIBs are mixture models, meaning that each consists of two logistic

regressions, one to represent “false zeros” (the zero inflated part), and one to represent the rest of the data (the conditional part). Because ZIBs are mixture models, zeros may come from either the zero inflated part or the conditional (binomial) part (Zuur et al., 2009; Zuur and Ieno, 2016). We used backward selection to determine the conditional part of each model. The same variables can be used to generate the zero inflated part (Zuur et al., 2009), and because each part only had 2 to 3 potential zero inflated covariates, we tried all possible uncorrelated combinations of the zero inflated covariates that allowed model convergence and used the Akaike Information Criterion (AIC) to select the final model (Zuur et al., 2009). Additionally, the data were tested for spatial autocorrelation using a semivariogram. All model visualization was conducted using the ggplot2 package (Wickham, 2009). Because an r2 value cannot be calculated for a GLM, we calculated a pseudo r2 using the residual and null deviance explained for each model (Zuur et al., 2009).

We calculated the size at which an agency fire has a 50% detection likelihood by the MODIS burned area and active fire products in the east and the west. To do this, we created new data frames based on each of the four satellite detection of agency fire models. The new data frames are a representation of model predictions based on covariate values of interest. This method was necessary because the nature of the models does not allow a 50% detection likelihood to be calculated Fires identified by the MODIS across all observations. Instead it is necessary to determine scenarios of interest based on the covariates. We chose scenarios of interest representing two high likelihood U.S. states, and a high and low likelihood for the remaining non-continuous covariates based on our model visualization (Figs. S1–S6). For each continuous covariate (cloud cover and leaf area index) we used the mean for observations across the corresponding state. In combination, these covariates represent high and low probability detection scenarios and should provide the range of values required for a 50%

detection likelihood. For example, the high probability detection scenario for the active fire product in the west would be in Idaho, on the herb landcover type, in August of 2003. The data frames for these covariates also included a range of final fire sizes from the minimum to the maximum observed final fire size. Once the data frames were constructed, we used the predict function to calculate the fitted values (detection probability) in each data frame and then found the detection probability for fires 10ha, 100ha, and 500ha in size. We also determined what final fire size input was required to generate a 50% detection probability for each set of scenarios.

1.4 Results

1.4.1 Overall product agreement

According to the agency fire records, there were a total of 252,274 fires over 1ha in size in the conterminous U.S. from 2003 to 2013, burning an estimated total of 245,333km2. Of these, 248,863 (98.6%) had information for all required covariates and were included in the modeling process. By aggregating individual MODIS pixels into fire event perimeters (Dadashi et al., 2017) we identified 24,497 fires associated with the burned area product (216,194km2; 463m pixels) and 249,190 fires associated with the active fire product (552,471km2; assuming that each of the 926m pixels burned entirely and only once each year). Fire event size and duration for the MODIS fire products and agency fire product were right skewed (Figs. S7–S9). Fires in the agency database with positive MODIS burned area and active fire detection accounted for 72% and 74% of the total burned area in the agency database, respectively, while the total area burned in the MODIS burned area database is 88% of the total area burned in the agency database.

MODIS satellite products positively detected agency fires at rates ranging from 3.5% for the burned area product in the eastern U.S. to 23.4% for the active fire product in the western

U.S. In contrast, agency records positively detected MODIS fire events at rates ranging from 23.5% for the active fire product in the eastern U.S. to 48% for the burned area product in the western U.S. (Table 1.1).

1.4.2 Satellite detection of agency fires

In order to assess the conditions when agency fires are more likely to be detected by satellite, we modeled satellite detection of agency fires using fire size, landcover, state, leaf area index, average annual cloud cover, month, and year in the conditional model. After covariate selection, all of these covariates were used in each of the four models with the exception of leaf area index for active fire detection in the east, and average annual cloud cover for burned area in the east. Of the conditional model covariates used, all were highly significant ($p < 0.001$) with the exception of leaf area index which was included but not significant for burned area detection of agency fires in the east, and average annual cloud cover which was included but not significant for burned area detection of agency fires in the west (Table 1.2).

Both average annual cloud cover and leaf area index were highly significant ($p < 0.001$) in all of the zero inflated models with the exception of cloud cover for burned area in the east where it was not used, and LAI for active fire in the east where it was included but not significant. The zero inflated part of the models accounts for conditions under which satellite detection of agency fires would be impossible regardless of other favorable conditions (Table 1.2). The total deviance explained by each of the models (indicative of how well the model explains detection probability) ranged from 10% for active fire detection of agency fires in the east, to 33% for burned area detection of agency fires in the west (Table 1.2).

Fire size was the most important predictor determining satellite detection of agency fire records for all four models. Not surprisingly, likelihood of satellite detection increased with fire

size (Figure 1.3). For state and year with the highest detection probabilities, we determined best and worst-case detection scenarios for benchmark fire sizes 10ha, 100ha, and 500ha and calculated the likelihood of satellite detection. For example, the mean probability of detection by the active fire product for a best-case scenario in the west (Idaho, herb, August 2003) ranged from 25.9% (se ± 1.3%) for 10ha fires, to 71.9% (se ± 1.3%) for 500ha fires (Table 1.3). We also provide estimates of fire sizes required for a mean 50% detection probability. Under best-case scenario conditions, MODIS active fire product had a 50% detection probability of agency fires with a fire size>78ha in the western U.S. (Idaho, herb, August 2003) and 10ha in the eastern U.S. (Kansas, tree, March 2004). For these size estimates, the 95% confidence interval for a 50% detection ranged from 47% to 53% and 46% to 54%, respectively. The MODIS burned area product had a 50% detection probability of agency fires with a fire size>234ha in the western U.S. (Idaho, herb, August 2012), and 169ha in the eastern U.S (Kansas, herb, March 2004). For these size estimates, the 95% confidence interval for a 50% detection ranged from 46% to 54% and 44% to 56%, respectively.

Both conditional and zero inflated covariates with expectations of directionality (i.e., highest detection rates at low levels of leaf area index) acted as predicted, except for cloud cover which appeared to have the highest likelihood of detection at intermediate values. We also looked at detection rates based on year, state, month, and land cover. Monthly detection rates showed higher likelihood of detection for both the active fire and burned area product in the west during summer and fall months, while the burned area product showed better detection in the east during spring and fall months. In the western U.S., both the active fire and burned area product had a similarly high detection likelihood in tree and herb land cover types, while the active fire product in the east had a slightly higher detection likelihood in the tree land cover type.

1.4.3 Agency detection of satellite fires

In order to assess the conditions under which agencies are likely to identify, record, and report fires observed by MODIS, we again created zero inflated binomial models. The conditional portion of these models included the covariates state, percent prescribed burn, percent agriculture, distance to road, distance to development, and presence of public land (Table 1.2). Distance to road or development was also significant as an interaction with public lands and was included when this interaction did not violate assumptions of independence and remained significant in the models. The models for agency detection of active fires were more complex and included some combination of all possible covariates, while the agency detection of burned area models were simpler and included fewer covariates (Table 1.2). Distance to development was included in all four of the models and was included as an interaction with presence of public land for both agency detection of active fire in the east, and agency detection of burned area in the west. Where the distinction between public and private land was included, detection likelihoods were higher on public land. The total deviance explained by each of the models ranged from about 8.5% for agency detection of active fire in the west, to about 23% for agency detection of burned area in the west (Table 1.2).

State was the most important predictor of likelihood of detection and was highly significant ($p < 0.001$) in all models except for agency detection of burned area in the east (Table 1.2). Individual states varied greatly in their predicted likelihood of detection (Figure 1.4). For example, when modeling agency detection of burned area fires in the west, Nevada and Utah had about a 75% detection likelihood while Washington's mean predicted detection likelihood was about 10% (Figure 1.4).

The zero inflated models account for structural zeros in the data, and included the covariates state, percent agriculture, and percent prescribed burn. All covariates were

significant, with the exception of state in the eastern U.S. (Table 1.2). Both conditional and zero inflated covariates with expectations of directionality acted as predicted. For example, there was a negative relationship between likelihood of detection and percent agriculture.

Table 1.1: The total number of fire events in each dataset >1ha that were included in the analysis with the percent of those fires detected by the indicated fire database. Positive detection rates ranged from 3.5–48%.

Model (Direction and Region)	Number of Fires	Detection Rate (%)
Satellite Detect Agency		
Active Fire- West	40,386	23.4
Burned Area- West	40,386	11.1
Active Fire- East	208,477	21.7
Burned Area- East	208,477	3.5
Agency Detect Satellite		
Active Fire- West	42,439	26.3
Burned Area- West	6,036	48.0
Active Fire- East	206,751	23.5
Burned Area- East	18,461	25.7

Table 1.2: There are eight generalized linear models (GLMs) for fire detections. Each GLM consists of a conditional and zero inflated part which together comprise the full model. For each model type, we list all potential model variables for both the conditional and zero inflated model parts. Then for each region and product, we show the variables used, their significance in the model, and the total deviance explained (pseudo r2; Zuur et al., 2009).

	Conditional Model Variables	**Zero Inflated Model Variables**	**Deviance Explained**
Satellite Detect Agency	*Fire Size, LC, State, LAI, Cloud, Month, Year*	*Cloud, LAI*	*potential variables*
Active Fire - West	Fire Size***, LC ***, State***, LAI***, Cloud***, Month***, Year***	Cloud***, LAI***	19.79
Burned Area - West	Fire Size***, LC ***, State***, LAI***, Month***, Cloud, Year***	Cloud***, LAI***	32.97
Active Fire – East	Fire Size***, LC ***, State***, Cloud***, Month***, Year***	Cloud***, LAI^	10.11
Burned Area - East	Fire Size***, LC **, State***, LAI, Month***, Year***	LAI***	15.27
Agency Detect Satellite	*Dev by Road, Road by Pub, Ag, Pr Burn, State*	*Ag, State, Pr Burn*	*potential variables*
Active Fire - West	Dev ***, Road by Pub***, Ag*, Pr Burn***, State***	Ag***, State***, Pr Burn***	8.43
Burned Area - West	Dev by Pub***, State***	Ag***, State***, Pr Burn***	23.33
Active Fire - East	Dev by Pub ^, Road, Ag ***, Pr Burn***, State***	Ag***, Pr Burn***	12.53
Burned Area - East	Dev, Ag ***, Pub*	Ag***, Pr Burn*	13.19
Key			**Significance:**
Fire Size- Log Fire Size	Road- Distance to Road	Dev- Development	p< 0.001 '***'
LC- Landcover Type	Ag- Percent Agriculture	by- Interaction	p<0.01 '**'
LAI- Leaf Area Index	Pub- Public Land		p<0.05 '*'
Cloud- Annual Cloud Cover	Pr Burn- Percent Prescribed Burn		p<0.1 '^'

Table 1.3: Detection probability for fire sizes 10ha, 100ha, and 500ha as well as the fire size required for a 50% probability of detection were determined for each product/region based on the high detection scenarios. The fire size for 50% detection probability includes a 95% confidence interval (CI) for the detection probabilities associated with that fire size. The active fire performs best in the eastern U.S. where it has a 50% detection probability of wildfires with a final size of 10ha.

Mean (SE) Detection Probability for Benchmark Fire Sizes and Size (CI) required for 50% Detection Probability		
Product / Region	**State / Year**	**Month / Landcover**
Active Fire / West	*ID / 2003*	*August / Herb*
	10 ha	25.9 (1.3)
	100 ha	53.0 (1.6)
	500 ha	71.9 (1.3)
50% Detection Probability Size	Size (CI%)	78 ha (47-53)
Active Fire / East	*KA / 2004*	*March / Tree*
	10 ha	49.9 (2.3)
	100 ha	68.8 (1.9)
	500 ha	79.0 (1.4)
50% Detection Probability Size	Size (CI%)	10 ha (46-54)
Burned Area / West	ID / 2012	August / Herb
	10 ha	12.0 (0.8)
	100 ha	36.9 (1.9)
	500 ha	61.8 (2.0)
50% Detection Probability Size	Size (CI%)	234 ha (46-54)
Burned Area / East	KA / 2004	March / Herb
	10 ha	20.0 (2.0)
	100 ha	43.5 (3.0)
	500 ha	62.8 (2.9)
50% Detection Probability Size	Size (CI%)	169 ha (44-56)

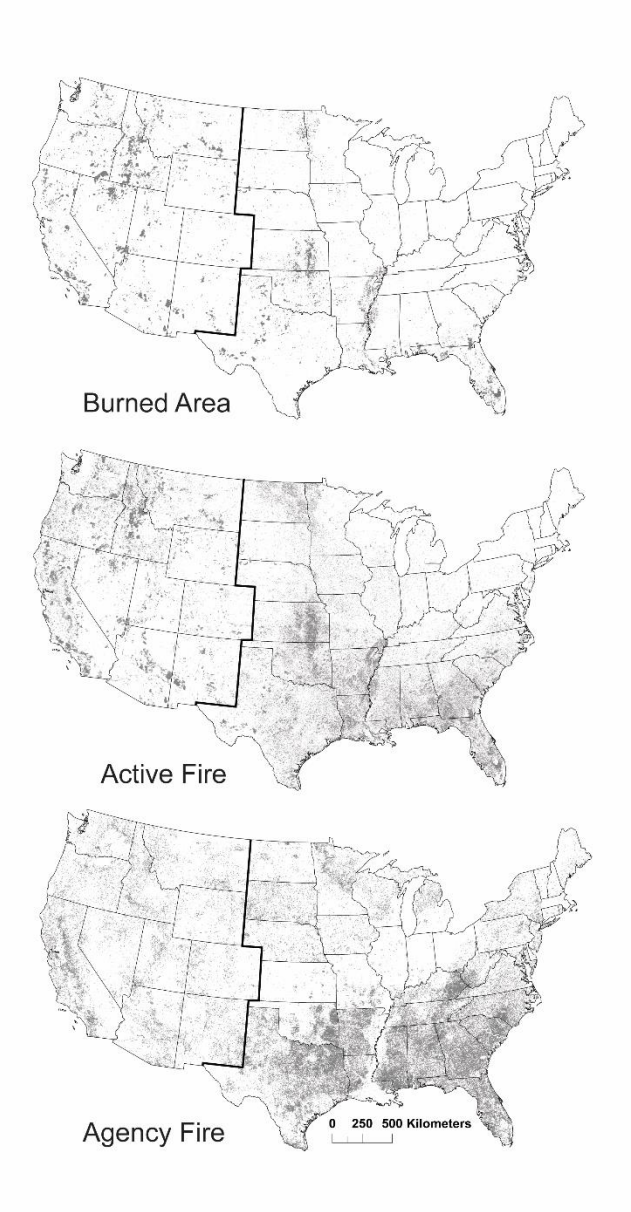

Figure 1.1: There are clear spatial disparities between A) the MODIS burned area product, B) the MODIS active fire product, and C) the agency fire records>1 ha. Agency fire product points and MODIS burned and active fire product pixels from 2003 to 2013 are shown in gray and a black line separates the eastern and western U.S. states. All agency fire point locations are the same size regardless of final fire size. Maps are in an Albers equal area conic projection.

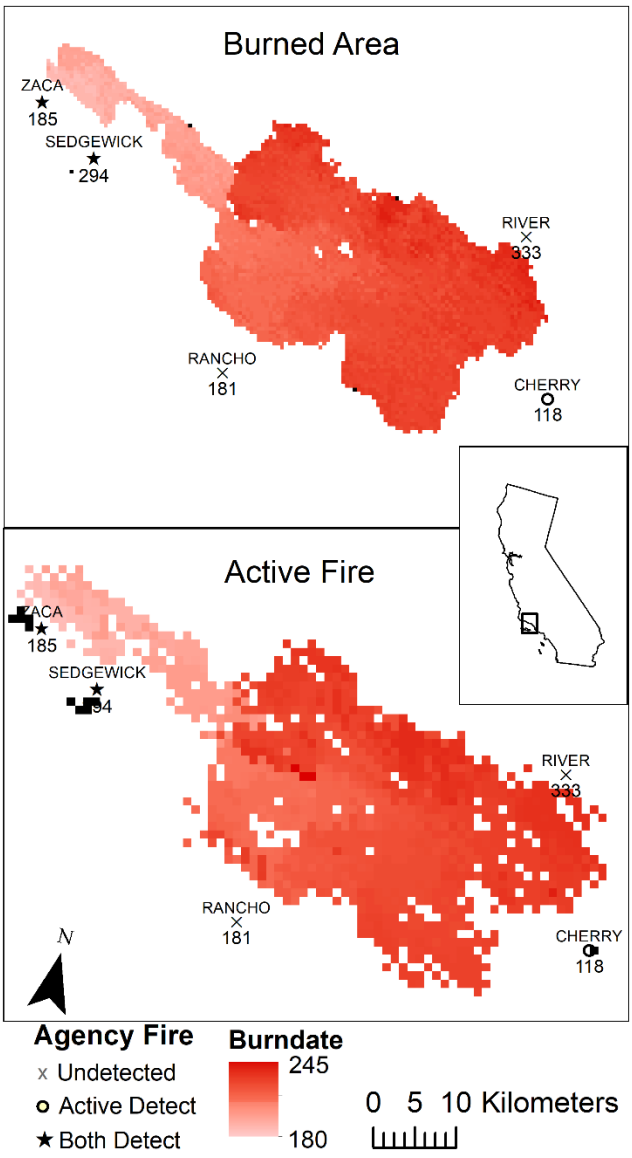

Figure 1.2: An illustration of the 2007 Zaca fire as seen by MODIS burned area (above) and active fire (below) products. Included are points associated with all fires>1ha near the Zaca fire as recorded by the agency database. Each point location for an agency fire is named, with the Julian date of discovery below the fire point. For example, the agency record of the Zaca fire is located in the northwest corner and was discovered on Julian day 185. The Zaca fire is counted as "detected" by both MODIS products because they are within 10km and±7days of at least one burned area and one active fire pixel. The Sedgewick fire, which burned on Julian day 294 is counted as detected because of the nearby MODIS pixels outside the range of the Zaca fire perimeter (burn dates outside Julian dates 180–245 have pixels shown in black). The Rancho fire, while within 10km of the overall perimeter, is not considered detected because its discovery date was not within±7days of the MODIS pixels within 10km.

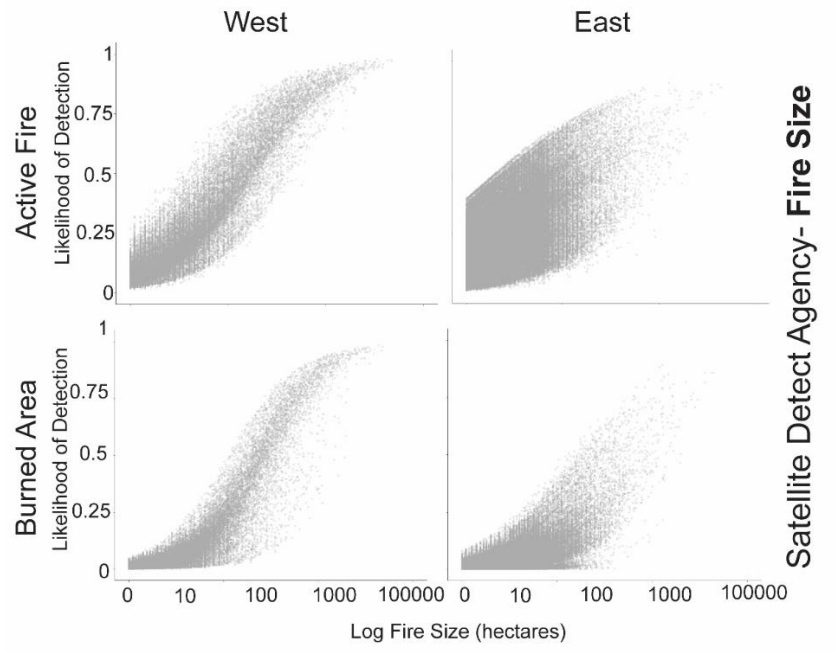

Figure 1.3: The ability of MODIS products to detect agency fire records was strongly dependent on fire size. As expected, likelihood of detected increased with fire size for each of the products and regions (such that the top left plot is for active fire in the west). Under best-case scenarios, the active fire product detected 50% of agency fires if fire size was >78ha in the west and 10ha in the east. The burned area product detected 50% of agency fires under best-case scenarios if fire size was >234ha in the west, and 169ha in the east.

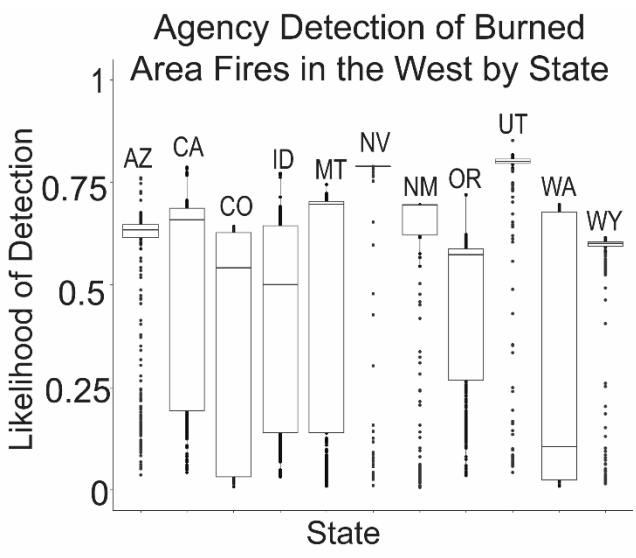

Figure 1.4: Agency fire data has the highest percent detection in the western U.S. for the MODIS burned area product. However, the likelihood that agency fire records correctly identified fire perimeters from the MODIS burned area product in the western U.S. varied markedly by state. For example, agency records from Washington were least likely to detect MODIS burned area events, whereas agency records from Nevada and Utah had a>75% likelihood of detection.

1.5 Discussion

1.5.1 Overall product agreement

With ongoing alteration of fire regimes (Balch et al., 2017) and increasing area burned (Westerling et al., 2006; Dennison et al., 2014; Westerling, 2016; Abatzoglou et al., 2017), documenting the spatial and temporal patterns of fire events is critical for understanding fire risk. Yet, our analysis shows that commonly used MODIS based satellite products and government records used to identify fire events and model fire regimes are reporting vastly different records of fire occurrence. Overall, satellite and agency fire records tend to overlap for only about a quarter of all events (Table 1.1). MODIS active fire and burned area products are likely to detect 50% of agency wildfires only when fire size reaches tens to hundreds of hectares, respectively, which is considerably larger than previously reported under theoretical conditions (Giglio et al.,2003; Giglio et al., 2009).Agency fire records show strong heterogeneity in reporting rates between states, suggesting that apparent spatial and temporal trends in fire are inconsistent across political boundaries(Short, 2014; 2015b),which could lead to questionable results of trends using agency data in these regions. This analysis highlights the need for more careful consideration of the limitations of underlying fire records in scientific analyses.

1.5.2 Satellite detection of agency fires

Satellite detection of agency fire records was relatively low, ranging from 3.5–23.4% of all fires>1ha. These values are consistent with satellite detection rates based on ground records estimated in the state of Georgia, U.S. (12%; Hu et al., 2016), Brazil (1%; Cardoso et al., 2005), and multiple regions (17%; Benali et al., 2016). However, detection rates are considerably lower than estimates using satellite to satellite comparisons, which can be as high as 86% within the conterminous U.S. when using fires>15ha in size (Hawbaker et al., 2008). The current use of

satellites for satellite fire data validation is useful for determining agreement in overall burned area when a fire event is detected by both satellite sources (e.g. Padilla et al., 2015; Zhu et al., 2017). However, this method does not fully evaluate a satellite's ability to detect a fire because remotely sensed products have many similar limitations such as difficulty detecting small fires, satellite overpass time, and satellite view obstruction from cloud or canopy cover (Cardoso et al., 2005; Hawbaker et al., 2008). Similar limitations between satellites could lead to a circular validation process, inflating perceived detection rates.

While previous studies have selected large reference fires to assess satellite detection rates (e.g. Hawbaker et al., 2008), this approach could inflate overall detection rates of the MODIS products (Hawbaker et al., 2008). By including all fires reported of at least 1ha, we were able to directly assess detection rates across a range of fire sizes. The overall detection rates reported here would be lower if we included fires smaller than 1ha reported in the agency database. The overall detection rates reported here would also be lower if we reduced our search window used to pair agency points with MODIS pixels to<10 km. We used the larger search window to encompass the extents of all agency fires, but it is likely overly generous for the smaller fires in the database. Thus, reported detection rates would be lower if we used a more stringent criterion to identify overlapping events. Finally, while the agency database preferentially retains records of individual fire events rather than fire complexes (Short, 2014), in cases where the agency database retains only one point record of many non-contiguous events as a complex, our method could underestimate detections of these events.

Our models provide new estimates for the final wildfire sizes for reliable detection (≥50% probability of detection) by the active fire and burned area products. Previous validations of the MODIS active fire product based on fires detected by ASTER suggest that MODIS is capable of detecting instantaneous hotspots between 2 and 7ha (Morisette et al., 2005; Csiszar

et al., 2006; Schroeder et al., 2008), while calculations for the burned area product suggest minimum detection sizes of 40–120ha under ideal conditions (Giglio et al., 2009; Giglio et al., 2013). Based on our analyses, it is evident that these ideal conditions are relatively rare for detecting U.S. wildfires. In our analysis, for the MODIS active fire product to reach a 50% detection probability, wildfire sizes had to reach 10ha in the east and 78ha in the west (Figure 1.3; Table 1.3). This estimate of detection likelihood differs from previous satellite-based estimates in that it is based on the final fire size, rather than the instantaneous area of the hotspots at the time of observation (Morisette et al., 2005; Csiszar et al., 2006; Schroeder et al., 2008). Although the MODIS active fire product detects hotspots, it is likely that fires with larger final fire sizes have a higher likelihood of detection because as fires continue to burn and increase in size, MODIS has more detection opportunities. Thus, this analysis provides a useful metric for estimating counts and size distributions of fires missed by MODIS products.

For the MODIS burned area product to reach a 50% detection probability, wildfire sizes had to reach 169ha in the east and 234ha in the west (Figure 1.3; Table 1.3). These estimates suggest that MODIS burned area is effective for detecting large fire events. However, analyses derived from products that preferentially detect large fires can be problematic because relatively small fires define fire regimes in some regions (Fornacca et al., 2017; Nagy et al., 2018). In the overall agency database, 91.5% of reported fires were <10ha, suggesting that small fires are an important component of fire regimes in the U.S.

Although final fire size was the most important predictor of MODIS' ability to detect fire, our results are consistent with previous work that suggests satellite detection of fires is also influenced by cloud cover, canopy cover, land cover, and seasonality (e.g. Giglio et al., 2009; Hantson et al., 2013; Hu et al., 2016). For example, our models suggest that MODIS has a slightly higher likelihood of detection on tree and herb land cover types compared to shrub land cover.

Our results are consistent with previous work that shows low detection on shrubs and higher detection on trees (Hantson et al., 2013). Our models were also consistent with previous work that showed a low likelihood of detection with high levels of cloudiness and leaf area index (Giglio et al., 2009; Hu et al., 2016). However, our models also suggest the highest levels of detection in places with intermediate levels of average annual cloud cover. High detection rates at intermediate levels of average annual cloud cover may be an artifact of the associated precipitation and fuels associated with intermediate cloud cover rather than cloud obstruction of satellite detections. This is supported by the intermediate fire-productivity hypothesis (van der Werf et al., 2008; Pausas and Ribeiro, 2013) which suggests high fire activity in areas of intermediate productivity and aridity. However, future work could improve these analyses using temporally explicit cloud cover indices.

While several covariates were significant predictors of MODIS' ability to detect agency fires (Table 1.2), the overall deviance explained by the satellite detection of agency fire models ranged from 10 to 32%. This relatively low explanatory power suggests that there may be other spatial or temporal conditions that limit MODIS fire detections. Time of day, fire duration, and fire radiative power can also impact satellite fire detection as longer, hotter fires that coincide with satellite overpass are more detectable (Cardoso et al., 2005; Hantson et al., 2013; Hu et al., 2016) but this information was not available for our analyses. Future work that examines these potential covariates, and future data collection that includes these covariates would be helpful in furthering our understanding of satellite fire detection limitations. The low predictive power of our models suggests that the spatial and temporal conditions under which MODIS has poor detection remain challenging to identify.

1.5.3 Agency detection of satellite fires

Our models suggest that variable reporting between U.S. states strongly limits the likelihood that fires will be present in the agency fire database. Although state variability is a recognized issue in the agency database (Short, 2014; 2015b), our results reveal marked discrepancies in detection likelihood. The likelihood that the agency database reported a fire detected by the MODIS burned area product ranged from as low as 10% for the state of Washington to higher than 75% for Nevada and Utah (Figure 1.4). Similarly, the likelihood that the agency database reported a fire detected by the MODIS active fire product ranged from <15% for the state of Massachusetts to >60% for the state of Nevada. These detection rates are likely overestimates. The large spatial search window (10km) used to determine fire event detection may have led to an overestimate in detection rates. Similarly, using broader spatial criteria to cluster fire events would lead to higher detection estimates because it would decrease the total number of events (by over clustering) while the number of detected events would remain the same. However, our results are consistent with analysis that suggests agency fire reports in California only include a fraction of fires detected by the MODIS active fire product (Butry and Thomas, 2017). These state differences suggest substantial inconsistencies in reporting rates based on political boundaries, which adds uncertainty to spatial models of U.S. fire regimes based on these data.

While the Department of Interior and U.S. Forest Service successfully suppress 95%–98% of unwanted wildfires, respectively (U.S. Department of Agriculture Forest Service, 2015), our analysis shows that the agency reports (which include only fires that require an agency response) only account for 23.5% to 48% of satellite fires. Satellite fire data tend to have low rates of false positive detections (Cardoso et al., 2005; Giglio et al., 2009). Thus, these differences suggest that there may be many more fires burning in the U.S. than agencies are

detecting and reporting. However, it is important to note that the MODIS products may contain fire information from agricultural and prescribed burns that are not included in the agency database (Short, 2014; 2015b). For example, differences in rates of crop burning may explain the low detection rates in Washington and Idaho which have relatively high rates of emissions from agricultural burning (Pouliot et al., 2017) because MODIS may detect many agricultural burns that would not be in the agency database. Alternatively, Nevada and Utah have lower rates of agricultural burning emissions (Pouliot et al., 2017) and higher detection likelihoods. Therefore, fire omissions in the agency database could contain a large proportion of agricultural and prescribed burns.

It is again important to note that while these factors were all significant, the total deviance explained by the models was low (8–23%) suggesting that there are additional reasons why the agency database may be missing satellite fire detections. It is possible that some variation is due to differences in socioeconomic status where the fires take place, as well as population density or number of local fire departments available to record data (Butry and Thomas, 2017). The agency data may also suffer from a lack of quality control at the initial recording level (Butry and Thomas, 2017) and inconsistencies among agencies (Short, 2015b), which could lead to spatial or temporal errors in the records. While our analysis emphasizes differences in state reporting as well as the impacts of prescribed burns and agricultural fires on agency fire detection rates, the low predictive power of our models suggests that additional biases in the agency fire records likely exist.

1.6 Conclusion

We compared satellite and agency fire data and demonstrated that these existing products have specific limitations in their scope to provide a true representation of all fire

occurrence in the U.S. However, they can be used in conjunction with one another to expand understanding of current fire regimes (e.g. Benali et al., 2016; Fusco et al., 2016). To most effectively use these data products, it is necessary to understand which fires each product represents. For example, burned area product in the western U.S. is much more likely to detect large fire events and performs best during the summer season on tree and herb land cover types. Therefore, fires in shrub land cover and in regions characterized by small fire events may be better represented with a ground-based agency database. In contrast, agency products in the western U.S. are more likely to contain fires that occurred on public lands and exclude agricultural and prescribed burns. Therefore, the MODIS fire products may be best for research that seeks to quantify overall fire emissions. Finally, the limitations of agency data based on political boundaries suggest that inter-state comparisons require careful interpretation and support the recommendation that these data are most useful for analysis over the entire U.S. (Short, 2015b).

Currently, there are at least eight active fire and burned area products that utilize various satellite sensor platforms and detection algorithms (e.g. MODIS burned area (MCD 64; Giglio et al., 2009), MODIS active fire (MCD14; Giglio et al., 2006), VIIRS (Schroeder et al., 2014), MTBS (Eidenshink et al., 2007), BAECV (Hawbaker et al., 2017) MERIS Fire CCI (Alonso-Canas and Chuvieco, 2015)), with others in development. Moreover, there are multiple sources of agency fire reports both in the U.S. and in other national systems (e.g., FPAFOD (Short, 2015a), Incident Command reports (GeoMAC, 2017)). However, based on our comparison of MODIS and agency fires, none of these sources is likely to offer a complete picture of fire activity. In the absence of a single, integrated fire product, fire scientists should be aware of the pronounced differences between products illustrated here and the influence of these detection differences on modeled fire regimes.

CHAPTER 2

QUANTIFYING THE HUMAN INFLUENCE ON FIRE IGNITION ACROSS THE WESTERN USA

2.1 Abstract

Humans have a profound effect on fire regimes by increasing the frequency of ignitions. Although ignition is an integral component of understanding and predicting fire, to date fire models have not been able to isolate the ignition location, leading to inconsistent use of anthropogenic ignition proxies. Here, we identified fire ignitions from the Moderate Resolution Imaging Spectrometer (MODIS) Burned Area Product (2000–2012) to create the first remotely sensed, consistently derived, and regionally comprehensive fire ignition data set for the western United States. We quantified the spatial relationships between several anthropogenic land-use/disturbance features and ignition for ecoregions within the study area and used hierarchical partitioning to test how the anthropogenic predictors of fire ignition vary among ecoregions. The degree to which anthropogenic features predicted ignition varied considerably by ecoregion, with the strongest relationships found in the Marine West Coast Forest and North American Desert ecoregions. Similarly, the contribution of individual anthropogenic predictors varied greatly among ecoregions. Railroad corridors and agricultural presence tended to be the most important predictors of anthropogenic ignition, while population density and roads were generally poor predictors. Although human population has often been used as a proxy for ignitions at global scales, it is less important at regional scales when more specific land uses (e.g., agriculture) can be identified. The variability of ignition predictors among ecoregions suggests that human activities have heterogeneous impacts in altering fire regimes within different vegetation types and geographies.

2.2 Introduction

Although fire is a natural component of most ecosystems and pre- dates the evolution of hominids (Pyne, 1982; Bond et al., 2005; Bond and Keeley, 2005; Bowman et al., 2009), humans are altering fire dynamics worldwide (Stephens, 2005; Korontzi et al., 2006; Archibald et al., 2008; Bowman et al., 2011). Anthropogenic changes that influence the fire cycle include changing climate (Westerling et al., 2006; Littell et al., 2009), fire suppression (Archibald et al., 2012), fuel alteration via the introduction of agriculture and pasture and through the introduction of nonnative grasses, which increase fine fuels and connectivity (D'Antonio and Vitousek, 1992), and the addition of anthropogenic ignition sources (Cardille et al., 2001). Fire is an important regulator of ecosystems, influencing succession and vegetation assemblages at local scales and the distribution of biomes at global scales (Bond and Keeley 2005, Bond et al., 2005). Fire is also economically costly (Butry et al., 2001); the USA spends over US$1 billion per year in suppression costs alone (Abt et al., 2009). Because of these ecological and economic impacts, it is necessary to understand how humans have altered fire cycles. We use a novel remote sensing approach to quantify anthropogenic impact on fire ignitions in seven western US ecoregions.

The western USA is an ecologically diverse region that includes many species such as Douglas fir forest in the Pacific Northwest, pinyon juniper in the Southwest, and ponderosa pine forest in the Southwest and northern Rockies (Pyne, 1982; Keane et al., 2008; Dennison et al., 2014). Human activities are strongly altering western fire regimes. For example, increased fire frequency in forested systems in the last 50 years has been observed in the western USA and has been partially attributed to rising regional temperatures and earlier spring snowmelt (Westerling et al., 2006; Dennison et al., 2014). Historical land- use change also influences fire. Since the early 1900s, fire has been substantially reduced in many western US ecosystems via

fire suppression (Pyne, 1982; Moore et al., 1999; Allen et al., 2002; Schoennagel et al., 2004). Suppression efforts resulted in an increase of fuels in certain ecosystems (e.g., ponderosa pine ecosystems), as well as an initial decrease in fire occurrence (Marlon et al., 2012). Although these western US forested systems have species with adaptations to fire, altered frequency and severity of fires associated with climate and land- use change can lead to different dominant species and overall changes in community composition (Keane et al., 2008). In addition to human impacts from climate and suppression, western US fire regimes have been impacted by the introduction of invasive plants. Nonnative grasses, such as *Bromus tectorum* and *Bromus rubens*, are known to alter fire regimes by increasing fine fuels and fuel continuity (D'Antonio and Vitousek 1992; Lambert et al., 2010; Balch et al., 2013). As invasive grasses continue to spread and human settlement near wildland areas increases (Theobald and Romme, 2007), ecosystems across the western USA are increasingly susceptible to fire.

Humans can alter fire ignitions intentionally or through accidental fire starts. People use fire intentionally for many purposes, including for land management (e.g., agriculture and pasture maintenance) and for ecosystem management (e.g., prescribed fires; Pyne, 1982; Bowman et al., 2011). Some of these intended fires may escape and start wildfires. Unintended fire starts associated with people include smoking, railroad sparks, equipment use, and powerlines (National Wildfire Coordinating Group, 2005). While some of these sources, such as campfire, debris burning, and arson, have obvious links to fire ignition, others are less intuitive. In the case of railroads, brake sparks and right of way track maintenance are known to cause fire ignition (Harrington and Donnelly, 1978), while extreme winds can knock down powerlines that may ignite fires (Tse and Fernandez- Pello, 1998).

Despite these strong relationships between humans and fire ignition, regional- scale spatial analyses of anthropogenic influences on fire ignition are lacking. Previous studies

investigating the influence of humans on fire ignition have typically been at landscape scales (e.g., Vega- Garcia et al., 1995; Syphard et al., 2007; Wu et al., 2014; Argañaraz et al., 2015). Regional and global- scale models of fire probability and human impact on fire have not empirically tested patterns of fire ignitions, but instead use spatial layers, such as roads or human population density, as proxies for human ignition pressure (Parisien et al., 2012; Hawbaker et al., 2013; Knorr et al., 2014). To date, both landscape and regional scale analyses assume that the importance of different anthropogenic predictors of fire ignition is constant across space and have not tested whether human influence on fire varies between ecosystems. Anthropogenic ignitions can be controlled reasonably well by fire management, (Hawbaker et al., 2013), and therefore understanding the spatial patterns of anthropogenic fire ignitions may help with the prediction and mitigation of future fire risk.

While we know that anthropogenic ignition pressure varies globally (Pechony and Shindell, 2009), previous studies have focused on roads and population density as proxies for anthropogenic ignition when predicting fire (Yang et al., 2007; Siljander 2009). It is unlikely that human presence alone is consistently the best predictor of fire occurrence. Thus, a better understanding of how specific human activities relate to fire ignitions would improve spatial models of fire risk.

We use a novel remote sensing approach to distinguish anthropogenic fire ignitions from lightning ignitions across the western USA. We then quantify the spatial relationship between anthropogenic predictors and fire ignition within seven western US ecoregions to answer the following questions: (1) What is the relative importance of anthropogenic features for predicting fire ignition in seven western US ecoregions? and (2) How does the influence of anthropogenic features on fire ignition vary among western US ecoregions. This study presents the first regional- scale analysis of the spatial variability of human influence on fire ignitions.

2.3 Methods

2.3.1 Fire data

We used the Moderate Resolution Imaging Spectrometer (MODIS) Collection 5 Burned Area Product (Roy et al., 2002; 2005; 2008) to identify ignition pixels. The MODIS Burned Area Product (MCD45A1) uses a bidirectional reflectance model- based change detection algorithm (Roy et al., 2005). Burned areas are distinguished at an approximate 500- m resolution based on rapid changes in surface reflectance due to removal of vegetation and subsequent deposition of charcoal and ash (Roy et al., 2005). Although the collection 6 MODIS Burned Area Product (MCD64A1) demonstrates superior fire detection rates, particularly for infilling fire perimeters (Giglio et al., 2009), these data were not available at the time of the analysis. The locations of potential ignition pixels associated with the two products are likely to be similar. In addition to providing a spatial location for burned areas, MCD45A1 also assigns a Julian day to each burned pixel which signifies the date of fire detection. In areas with limited cloud cover, such as the western USA during summer months, MCD45A1 has higher accuracy than in areas with higher levels of cloud cover (Boshetti et al., 2010). These daily data span 1 January 2000–31 December 2012 (except June 2001, when there was an error in the fire detection instrument) for the 11 westernmost contiguous states (Figure 2.1). We only considered fires that burned from May to October because this time frame is considered the typical fire season in the western USA (Westerling et al., 2003). We retained ignitions associated with all land cover classes in the modeling analysis assuming that all ignitions have the potential to spread into wildland fires. We aimed to characterize the overall pattern of anthropogenic ignitions associated with all sources.

2.3.2 Response variables

The MCD45A1 product identifies burn dates for individual (~500 m) pixels but does not identify unique fire perimeters. We grouped the burned pixels into unique fire perimeters based on spatial and temporal proximity. Pixels were considered part of the same fire event if they were within 2 d and two pixels of one another or within 3 d and adjacent. Temporal proximity was only considered when pixels burned in ascending order such that large fires that eventually merge would maintain unique perimeters and ignition points. In some cases where large fires burned for multiple weeks, these criteria were not appropriate. For these complex fires, we grouped pixels into a single event if burned pixels were within two pixels and there were no time gaps longer than 3 d during the entire event. After grouping all unique fire perimeters or complexes, we identified the earliest burn date. Pixels burning on the first day of multiday fires and all burned pixels in single date fires were identified as potential ignition pixels. Based on these criteria, a single fire event could have multiple potential ignition pixels. To test whether this biased our modeling results, we also averaged predictor variables for all ignition pixels in every unique fire event and repeated out analysis using only a single ignition per fire.

In order to isolate ignitions likely caused by anthropogenic activity, we excluded ignitions likely to have been caused by lightning. Cloud- to- ground lightning strikes were acquired from the Vaisala National Lightning Detection Network lightning density data from 2000 to 2009 and the North American Precision Lightning Network from 2010 to 2012 to identify ignitions potentially attributable to lightning. These data included information on the location and timing of lightning strikes and have a reported median spatial accuracy of 500 m in the western USA (Cummins and Murphy, 2009) with over 95% of strikes having uncertainties in location of <4 km (Biagi et al., 2007). If an ignition pixel was within a 4- km radius and burned within 3 d after a lightning strike, it was considered a potential lightning ignition. We used a 3 d buffer as lightning ignitions can remain undetected by satellites for several days until weather

conditions become conducive to fire spread. All other ignitions that were not spatially or temporally proximal to lightning strikes were assumed to originate from an anthropogenic source.

2.3.3 Validation of ignition sources

We used the Fire Program Analysis fire- occurrence database (FPA FOD; Short, 2015a) to test the relative accuracy of the in anthropogenic vs. lightning ignition classification. The FPA FOD is a compilation of fires reported by federal, state, and local agencies and encompasses the entire study period, 2000–2012 (Short, 2015a). The completeness and accuracy of these records varies by state and reporting abilities, and while extensive, is an incomplete record of all fire activity (Short, 2014). Therefore, a lack of corresponding ignition records between FPA FOD and MCD45A1 may be due to reporting errors in FPA FOD and not necessarily attribution errors in our method. Nonetheless, as the only other ignition dataset available, the comparison provides an important initial estimate of MCD45A1 ignition accuracy.

The goal of identifying lightning ignitions was to exclude them from the analysis, thus creating a clearer picture of anthropogenic ignition. In order to test our classification of lightning ignitions, we identified data points from the FPA FOD that overlapped with fire perimeters from the MCD45A1 data. The spatial and temporal accuracy of the FPA FOD dataset are unknown, and it is likely that some spatial and temporal errors exist (Short 2014). As such, we set a wide search window for overlap. Points and perimeters were considered overlapping if they were within 10- km spatially and burned within 7 d temporally. The FPA FOD fire causes listed for each fire were then assigned to ignition points associated with that perimeter. Fires that had arson, railroad, power line, smoking, children, debris burning, structure, fireworks, campfire,

equipment use, or miscellaneous listed as the cause were considered anthropogenic, while FPA FOD listed as lightning caused were considered lightning ignitions.

2.3.4 Predictor variables

We chose anthropogenic features potentially associated with wildfire ignitions based on fire causes listed in the National Wildfire Coordinating Group Cause and Determination Handbook (National Wildfire Coordinating Group, 2005; Table 2.1). We used the LandFire Existing Vegetation Type 120 (LANDFIRE, 2008; Rollins, 2009) to determine presence or absence of agriculture in each 500- m ignition pixel. We chose to include ignition pixels that burned on agricultural land because agricultural fires are a potentially important component of anthropogenic ignitions across the western US region. We used the USGS SAGEMAP (Sagebrush and Ecosystem Map Assessment Project) Human Footprint data relating to roads, power lines, railroads, interstates, campgrounds, and population density (Leu et al., 2008). We calculated distance to roads, power lines, railroads, and interstates from the centroid of each pixel. If any of these features were present within the pixel, the distance value was set to zero. Campgrounds were treated as a binary variable denoting presence or absence in each pixel. We used the mean population density for each pixel to represent the population density for the entire pixel. Population density was log transformed to deal with outliers with large population sizes.

We used the SILVIS (Spatial Analysis for Conservation and Sustainability) 2010 WUI (Wildland Urban Interface) stand- alone data to determine the percent of development within each pixel (Radeloff et al., 2005). Overall WUI development was calculated as the sum of high density interface, high density intermix, medium density interface, medium density intermix, low density interface, and low density intermix based on the WUICLASS10 designation.

2.3.5 Modeling

For each of the seven Omernik Level I Ecoregions in the western USA (Omernik, 1987; Figure 2.2), we first modeled the presence/absence of ignitions as a function of the predictor variables using generalized additive models (GAMs) in the mgcv package (Wood, 2011) in R version 3.1.2. Anthropogenic ignitions were treated as presence, while randomly selected unburned areas from 2000 to 2012 were treated as absence. Lightning ignitions and associated fires were excluded from analysis. We calculated the generalized variance inflation factors (GVIF; Fox and Monette, 1992) for predictor variables separately in each ecoregion to test for multicollinearity. We removed variables with GVIF values above 3 to avoid violations of multicollinearity. The campground predictor was removed from analysis because there were too few observations to create an effective model. The GAMs were used to explore the relationship between predictor and response variables, for variable selection and to identify type of relationship (e.g., linear, quadratic). Based on the predictor variables and relationships identified in the GAM analysis, we then used generalized linear models (GLMs) to identify the relative contribution of predictors within each ecoregion. If a variable was best modeled with a quadratic or cubic polynomial based on the relationship displayed in the ecoregion GAM, we kept all lower order forms (linear, or quadratic and linear, respectively) of that variable in the GLM analysis. This resulted in first, second, and third order polynomials in the construction of ecoregion GLMs. We performed backward stepwise selection for each ecoregion model until there were 12 (the maximum allowable in the hier.part package) or fewer variables and selected the GLMs with the lowest Akaike's information criteria (AIC) value.

We tested the relative importance of each anthropogenic predictor, using hierarchical partitioning (Chevan and Sutherland, 1991) to determine the independent model contribution for each variable included in the GLM. Hierarchical partitioning was done in R using the hier.part

package (Walsh and MacNally, 2013). To find the independent model contribution of each variable, we summed the percent model contribution of each term containing the variable. A variable with a quadratic and linear term would count as two terms in the 12 term limit. We assessed each model fit by calculating the deviance explained by the model. We tested the direction of the relationship for the top two predictors with anthropogenic ignition in each ecoregion using both a linear regression and loess smoother. We also tested the direction and strength of the relationship for the top two predictors using only anthropogenic ignitions confirmed by the FPA FOD data.

2.4 Results

We identified 47,495 unique fire events in the western USA from 2000 to 2012, with a total of 129,332 potential ignition pixels (fire events often had multiple pixels burning on the first day). Of these ignition pixels, the vast majority (90%) occurred in the May– October time frame and were included in this analysis (Figure 1.2). 26,402 ignitions (23%) were identified as potentially caused by lightning based on the 3 d and 4 km criteria, leaving a total of 90,278 ignition pixels likely attributable to anthropogenic sources. Pixels that burned exclusively on agricultural land made up a minimal (<2%) number of ignition pixels in all ecoregions except in the Marine West Coast Forest, where they made up 6.6%. The total number of anthropogenic and lightning ignitions varied among ecoregions. The most anthropogenic ignitions occurred in the North American Desert and Mediterranean California ecoregions, and the fewest occurred in the Southern Semiarid Highlands and Temperate Sierra ecoregions (Table 2.2).

Of the 116,680 total potential ignition sources in the May–October time frame, a total of 13,170 aligned with the FPA FOD fire database when ignitions with unknown sources were excluded from analysis. This low overlap rate could reflect differences in fire size and detection

likelihood. The FPA FOD fire database identifies all fires that were treated (and often extinguished) by government agencies, while MCD45A1 identifies burned area detectable within at least one 500- m pixel, likely including fires not reported in agency databases (e.g., agricultural fires that did not require agency response). Of the ignitions in the overlapping subset, we identified 4,093 as lightning, 83% of which were confirmed by the FPA FOD. Of the remaining ignitions, 4,372 (48%) were confirmed by the FPA FOD as anthropogenic (Figure 2.3, Table 2.3).

These confirmation rates match our initial goal of including all anthropogenic and potentially anthropogenic ignitions in our dataset. However, we repeated our modeling analyses using only the confirmed anthropogenic ignitions and found very similar results, suggesting that our analysis is robust to the potential inclusion of some percentage of lighting ignitions.

There was substantial variability in the deviance explained by each ecoregion model. The ecoregion GLMs used for hierarchical partitioning are less flexible and therefore explain less than ecoregion GAMs, however, they still perform comparably for the majority of ecoregions (Table 2.4). The best model GLMs based on deviance explained were in the Marine West Coast Forest (69.2%) and North American Desert (28.6%), whereas anthropogenic predictors only explained 5.4% of the spatial pattern of ignition in the Great Plains (Table 2.4). For most ecoregions, the GLMs performed similarly to the GAMs in terms of overall deviance explained, suggesting that relationships between anthropogenic predictors and ignition are reasonably well explained with linear, quadratic, or cubic functions.

After using model selection criterion, all predictor variables were retained in all ecoregion GLMs except for the Southern Semiarid Highlands and Temperate Sierras where powerlines, and powerlines/agriculture, respectively were excluded (Table 2.5). The polynomial term used to include predictors varied among ecoregions but was most commonly linear or quadratic. The 12

variable maximum allowed in the hier.part package only affected the GLM created for the Great Plains ecoregion.

Model contribution from each predictor varied substantially among ecoregions. Proximity to railroads was the most consistently important predictor, with the highest or second highest model contribution in all ecoregions except for in the Great Plains and Mediterranean California. Agricultural presence had the highest model contribution in the Marine West Coast Forest (45%) and Northwest Forested Mountains (41%). Presence of wildland urban interface had the highest model contribution in the Southern Semiarid Highlands (39%) and Mediterranean California (36%). The most important predictor of anthropogenic ignition was different for the remaining three ecoregions with distance to railroad in the North American Desert (36%), distance to road in the Temperate Sierras (57%), and distance to interstate in the Great Plains (35%; Figure 2.4). Relative contributions of predictor variables for models run with a single ignition per fire event were largely the same in each ecoregion.

If anthropogenic features are indeed influencing fire ignitions, we expect their relationships to have a predictable directionality. For example, anthropogenic ignition should decrease with distance to roads, resulting in a negative relationship. In contrast, anthropogenic ignition should increase with higher wildland urban interface (i.e., more urban areas within wildlands), resulting in a positive relationship. This is the case for the top predictors in the regions with the highest explanatory power: Marine West Coast Forest, North American Desert, Northwest Forested Mountains, and Mediterranean California ecoregions (Figure 2.5a–d). However, the expected relationships are not evident in the regions with the lowest explanatory power (Temperate Sierras, Southern Semiarid Highlands, and Great Plains; Figure 2.5e–g).

Table 2.1: Predictor data layers used in this analysis are associated with one or more of the wildfire causes listed in the National wildfire coordinating group origin and cause determination handbook.

Data Layer	Data Source	National Wildfire Coordinating Group Ignition Cause Category
Lightning	Vaisala NLDN	Lightning
Roads/ Interstates	SAGEMAP (Leu et. al., 2008)	Smoking, Arson, Equipment Use
Powerlines	SAGEMAP (Leu et. al., 2008)	Powerlines
Railroads	SAGEMAP (Leu et. al., 2008)	Railroads, Arson, Equipment Use
Campgrounds	SAGEMAP (Leu et. al., 2008)	Campfire
*WUI/ Population	SILVIS/ SAGEMAP (Radeloff et al.,2005; Leu et al, 2008)	Smoking, Arson, Children, Fireworks, Cutting, Welding
Vegetation Type	LANDFIRE	Agriculture

Table 2.2: The total number of lightning and anthropogenic ignitions in each of the seven western US ecoregions. Ecoregion

Ecoregion	Lightning	Anthropogenic	Total Ignitions	Anthropogenic Ignitions/km2
Great Plains	36%	64%	9283	0.01
Marine West Coast Forest	17%	83%	10620	0.11
Mediterranean California	7%	93%	18582	0.10
North American Desert	26%	74%	60660	0.03
Northwestern Forested Mountain	20%	80%	14977	0.01
Southern Semiarid Highlands	20%	80%	776	0.01
Temperate Sierras	42%	58%	1782	0.01
All Ecoregions	23%	77%	116680	0.03
Ignitions Not Analyzed			12652	

Table 2.3: MODIS Burned Area Product (MCD445A1) ignitions that overlapped with the Fire Program Analysis fire- occurrence database (FPA FOD) data set were used to validate attribution of lightning as an ignition source.

		MCD45A1		
		Anthropogenic	Lightning	
FPA FOD	Anthropogenic	4372	703	5075
	Lightning	4705	3390	8095
		9077	4093	13170 Total Overlap
		48% confirmed anthropogenic	83% confirmed lightning	

Table 2.4: The deviance explained by the best generalized linear model (GLM) varied by ecoregion but was comparable to the deviance explained by the general additive model (GAM) with the same variables for each region.

Ecoregion	Deviance Explained (GLM)	Deviance Explained (GAM)
Marine West Coast Forest	69.2%	74.0%
North American Desert	28.6%	30.2%
Northwest Forested Mountains	17.0%	20.1%
Mediterranean California	15.8%	18.5%
Temperate Sierras	8.2%	16.7%
Southern Semiarid Highlands	8.2%	10.5%
Great Plains	5.4%	6.8%

Table 2.5: After testing for multicollinearity, the remaining predictor variables were used to create ecoregion GLMs.

	Predictor Variables Modeled by Ecoregion						
Ecoregion	Road	Interstate	Powerline	Railroad	WUI	Log Pop	Agriculture
Southern Semiarid Highlands	2	1		1	1	1	1
Temperate Sierras	3	2		3	1	1	
Mediterranean California	2	2	2	2	1	2	1
Marine West Coast Forest	1	2	2	1	1	2	1
Northwest Forested Mountains	2	2	2	3	1	1	1
Great Plains	2	3	2	1	1	2	1
North American Desert	1	2	1	3	1	2	1

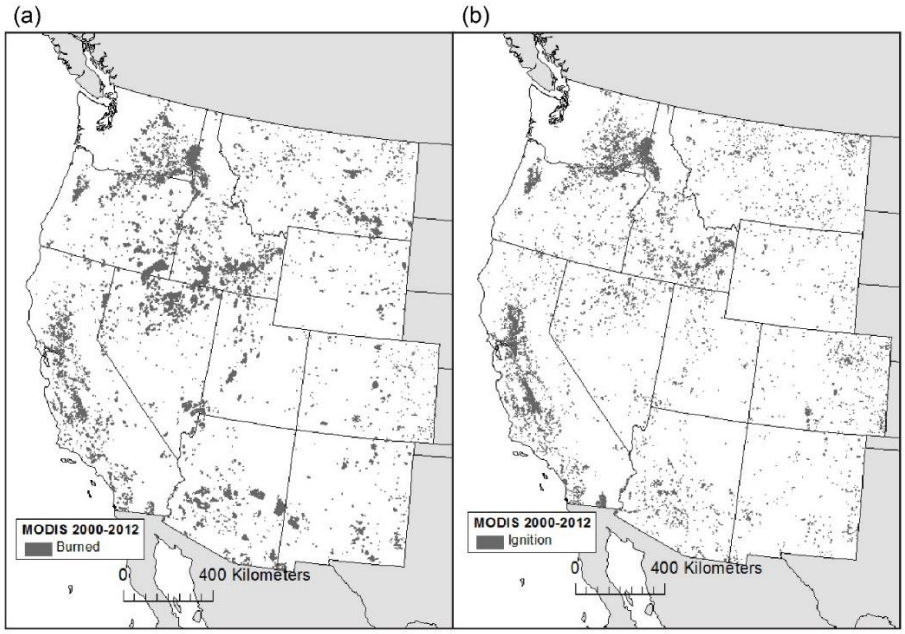

Figure 2.1: The study area is composed of the eleven westernmost contiguous US states. (a) Burned and (b) ignition pixels were determined using the MODIS Burned Area Product (MCD45A1).

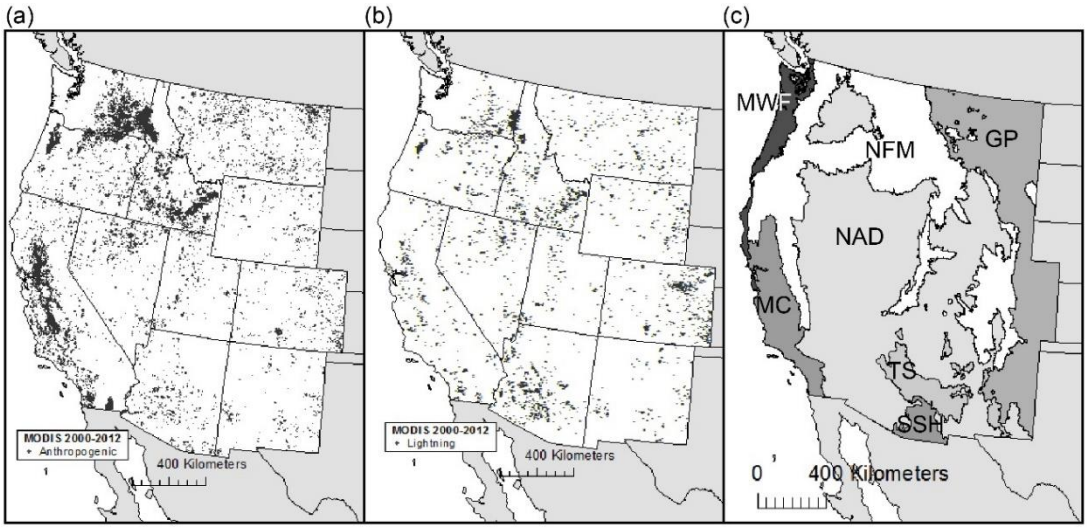

Figure 2.2: Fire ignitions are distributed throughout the western USA. For all ignitions that occurred from May to October 2000– 2012, we determined whether the ignition had an (a) anthropogenic or (b) lightning source using data from Vaisala National Lightning Detection Network. (c) The distribution of anthropogenic ignitions varied between ecoregions. The ecoregions are abbreviated as follows: MWF, Marine West Coast Forest; NAD, North American Desert; MC, Mediterranean California; TS, Temperate Sierras; SSH, Southern Semiarid Highlands; GP, Great Plains; NFM, Northwest Forested Mountains.

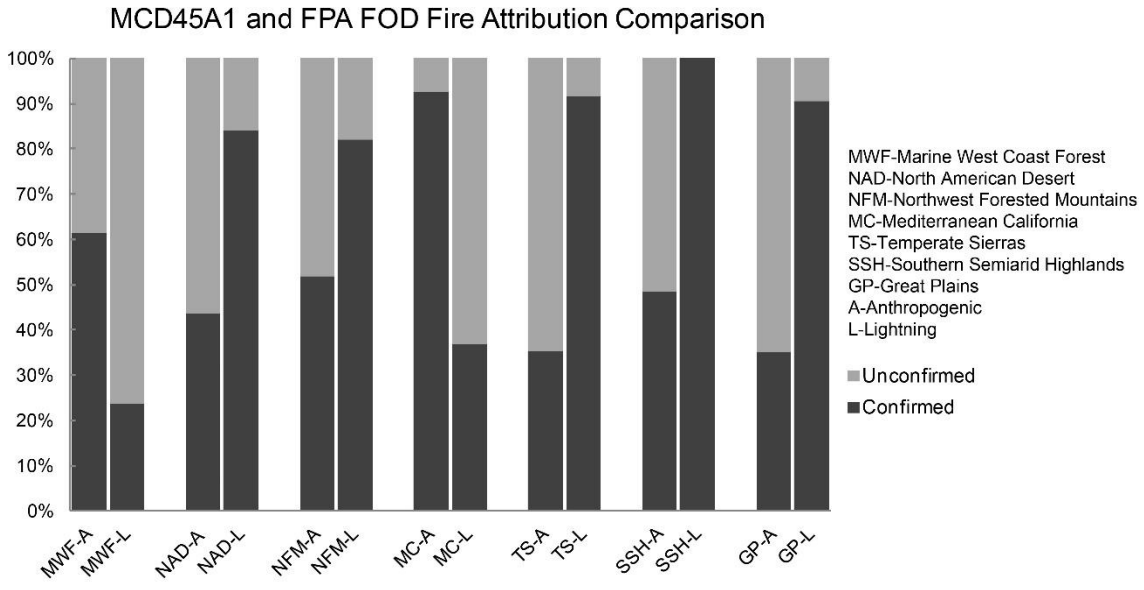

Figure 2.3: The percent of MODIS (MCD45A1) lightning ignitions that were confirmed by the Fire Program Analysis fire- occurrence database (FPA FOD) data varied among ecoregions, but averaged 83%. The average number of confirmed anthropogenic ignitions per region was 48%. We correctly identified lightning ignitions above a rate of 75% for five out of the seven ecoregions, with the lowest accuracy in the Marine West Coast Forest and Mediterranean California.

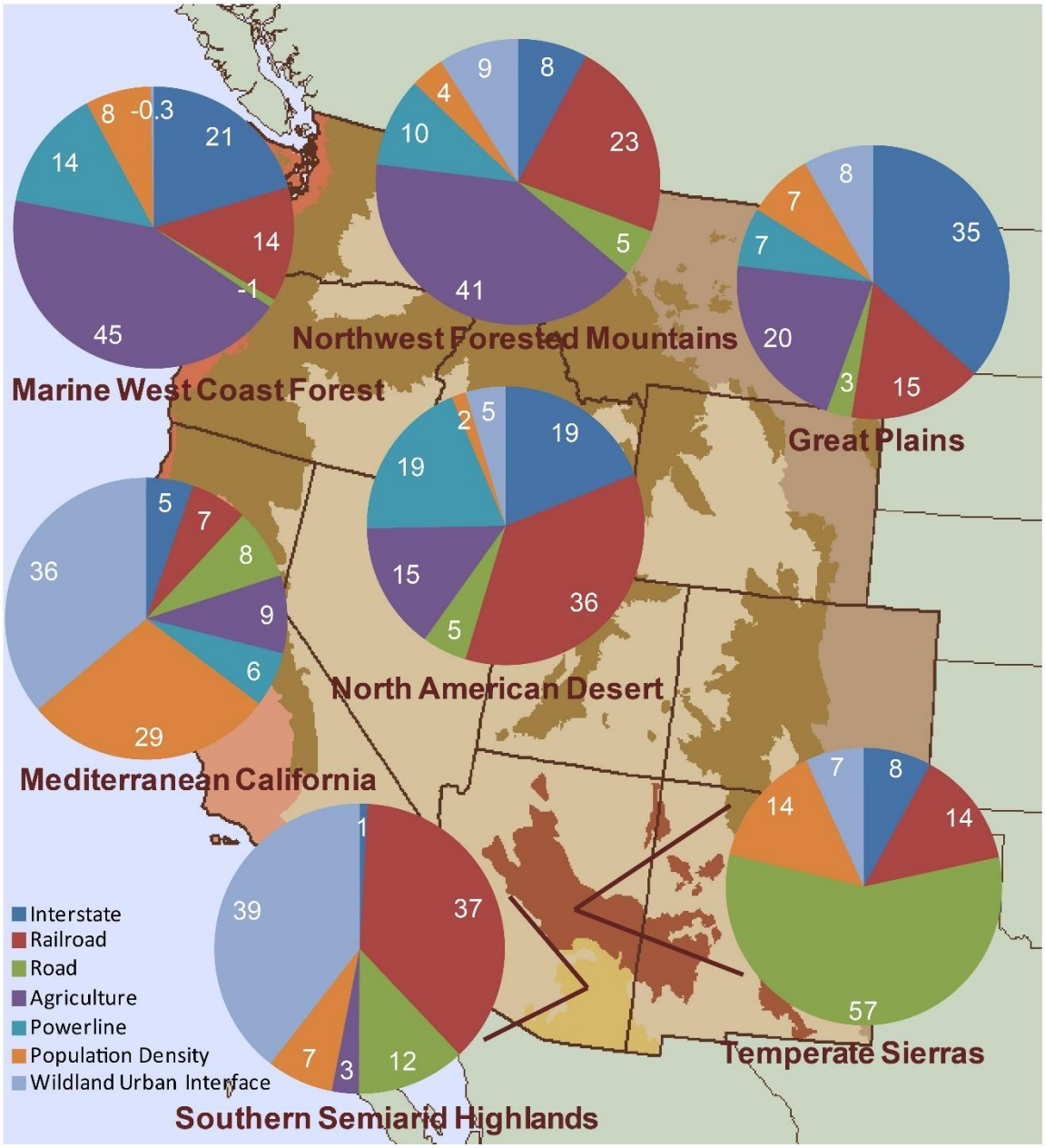

Figure 2.4: The top anthropogenic predictors of anthropogenic ignition varied widely between ecoregions. Pie charts show the independent model contribution of each predictor variable for the best ecoregion model. Negative values show that the variable acts as a suppressor of other model variables, meaning that it is not a great predictor itself, but suppresses the residual error of the model.

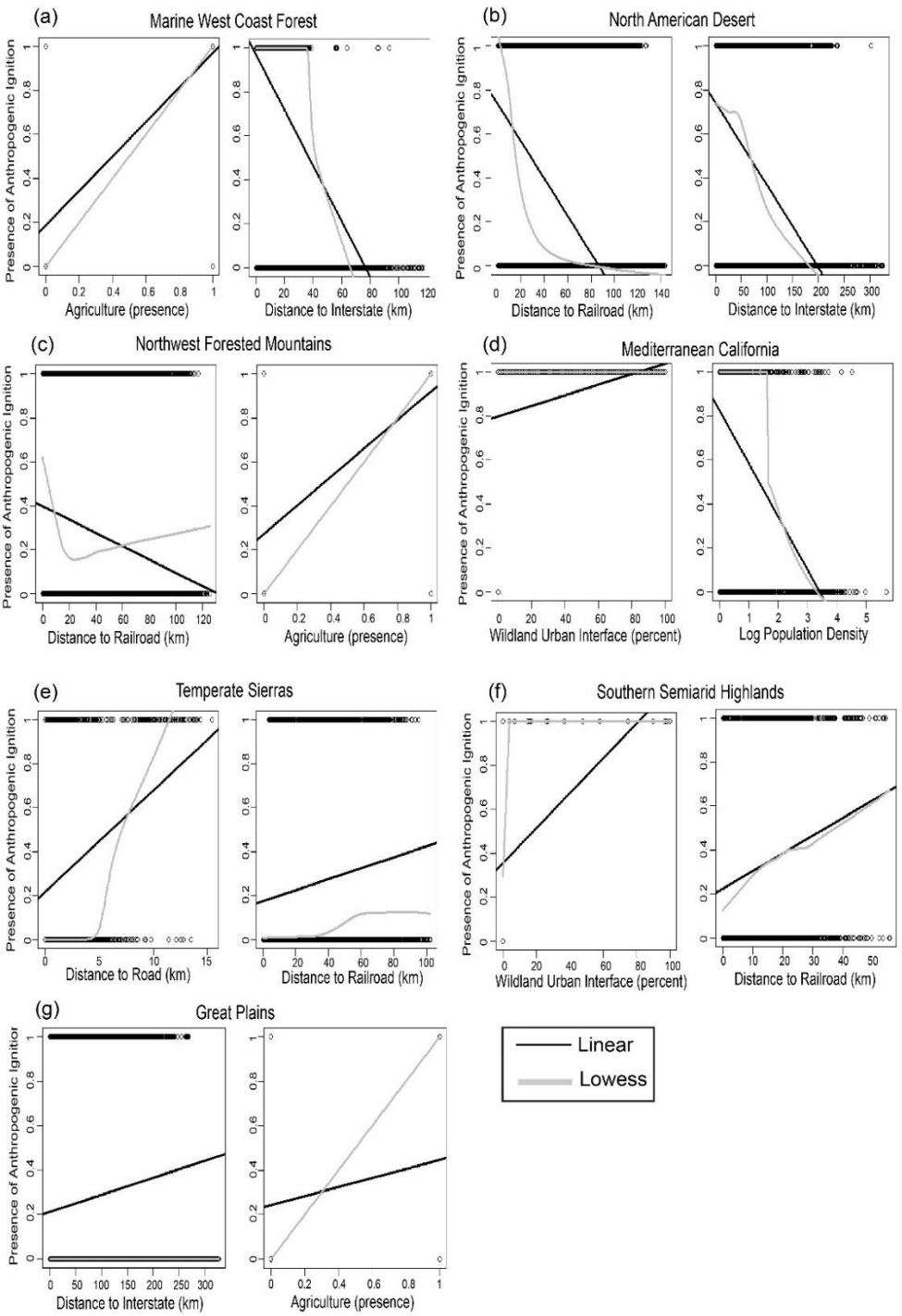

Figure 2.5: The relationship of the two best model predictors and anthropogenic ignition are shown for each ecoregion. These relationships are in (a–d) the expected direction in the four ecoregions with the highest explanatory power, but (e–g) are counter intuitive in the three ecoregions with poor explanatory power. The black line denotes a linear relationship, while the gray line shows the loess smoother.

2.5 Discussion

Our analysis reveals strong spatial variability in the relationship between human land- use and anthropogenic fire ignitions. This variability in anthropogenic influence suggests that humans impact ignition differently across ecoregions due to interactions with climate and land cover, and spatial variation in human land- use across regions (Archibald et al., 2008; Littell et al., 2009; Marlon et al., 2012). For example, environments with wetter, larger fuels and humid weather would be less likely to carry a spark that results in ignition than those with dry, fine fuels and frequent fire weather. They would also be more fire- limited as a consequence of shorter- lived fire potential through the season. In addition, human impact on the landscape varies among ecoregions (Leu et al., 2008). The results of this study underscore the complexity of the interplay between humans, climate, and fuels and their relationship with fire ignition across the western USA. Given the considerable variation in the relationship between anthropogenic influence and fire ignitions across broad ecoregions, it is likely that the similar variance will also be evident at landscape scales.

In the Marine West Coast Forest, agricultural presence was the best predictor of anthropogenic fire with an independent model contribution of 45%, suggesting that human agricultural practices in this region are strongly linked to fire ignition. While many regions contain agricultural areas, variation in crop types and agricultural burn calendars impact the patterns of agricultural influence on the landscape (Korontzi et al., 2006). For example, the Marine West Coast Forest consists largely of the Willamette Valley region, which has a long history of grass seed production beginning with rye grass and turf grass in 1935 (Conklin and Fisher, 1973). In order to prevent the spread of disease and to remove agricultural residue which can inhibit future growth, fire is used as a regular management tool (Conklin and Fisher,

1973; Hardison, 1980). It is likely that the heavy use of fire to manage these grass crop systems contributes to the high influence of agriculture on fire ignition in the Marine West Coast Forest.

Although the practice of agriculture burning is not restricted to Willamette Valley (McCarty et al., 2009), agricultural presence did not have a high model contribution in any of the remaining ecoregions except for the Northwest Forested Mountains, where post- harvest burning of wheat crops may be responsible. This may be due to the unique climate in the Marine West Coast Forest, which is one of the wettest in North America (Commission for Environmental Cooperation, 1997). In this wet area, it may be necessary to have a hotter and more intentional ignition source, such as crop residue burning, for successful ignition. However, in more arid regions, less powerful sources of ignition may be enough to ignite fuels. For example, cigarette butts require relative humidity levels below 22% for fire ignition (National Wildfire Coordinating Group, 2005) and would be more likely to start a fire in arid regions such as the North American Desert where distance to interstate (and associated cigarettes and automotive sparks) is an important predictor of ignitions.

Another important predictor in the North American Desert, characterized in part by a desert steppe climate (Commission for Environmental Cooperation, 1997), is distance to railroad, with a total model contribution of 39%. The dry climate in this region likely encourages fire spread from railroad ignitions attributed to brake sparks and track maintenance (Harrington and Donnelly, 1978; National Wildfire Coordinating Group, 2005), whereas these sparks would be less likely to ignite larger, wetter fuel sources. Another potential reason why railroads are such a strong predictor of fire ignition in this ecoregion is because of their association with cheatgrass (*B. tectorum*), which was originally introduced in the west via railroad lines (Knapp, 1996). Cheatgrass is a fire prone invasive species (D'Antonio and Vitousek, 1992) that has been shown to increase the fire activity in invaded areas (Balch et al., 2013). Although cheatgrass is

widespread in the west, it is most dominant in the Great Basin region, covering 40,000 km2 (Bradley and Mustard, 2005), which makes up a large portion of the North American Desert ecoregion. In this region, the distinctive combination of arid climate and fire prone fine fuels in close proximity to an ignition source likely contribute to the unique contribution of railroads to overall anthropogenic ignition in the North American Desert.

Although population density is often used as a proxy for human ignition (Cardille et al., 2001; Syphard et al., 2007; Hawbaker et al., 2013), in our western US study, it was a poor predictor. (The only notable influence was in Mediterranean California.) At global scales, spatial population density is more widely available and likely provides a reasonable proxy for other anthropogenic land- use features. However, the low contribution of population density in most western US ecoregion models suggests that human use of the landscape has a greater impact on fire ignition than just the number of people per square kilometer. This understanding will enhance our ability to include human variables in predictive fire models.

In Mediterranean California, where population density was an important predictor of ignition, it showed a negative monotonic relationship with anthropogenic fire ignition (e.g., Figure 2.5d). In contrast, previous work suggests fire density is highest at intermediate levels of population density (Syphard et al., 2007; Archibald et al., 2008). An association with intermediate population densities could be due to increased levels of fire detection and suppression, as well as more fuel breaks in highly populated areas, and a lack of anthropogenic ignition sources in sparsely populated areas (Guyette et al., 2002; Syphard et al., 2007). However, fire frequency has also been found to have a negative relationship with population density regionally, for example in the Missouri Ozarks (Guyette et al., 2002), and globally (Knorr et al., 2014). Our results for the Mediterranean California ecoregion model are consistent with Guyette et al. (2002) and Knorr et al. (2014). It is likely that fires throughout the heavily

populated Mediterranean California are quickly suppressed, before becoming detectable by MODIS, because they pose a threat to people and infrastructure.

Human impact (Sanderson et al., 2002) and ignition pressure (Pechony and Shindell, 2009) are not homogenous across the globe. Therefore, how anthropogenic ignitions vary must be accounted for when predicting fires. Currently, predictive fire models typically rely on population density as a proxy for anthropogenic ignition (Yang et al., 2007; Pechony and Shindell, 2009; Siljander 2009) and do not consider regional differences in ignition pressure. We suggest that regional differences in fire ignition should be taken into account when creating regional and global fire models. For example, more specific measures of human activity, such as railroads and interstates, should be tested where available when determining the best proxy for anthropogenic ignition in fire models. However, population density is included in each ecoregion model despite its generally low overall model contribution. Therefore, it may be used to improve predictive fire models when more specific spatial information is unavailable.

The variation in anthropogenic influence on fire ignition across ecoregions shown in this study emphasizes that human presence alone is not the best predictor of ignitions. Rather, human use of the landscape, likely combined with flammability of surrounding vegetation, influences regional patterns of fire ignition. This is the first study to address how human drivers of ignition vary by ecoregion using a remote sensing approach. By better understanding how humans influence ignition and how humans interact with regionally varying climate and fuels, we can more accurately include anthropogenic variables in predictive fire models.

CHAPTER 3

INVASIVE GRASSES INCREASE FIRE OCCURRENCE AND FREQUENCY ACROSS U.S. ECOREGIONS

3.1 Abstract

Fire prone invasive grasses create novel threats to ecosystems by increasing fuel load and continuity, which can alter fire regimes. While the existence of an invasive grass-fire cycle is well known, evidence of altered fire regimes is typically based on local scale studies or expert knowledge. Here, we quantify the effects of twelve non-native, invasive grasses on fire occurrence, fire size, and fire frequency across twenty-nine U.S. ecoregions. We combined both agency and satellite fire records with spatial records of abundant grass invasion to test for differences in fire regimes between invaded and nearby 'uninvaded' habitat. Additionally, we assessed whether invasive grass presence is a significant predictor of altered fire by modeling fire occurrence, size, and frequency as a function of grass invasion as well as anthropogenic and ecological variables relevant to fire. Eight of the twelve target species showed significantly higher rates of fire occurrence, with fire occurrence more than twice as likely for four grasses. Two species showed significantly larger mean fire size. Six species demonstrated significantly higher mean fire frequency, with fires more than twice as frequent for two grasses. Grass invasion remained a significant predictor in the modeling results for fire occurrence and frequency, however, it was not significant in any of the fire size models. The significant differences in fire regimes between invaded and uninvaded areas coupled with the importance of grass invasion in modeling these differences, suggest that invasive grasses are altering U.S. fire cycles at regional scales. As concern about U.S. wildfires continues to grow, accounting for the interaction of these widespread fire promoting invasive grasses with climate change and human ignition will be imperative for effectively managing wildfires.

3.2 Introduction

Non-native invasive grasses can promote fire, altering fire regimes to the detriment of native species. Altered fire regimes create favorable conditions for these invasive grasses, which recover and spread quickly post fire, resulting in a 'grass-fire cycle' (D'Antonio and Vitousek, 1992). Despite the ubiquity of invasive grasses identified as fire-prone (e.g. Beatley et al., 1966; Greenall, 1995; Lippincott, 2000; U.S. Department of Agriculture, 2018), alteration of fire regimes at the regional scale has been quantified for only a single species (*Bromus tectorum*; Knapp, 1998; Balch et al., 2013; Bradley et al., 2018). Given the increasing frequency of fires in the U.S. (Westerling et al., 2006; Balch et al., 2017), it is critical to identify the broad-scale effects of the grass-fire cycle.

Grass invasion adds novel fuels to ecosystems, altering fuel properties and promoting fire (D'Antonio and Vitousek, 1992; Brooks et al., 2004). For example, invasive grasses can increase rates of fire occurrence because they dry quickly, making them more receptive to ignition relative to other vegetation types (Kauffman and Uhl, 1990; D'Antonio and Vitousek, 1992; Brooks et al., 2004). Further, invasive grasses can support a microclimate more conducive to fire ignition (D'Antonio and Vitousek, 1992), suggesting that fire can occur in invaded systems even at times when the ambient climate may not be amenable to fire ignition. The presence of invasive grasses can increase fire size because they alter horizontal and vertical fuel continuity, resulting in increased fire spread and the potential for crown fires (D'Antonio and Vitousek, 1992; Brooks et al., 2004). Increased fuel loads from grass invasion can also lead to higher fire intensity (Brooks et al., 2004), and hotter fires have been documented in multiple grass species currently invading the U.S. (e.g. Lippincott, 2000; Platt and Gottshalk, 2001; McDonald and McPherson, 2013). Finally, invasive grasses can increase fire frequency because they recover quickly post fire, providing additional fuel sources, and potentially resulting in shortened fire

return intervals (e.g. Whisenant 1989; Lippincott 2000; Brooks et al., 2004; Coffman et al., 2010). These mechanisms by which invasive grasses promote fire are likely applicable across large spatial scales and ecosystems, suggesting that many invasive grass species could impact fire at regional scales.

In the U.S., non-native invasive grasses suspected of promoting fire are established in ecosystems across the country, including pine savannah in the southeast (Lippincott, 2000; Platt and Gottshalk, 2001), temperate deciduous forest in the mid-Atlantic (Flory et al., 2015), wetlands in the Great Lakes region (Gucker, 2008), deserts in the southwest (Brooks et al., 1999), and semi-arid shrublands in the Great Basin (Knapp 1998; Balch et al., 2013; Bradley et al., 2018; Figure 3.1). Invasive grass alteration of fire regimes is likely to negatively affect native species regardless of region, from ecosystems where fire is infrequent (e.g. sagebrush systems in the intermountain west; Whisenant, 1989), to those that are fire dependent (e.g. pine savannah in Florida; Lippincott, 2000) by increasing fire frequency to a point where native vegetation is unable to recover. For example, increased fire intensity associated with grass invasion has been demonstrated to adversely affect native plants which evolved with low intensity fires (McDonald and McPherson, 2013), and frequent fires can negatively impact native species ability to resprout (Fairman et al., 2019).

Non-native, invasive grasses are increasingly introduced and dispersed by humans across the U.S. (Reichard and White, 2001; Bradley et al., 2015). But, despite the prevalence of invasive grasses across U.S. ecoregions and the pronounced economic and ecological consequences of wildfires (Calkin et al., 2005; Bowman et al., 2009), the regional impacts of these grasses on fire regimes remains unknown. Here, we calculate differences in fire occurrence, fire size, and fire frequency on invaded vs uninvaded landscapes for twelve invasive grass species. We further model these fire regime parameters as a function of anthropogenic

and ecological variables to test the contribution of grass invasion on observed differences in fire regimes. This study is the first to document the widespread impacts of invasive grasses on regional fire regimes across U.S. ecosystems.

3.3 Methods

3.3.1 Invasive grass data

We used the Invasive Plant Atlas of the United States (Invasive Plant Atlas of the United States, 2018) to identify invasive grass species in the U.S. For each of these species, we conducted a literature search on web of science (search terms: TS=(Scientific name OR common name) AND TS=(fire) AND TS=(increase OR promote OR cycle)) and, if available, reviewed the species summary on the Fire Effects Information System (FEIS; U.S. Department of Agriculture, 2018) to determine if the species is thought to promote fire based on the scientific literature or expert knowledge (Table 3.1). For species with a reported or hypothesized association with fire, we compiled spatial occurrence data from 33 local, state, and national databases (Allen and Bradley, 2016; EDDMapS, 2018).

Non-native grass invasions at very low abundance are unlikely to influence fire regimes (Bradley et al., 2018) and invasive plant occurrence data tend to be skewed towards low abundance because they are often collected for the purpose of early detection and rapid response (Marvin et al., 2009; Cross et al., 2017). Therefore, we focused this analysis on occurrence data with associated abundance information, reported as either percent cover, stem count, or density. We excluded points with very low abundance reported as either <1% (percent cover), a single plant (stem count), or as trace/ rare (density). However, data with very low abundance as well as data lacking abundance information (presence only) were retained to inform the selection of pseudo-absence points (see below). For each species, we aggregated

points at 500 m pixel resolution, and identified pixels as 'invaded' for those with any reported abundant infestation, and 'present' for pixels containing only points with very low abundance or unknown abundance.

For each grass species, we determined a study region by identifying areas where each species was reported to have invaded, and by assessing ecoregions where the literature reported a fire effect. The majority of invaded pixels were typically within the geographic regions reported as fire prone in the literature with the exception of *Arundo donax*, which had the majority of invaded pixels in Texas but was identified as fire prone in southern California. Next, we used a convex hull polygon to identify each study area based on the invaded pixels that fell within U.S. EPA Level III Ecoregions (U.S. Environmental Protection Agency, 2013) that encompassed the geographic regions identified in the literature (Figure 3.1). Finally, we created a set of random 'pseudo-absence' points to represent the uninvaded landscape for each invasive grass species (Franklin, 2010). Pseudo-absence points, hereafter referred to as uninvaded points, were randomly located within the convex hull polygon study area, were not within 500 m of a presence or invaded pixel centroid and were less than 5 km from an invaded pixel centroid. By restricting pseudo-absence sampling to areas within 5 km of invaded pixels, we increase the likelihood that these uninvaded pixels encompass similar habitats and land use conditions as invaded pixels (VanDerWal et al., 2009).

3.3.2 Fire data

We used U.S. fire records from the Fire Program Analysis fire occurrence database (FPA fod; Short, 2017) and Monitoring Trends in Burn Severity (MTBS; Eidenshink et al., 2007) from 2000-2015 to assess relationships between grass and fire. The FPA fod is a spatial database of federal, state, and local wildfires, and excludes agricultural fires and prescribed burns (Short,

2017). The FPA fod records are point data and contain attributes such as fire year, final fire size, and in some cases, an identifier that links the record to the MTBS database. The MTBS database is a compilation U.S. fires that reached a final fire size of 404 ha in the west and 202 ha in the east, and includes a final perimeter of the fire event. For each point in the FPA fod database that could be linked to a fire in the MTBS database, the fire perimeter from the MTBS database was retained (1.18% of fire records, 88% of total burned area). For the remainder of fire events in the FPA fod database, we estimated fire perimeters as a circular buffer based on final fire size. The MTBS records provide the precise geography of the burned area extents, while the circular buffers are an approximation. The resulting yearly files were converted into 500 m rasters (Albers equal area conic projection to cover the extents of the contiguous U.S.) and a pixel was identified as burned if any part of the fire perimeter overlapped the pixel. Yearly files were combined over the study period to create three fire datasets: fire occurrence (whether or not a pixel burned), fire size (maximum fire size associated with each pixel), and fire frequency (how many times a pixel burned during the 16 year study period; Romme, 1980).

3.3.3 Modeling

In order to quantify the degree to which an abundant invasive grass alters fire regimes, we calculated the fire occurrence, fire size, and fire frequency associated with invaded vs. uninvaded pixels. To ensure that fire occurrence did not drive results for size and frequency, fire size was only compared for pixels that burned, and frequencies were only compared when at least 10% (and >20) of pixels burned more than once. We checked for significant differences in fire occurrence of invaded and uninvaded pixels using Pearson's chi-squared test, fire size using a Welch's T-test, and fire frequencies using a Mann Whitney U test.

For the grasses that showed a significant difference in fire occurrence, size, or frequency, we extracted additional ecological and anthropogenic covariates to test whether grass presence remained a significant predictor of the altered fire regime. Cases where grasses are significant predictors provide further evidence that the observed alteration in fire regime is due to the presence of the invasive grass rather than correlated ecological or anthropogenic conditions. Ecological covariates included the EPA Level III ecoregion associated with the pixel centroid, and the most common potential vegetation on each 500 m pixel (BPS_Veg; 140BPS; LANDFIRE, 2014b; Rollins, 2009). Anthropogenic covariates included euclidean distance to road (Tiger lines, 2016), and percent development per pixel (EVT_PHYS; 140EVT; LANDFIRE, 2014a; Rollins, 2009). We created a generalized linear model (GLM) for each grass species using the ecological, anthropogenic, and grass invasion (invaded vs uninvaded) variables as predictors of fire occurrence, size, or frequency using binomial, gamma, and poisson distributions, respectively (R version 3.3.2). Covariates were checked for correlation using the corvif function (Zuur et al., 2009) and we did not use any combination of variables with a correlation variation inflation factor >6. We used backward selection and selected the best model for each grass and fire characteristic (occurrence, size, frequency) using AIC. The models were checked for spatial autocorrelation using a semivariogram. Cases where invaded pixels were significantly different from uninvaded pixels as well as significant predictors of fire in the GLM were interpreted as evidence that the invasive grass influences the regional fire regime.

3.4 Results

Based on our literature review and the availability of abundant, invaded pixels, we identified 12 grass species that were suitable for analysis (Table 3.1). These grasses were located

in 29 U.S. Level III ecoregions (Figure 3.1), and numbers of invaded pixels ranged from 35 for *A. donax* to 9,388 for *B. tectorum* (median invaded pixels 344; Table 3.2).

Eight of the twelve grass species had a significantly higher proportion of fire occurrence on invaded pixels when compared to uninvaded pixels and increased by 27-230% (Figure 3.2A). Of these species, *S. barbatus* showed the highest rate of increase, with 5% of uninvaded pixels burning during the 2000-2015 time period vs. 16.5% of invaded pixels. There was no significant difference in fire occurrence for three species, and for *P. australis* fire occurrence was significantly lower on invaded pixels (Figure 3.2A). Pixels invaded by *I. cylindrica* and *M. sinensis* had significantly larger fire size, while pixels invaded by *B. tectorum, P. ciliare,* and *T. caput-medusae* had significantly smaller fire size (Figure 3.2B). Of the six species with sufficient data, fire frequency was significantly higher on invaded pixels of *B. tectorum*, *I. cylindrica*, *M. vimineum*, *N. reynaudiana*, *P. ciliare*, and *T. caput-medusae* (Figure 3.2C). For *N. reynaudiana*, average fire frequency more than doubled on invaded pixels (0.38 vs 0.87 fires/ 16 years/ pixel).

For the grasses with significant differences in fire regime between invaded and uninvaded pixels, we created GLMs to predict fire occurrence, fire size, and fire frequency as a function of environmental variables, anthropogenic variables, and grass invasion. Results of these models generally support that grass invasion increases fire. Of the nine GLMs created for fire occurrence, presence of invasive grass remained a significant predictor in all models with the exception of *P. australis*. The deviance explained for these models ranged from 2.3% for *M. vimineum* to 13.8% for *N. reynaudiana*. Similarly, grass presence remained a significant predictor in all six of the fire frequency models tested (Table 3.3). The total deviance explained in these models ranged from 3.9% in *M. vimineum* to 14.8% for *T. caput-medusae*. Grass presence was not an important predictor in any of the fire size models.

Table 3.1: Invasive grass species in the U.S. and reported impacts on fire regimes.

***Indicates a review of the species in the FEIS (U.S. Department of Agriculture, 2018)**

Scientific Name	Common Name	Impact on Fire Regime	Selected Supporting Literature
Arundo donax	giant reed	high flammability, high intensity, increased fuel load, increased fuel continuity	McWilliams, 2004*; Lambert et al., 2010; Coffman et al., 2010
Bromus rubens	red brome	increased fire frequency, increased fuel load, increased fire occurrence, persistent flammability, increased fire spread, low fire intensity	Brooks, 1999; Simonin, 2001*; Brooks and Matchett, 2006; Lambert et al., 2010
Bromus tectorum	cheat grass/ downy brome	increased fire frequency, increased horizontal fuel continuity, increased spread, increase fire frequency, contributor to large fires in the Great Basin	Whisenant, 1989; Brooks, 1999; Zouhar, 2003*; Balch et al., 2013; Bradley et al., 2018
Imperata cylindrica	cogon grass	increase fuel loads, increase horizontal continuity, increase vertical continuity, increased fine fuels, increased fire intensity	Lippincott, 2000; Platt and Gottschalk, 2001; Howard, 2005*
Microstegium vimineum	Japanese stiltgrass	potential to increase fine fuel load, increased flame height, easily ignitable, particularly a hazard after senescence and in dry climates	Dibble et al., 2007; Fryer, 2011*; Flory et al., 2015; Wagner and Fraterrigo 2015
Miscanthus sinensis	Chinese silvergrass	increased fuel load, high flammability, particularly a hazard after senescence and in dry climates	Waggy, 2011*; Jorgenson 2011
Neyraudia reynaudiana	silk reed, burma reed	increase fuel load, increase fine fuel, increase vertical continuity, increase fire spread, increased fire severity, increase fire frequency	Platt and Gottschalk, 2001; Stone, 2010*
Pennisetum ciliare	buffelgrass	increase fine fuel load, increased flame length, increase fire spread, increased fire intensity, increased fire frequency, creates consistent fire hazard	Hauser, 2008*; McDonald and McPhereson, 2013
Phragmites australis	common reed	highly flammable, increase fire spread, increase fuel loads	Marks et al., 1994; Gucker, 2008*
Schismus arabicus	Arabian schismus	increase fine fuel, increase continuity	Brooks, 1999; Lambert et al., 2010
Schismus barbatus	Common Mediterranean grass	increase fine fuel, increase continuity	Brooks, 1999; Lambert et al., 2010
Taeniatherum caput-medusae	medusahead	increased fire frequency, highly flammable, high volumes of long lasting dry litter, increased horizontal continuity	Torrell et al., 1961; Archer 2001*; Davies and Svejcar; 2008

Table 3.2: Available spatial data and affected ecoregions for each grass species. The extents of invaded points within affected Level III Ecoregions (U.S. Environmental Protection Agency, 2013) were used to define each study area.

Scientific Name	Location of Suspected Fire Impacts	Level III Ecoregion(s)	Number of Invaded Pixels
Arundo donax	southern California	California Coastal /Sage Chaparral and Oak Woodlands (11.1.1)	35
Bromus rubens	Mojave Desert, Sonoran Desert, California chapparral	Arizona/ New Mexico Mountains (13.1.1), Arizona/ New Mexico Plateau (10.1.7), Madrean Archipelago (12.1.1), Mojave Basin and Range (10.2.1), Sonoran Basin and Range (10.2.2)	286
Bromus tectorum	great basin, mojave	Central Basin and Range (10.1.5), Columbia Plateau (10.1.2), Mojave Basin and Range (10.2.1), Northern Basin and Range (10.1.3), Snake River Plain (10.1.8)	9,388
Imperata cylindrica	south eastern U.S.	Southern Coastal Plain (8.5.3), Southern Florida Coastal Plain (15.4.1)	2,761
Microstegium vimineum	eastern temperate forest	Blue Ridge (8.4.4), Central Applachains (8.4.2), Interior Plateau (8.3.3), Interior River Valleys and Hills (8.3.2), Northern Piedmont (8.3.1), Piedmont (8.3.4), Ridge and Valley (8.4.1), Southwestern Applachains (8.4.9), Western Allegheny Plateau (8.4.3)	1,856
Miscanthus sinensis	south eastern U.S.	Blue Ridge (8.4.4), Central Applachains (8.4.2), Northern Piedmont (8.3.1), Piedmont (8.3.4), Rige and Valley (8.4.1), Southeastern Plains (8.3.5), Western Allegheny Plateau (8.4.3)	86
Neyraudia reynaudiana	south Florida	Southern Florida Coastal Plain (15.4.1)	295
Pennisetum ciliare	Sonoran Desert, Arizona	Sonoran Basin and Range (10.2.2), Sonoran Desert (10.2.2)	2,402
Phragmites australis	upper midwest wetlands, Atlantic coast	Huron/Erie Lake Plains (8.2.2), North Cenral Hardwood Forests (8.1.4), Northern Lakes and Forests (5.2.1), Southern Michigan/Northern Indiana Drift Plains(8.1.6)	3,539
Schismus arabicus	California, Mojave Desert	Sonoran Basin and Range (10.2.2), Sonoran Desert (10.2.2)	229
Schismus barbatus	arid shrublands California, Mojave Desert	Sonoran Basin and Range (10.2.2), Sonoran Desert (10.2.2)	236
Taeniatherum caput-medusae	Great Basin, western US	Central Basin and Range (10.1.5), Northern Basin and Range (10.1.3), Sierra Nevada (6.2.12), Wasatch and Uinta Mountains (6.2.13)	393

Table 3.3: Generalized linear models (GLMs) show significant relationships between invaded areas and fire occurrence and frequency.

Grass	Fire Occurrence Model	Fire Size Model	Fire Frequency Model
B. tectorum	Invaded***, Road***, BPS***, Ecoregion***, Dev***	BPS^, Ecoregion***	Invaded***, Road^, BPS***, Ecoregion***, Dev***
Deviance Explained	7.1	12	9.3
I. cylindrica	Invaded**, Road***, BPS**, Ecoregion***	BPS***, Ecoregion***, Dev***	Invaded^, Road***, BPS**, Ecoregion***
Deviance Explained	5.9	21.3	7
M. sinensis	Invaded*, Road**	Ecoregion***	n/a
Deviance Explained	10	39.2	n/a
M. vimineum	Invaded*, Road**, Ecoregion***	n/a	Invaded*, Road***, Ecoregion***
Deviance Explained	2.3	n/a	3.9
N. reynaudiana	Invaded***, Dev***	n/a	Invaded***, BPS***
Deviance Explained	13.8	n/a	11.3
P. ciliare	Invaded***, Road***, BPS*, Ecoregion**, Dev**	Invaded, BPS, Ecoregion, Dev	Invaded***, Road***, Ecoregion***, Dev*
Deviance Explained	7.4[2]	17.6	10.8[1,2]
P. australis	Road**, BPS***, Ecoregion***, Dev^	n/a	n/a
Deviance Explained	9.8	n/a	n/a
S. barbatus	Invaded*, Road**, BPS*	n/a	n/a
Deviance Explained	11	n/a	n/a
T. caput-medusae	Invaded***, Ecoregion***, Dev	Ecoregion***, Dev**	Invaded***, Ecoregion***, Dev^
Deviance Explained	10.1	15.8	14.8

Key: Road- distance to road BPS- biophysical setting Ecoregion- Level III ecoregion Dev- percent development, Invaded- grass invaded pixel
^ p<0.1 *p<0.05 ** p<0.01 ***p<0.001

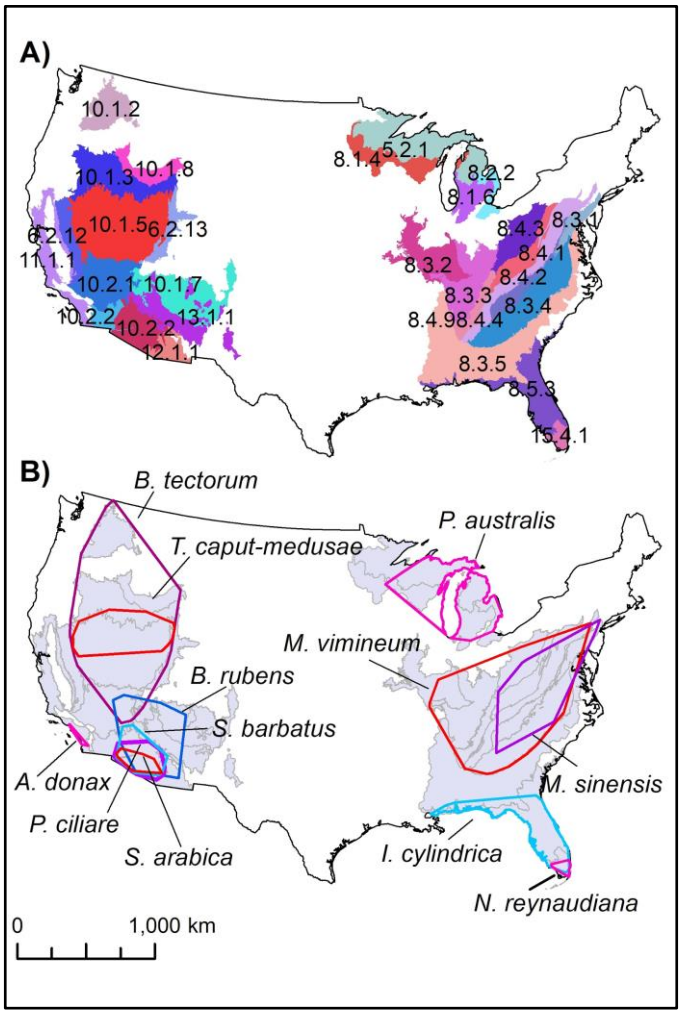

Figure 3.1: The grass species analyzed span U.S. ecoregions. A) Twenty-nine EPA level III ecoregions were included in the analysis. Ecoregion names are listed in Table 3.2. B) Study areas for the target invasive grass species based on convex hull polygons of invaded pixels located in fire-prone ecoregion(s). Both maps are displayed in U.S. Albers Equal Area Conic projection).

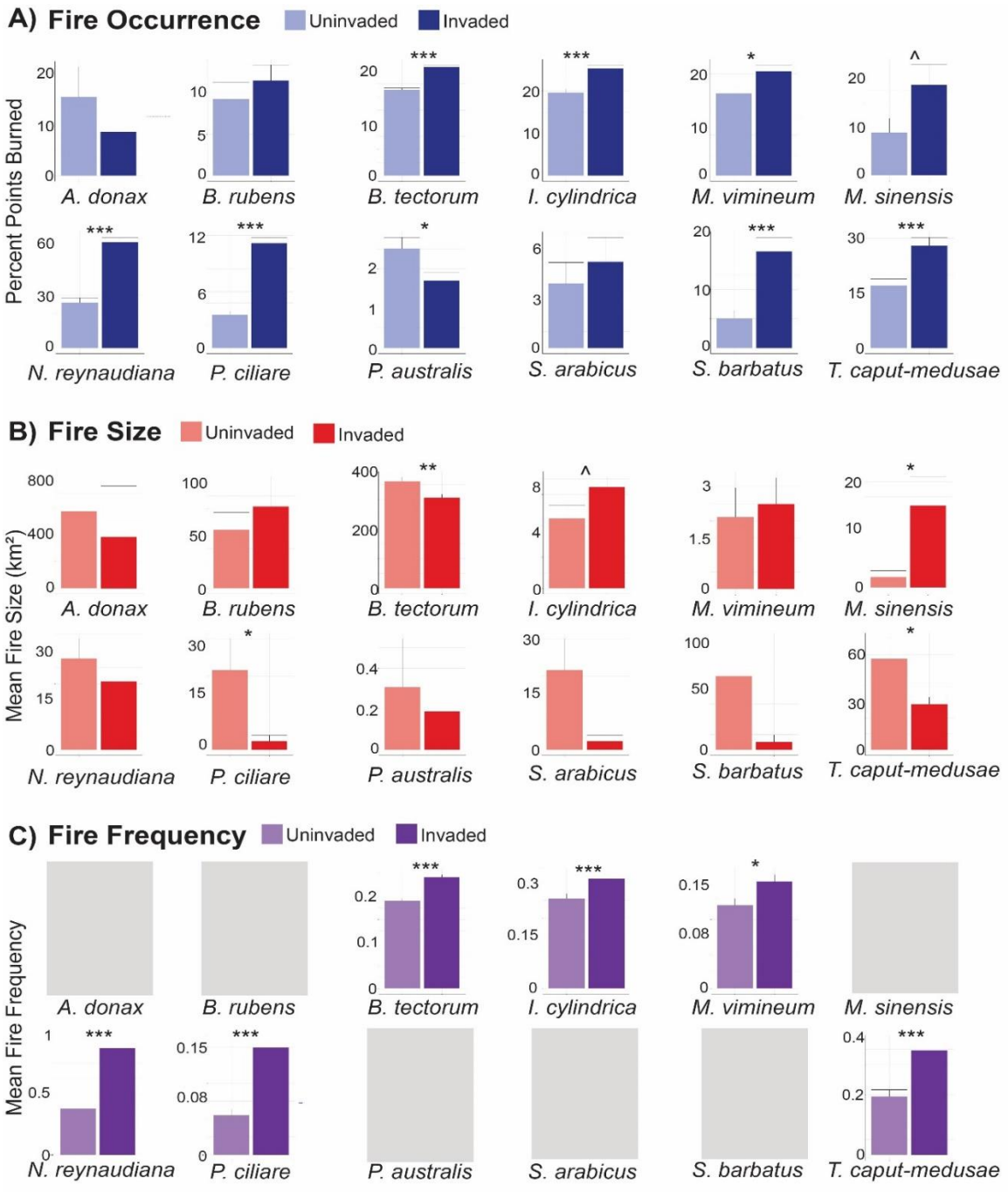

Figure 3.2: Invasive grasses are significantly related to changes in fire regimes. A) Of the twelve species tested, eight showed significant increases in fire occurrence, B) two showed a significant increase in mean fire size and C) six showed significant increases in fire frequency. Six species were not tested for changes in fire frequency because it was rare for invaded pixels to burn more than once. Significance: ***p<0.001, **p<0.01, *p<0.05, ^p<0.1.

3.5 Discussion

Humans undoubtedly influence fire regimes (Bowman et al., 2009; Bowman et al., 2011), increasing fire by providing ignition sources (e.g. Syphard et al., 2007; Fusco et al., 2016; Balch et al., 2017; Nagy et al., 2018), changing climate (e.g. Westerling et al., 2006; Westerling, 2016), and altering fuels sources through the introduction of non-native, invasive species (D'Antonio and Vitousek, 1992; Brooks et al., 2004; Balch et al., 2013). While there has been a focus on national and regional scale impacts of climate and human ignition on fire, this is the first analysis to quantify regional impacts of twelve invasive grasses on U.S. fire regimes. Our results are consistent with previous work that showed regional increases in fire occurrence for *B. tectorum* in the Great Basin region (Balch et al., 2013; Bradley et al., 2018). We also demonstrate significant alteration to regional fire regimes for seven additional species: *T. caput-medusae* in the Great Basin, *P. ciliare* and *S. barbatus* in the desert southwest, *M. vimineum* and *M. sinensis* in eastern temperate deciduous forests, and *I. cylindrica* and *N. reynaudiana* in southern pine savannah and pine rockland communities (Figure 3.1).

Climate change is expected to increase potential for fire occurrence by 150% by the end of the century based on projected changes in temperature and precipitation (Liu et al., 2010). Here we show that eight grass species have already increased rates of fire occurrence by 27-230% (Figure 3.2A), and six grass species increased mean fire frequency by 24-150% (Figure 3.2C), compounding the likelihood of increased fire risk across the U.S. The observed increases in fire occurrence and frequency were present for grasses across the U.S., suggesting that the introduction of fine flammable fuels, as well as the quick recovery of invasive grasses, could exacerbate increased fire potential from climate change.

Grass invasion was an important predictor of increased fire occurrence and frequency for eight and six invasive grass species, respectively (Table 3.3). This is not surprising given that

all species tested were suspected of increasing fine fuel loads (Table 3.1). Only invaded pixels of *P. australis* had significantly lower rates of fire occurrence when compared to uninvaded pixels (Figure 3.2A), but *P. australis* invasion was no longer significant when anthropogenic variables were included in the model, suggesting that other covariates explain this pattern (Table 3.3).

Interestingly, both invasive grass presence and anthropogenic predictors (distance to road or percent development) were significant in the majority of fire occurrence and frequency models (Table 3.3). In the U.S., human ignitions account for 84% of wildfires (400% more than lightning fires; Balch et al., 2017), and invasive grasses are strongly associated with anthropogenic activity (Reichard and White, 2001). Our results highlight the importance of both anthropogenic activity and invasive grasses on the grass-fire cycle, and it is likely that humans are adding both the ignition sources and highly flammable fuels that drive the fires closest to us.

While the majority of grasses tested showed regional impacts on fire occurrence and frequency, we found little evidence for regional impacts on fire size (Figure 3.2B). Our modeling results suggest that for the few species that demonstrated differences in fire size, these differences are a result of ecological and anthropogenic variables. For example, the significance of development in predicting fire size for *I. cylindrica* and *B. tectorum* (Table 3.3) could be because fire suppression near developed areas supersedes the importance of increased fuel continuity to reduce fire size in invaded landscapes. This suggests that while grass invasion may promote fire spread and size at the event level (e.g. Coffman et al., 2010), the multitude of small fires ignited and suppressed in human dominated areas make it challenging to identify a regional link between fire size and grass invasion.

Wildfires are costly to both ecosystems and economies (Calkin et al., 2005; Bowman et al., 2009), and climate change and human ignition sources have contributed to a regional scale increase in U.S. wildfires (Westerling et al., 2006; Flannigan et al., 2009; Balch et al., 2017; Nagy

et al., 2018). Here we show that a third global change, fuel alteration from the introduction of non-native, invasive grasses, also increases fire at regional scales. As invasive species success increases (Dukes and Mooney, 1999; Diez et al., 2012), the interaction of these three global changes will continue to promote wildfires across the U.S.

CHAPTER 4

ACCOUNTING FOR ABOVEGROUND CARBON STORAGE IN SHRUBLAND AND WOODLAND ECOSYSTEMS INCREASES TOTAL CARBON ESTIMATES IN THE GREAT BASIN REGION

4.1 Abstract

Improving the accuracy of carbon accounting in terrestrial ecosystems is critical for understanding carbon fluxes associated with land cover change, with significant implications for global carbon cycling and climate change. Semi-arid ecosystems account for an estimated 45% of global terrestrial ecosystem area and are experiencing high degrees of degradation. However, aboveground carbon accounting has largely focused on tropical and forested ecosystems, while drylands have been relatively neglected. Here, we used a combination of field estimates, remotely sensed data, and existing land cover maps to create a spatially explicit estimate of aboveground carbon storage within the Great Basin, a semi-arid region of the western U.S. encompassing 643,500 km^2 of shrubland and woodland vegetation. We classified the region into seven distinct land cover categories: pinyon-juniper woodland, sagebrush steppe, salt desert shrub, low sagebrush, forest, non-forest, and other/excluded, each with an associated carbon estimate. Aboveground carbon estimates for pinyon-juniper woodland were continuous values based on tree canopy cover. Carbon estimates for other land cover categories were based on a mean value for the land cover type. The Great Basin ecosystems contain an estimated 296.9 Tg in aboveground carbon, which is almost double previous estimates that only accounted for forested ecosystems in the same area. Aboveground carbon was disproportionately stored in pinyon-juniper woodland (43.5% carbon, 16.9% land area), while the shrubland systems accounted for roughly half of the total land area (49.1%) and one third of the total carbon. Our results emphasize the importance of distinguishing and accounting for the distinctive

contributions of shrubland and woodland ecosystems when creating carbon storage estimates for dryland regions.

4.2 Introduction

Quantifying aboveground carbon stored in ecosystems is a critical component of understanding overall carbon storage and measuring carbon fluxes associated with land cover change (Houghton, 2007). While dryland ecosystems make up more than 45% of land area globally (Lal, 2004), aboveground carbon mapping has tended to focus on tropical and forested ecosystems (e.g., Baccini et al., 2008; Saatchi et al., 2011; Cartus et al., 2014) because their high productivity disproportionally contributes to carbon storage. However, the amount of aboveground carbon stored on a landscape is not constant, and semi-arid ecosystems have recently gained increased attention in global carbon cycling because of their role in driving the inter-annual variability in terrestrial carbon storage (e.g., Poulter et al., 2014; Ahlström et al., 2015; Haverd et al., 2017). In North America, semi-arid systems account for roughly 17% of the total land area (Lal, 2004), but the amount of carbon stored in these woodland and shrubland ecosystems has not previously been quantified.

The Great Basin is a semi-arid region of western North America with ecosystems ranging from sparsely vegetated salt desert shrubland (*Atriplex* spp.) to sagebrush steppe (*Artemisia* spp.) and pinyon-juniper woodlands (*Pinus* spp., *Juniperus* spp.). Dominant vegetation shifts with resource availability across elevational gradients (Blaisdell and Holmgren, 1984; Miller et al., 2008; Chambers et al., 2014), and ecosystems in the Great Basin are highly productive relative to other semi-arid systems (Brooks and Chambers, 2011). In particular, pinyon-juniper woodlands have the potential to contribute a significant amount of aboveground carbon storage (Huang et al., 2009); however, carbon storage in woodlands is directly related to tree cover and

can be highly variable in these ecosystems, even over short distances (Rau et al., 2012). To date, most carbon accounting in these woodland and shrubland systems has focused on calculating aboveground biomass and carbon at the organismal or plot scale (e.g. Rickard, 1985; Rau et al., 2010). While mapping carbon storage in pinyon-juniper woodlands using remote sensing rather than field population estimates can provide the combined benefits of high spatial detail and regional scale estimates (Chojnacky et al., 2012), most remote sensing-based studies of carbon in the Great Basin have focused on estimating expansion rates of pinyon-juniper woodlands over relatively small areas (Sankey and Germino, 2008; Strand et al., 2008; Huang et al., 2009). As a result, regional estimates of aboveground carbon are lacking. Understanding current carbon storage is critical because of the numerous large-scale threats to these ecosystems, including invasive species (Bradley et al., 2006), wildfire (Balch et al., 2013), woody plant encroachment (Miller et al., 2008), and land use/land cover change (Bradley, 2010). Creating a spatially explicit baseline estimate of aboveground carbon storage in this region is critical for future carbon management.

Methods used to develop large scale carbon maps include assigning fixed carbon values based on land cover designations (termed “stratify and multiply”; Goetz et al., 2009). A stratify and multiply approach is more appropriate in cases where canopy cover estimates and/or relationships between canopy cover and aboveground carbon are unknown. In forested systems, satellite observations can more reliably estimate continuous canopy cover, which can be related to aboveground carbon storage using field measurements (termed “direct remote sensing”; Goetz et al., 2009). Direct remote sensing has been employed globally to create carbon estimates for tropical and forested regions (e.g. Baccini et al., 2008; Saatchi et al., 2011; Cartus et al., 2014).

In the U.S., the National Carbon and Biomass Database leveraged ground based data from the USDA Forest Service Forest Inventory and Analysis (FIA) and remote sensing data from the Shuttle Radar Topography Mission (SRTM) and Landsat reflectance to create a continuous estimate of aboveground biomass and carbon at 30 m resolution (Kellndorfer et al., 2013). However, this database estimates carbon in forests (Kellndorfer et al., 2013), and it is currently unknown whether the model is effective for estimating carbon in semi-arid systems like those in the Great Basin region, which often has tree cover lower than the 10%-25% necessary to be considered for forest carbon monitoring.

While the majority of carbon mapping in the U.S. focuses on forested systems, one study (Huang et al., 2009) quantified carbon storage in pinyon-juniper woodlands in the Colorado Plateau. Huang et al. (2009) leveraged field based measurements, and remote sensing images (hyperspectral AVIRIS and multispectral Landsat), to calculate pinyon-juniper canopy cover and aboveground carbon over a 30,000 km2 area (Huang et al., 2009). While this remains the most extensive, spatially explicit estimate of aboveground carbon to date in pinyon-juniper woodlands, it encompasses only a quarter of the Colorado Plateau and none of the Great Basin. Aerial photography (Strand et al., 2008) and Landsat imagery (Campbell et al., 2012) have also been used to map carbon in western juniper woodlands in the Pacific Northwest. There is potential to apply these remote sensing approaches for mapping carbon in the pinyon-juniper woodlands which cover more than 15% of the Great Basin.

A comprehensive understanding of carbon stocks globally must include dryland regions like the Great Basin, which will require different methods than those used for temperate and tropical forests. Here, we leverage field based carbon measurements, remotely sensed canopy cover estimates, and an existing land cover database to create the first spatially explicit estimates of aboveground carbon stored in the Great Basin.

4.3 Methods

4.3.1 Study region

Our study area encompasses the Great Basin region of the western U.S. The spatial extents of this region were defined using a combination of the EPA ecoregions (U.S. Environmental Protection Agency) and LandFire existing vegetation type (LANDFIRE.US_140EVT, Rollins, 2009; LANDFIRE 2014a). First, we selected EPA Level III ecoregions that are present within the Great Basin: Blue Mountains, Central Basin and Range, Columbia Plateau, Eastern Cascades Slopes and Foothills, Northern Basin and Range, and Snake River Plain. Within these Level III ecoregions, we removed Level IV subregions that had a primary designation in LandFire EVT of forest, thereby focusing our analysis on subregions containing woodland and shrubland. The resulting study region spans six western US states and encompasses 643,500 km2 of semi-arid ecosystems.

4.3.2 Land cover classification

Aboveground carbon is expected to vary considerably with land cover class across the Great Basin. In order to assess carbon, we created a spatially explicit 30 m land cover dataset for the study region. We classified the Great Basin into seven land cover categories: pinyon-juniper woodland, three shrubland categories (low sagebrush, salt desert scrub, and sagebrush steppe), forest/woodland, non-forest, and other/excluded based on their dominant plant functional groups and their possible aboveground carbon contributions. For example, pinyon-juniper is distinct relative to the other vegetation categories because it is the only woodland system. Woodland systems may contain large amounts of aboveground carbon but their contribution to carbon storage is dependent on tree cover which can be highly variable over short distances.

The three shrubland categories were based on the dominant species assemblages which are often determined by soil factors such as salinity, pH, and depth. These three shrub communities can have considerable variation in biomass and carbon storage depending on the localized growing conditions. For example, salt desert scrub communities are typically found on alluvial features adjacent to and in low lying areas with poor drainage where soils are saline such as playas and salt flats. The communities are typically dominated by *Atriplex* spp. or *Sarcobatus* spp. and the vegetation density and biomass can vary considerably (Tueller, 1989). Low sagebrush communities are typically found on shallow, rocky, and alkaline soils that are typically too dry to support big sagebrush (McArthur and Taylor, 2004). Low sagebrush communities tend to be lower in stature than big sagebrush but can vary significantly in density and biomass as well.

Land cover classifications were based on Falkowski et al. (2017a), who identified pinyon-juniper using object-based identification of tree crowns from aerial photos, and the LandFire Existing Vegetation Type 140 (LANDFIRE.US_140EVT, Rollins 2009; LANDFIRE 2014). LandFire EVT is a U.S. national scale land cover product that includes current vegetation information at 30 m resolution and is created using a decision tree approach based on satellite-derived predictors (Rollins, 2009).

Pixels were classified as pinyon-juniper if they had >0% cover as designated by Falkowski et al. 2017a, or were designated as ‘pinyon-juniper woodlands’ or ‘juniper woodland and savannah in the LandFire EVT group (GP_N, LANDFIRE, 2014a, Rollins 2009; Figure 4.1). Remaining pixels were classified using LandFire EVT groups (GP_N). EVT group designation is based on the National Vegetation Classification system which considers dominant and co-dominant plant species, the plant species growth forms, and regional ecology and biogeography to make a general land cover classification (Federal Geographic Data Committee, 2008). We

combined shrubland EVT groups into salt desert shrubland, low sagebrush, and sagebrush steppe. These shrub classifications represent a potential gradient of aboveground biomass and carbon. While the shrubland categories intuitively include vegetation groups named for the shrubs present in them, the sagebrush steppe classification also included pixels with a "grassland" designation. Here, "grassland" typically included some shrub vegetation (GAP-USGS, 2016) and comprised only 1.9% of the study area. We excluded many remaining pixels with categories of low carbon consequence (primarily agriculture, introduced grass, barren, developed, and water). The few remaining pixels were classified using the LandFire EVT life form (LF) and group name designations such that pixels designated as tree or had a group name (GP_N) of chaparral were placed into the forest/woodland category, while the remaining pixels designated as shrub or herb were classified as non-forest (Figure 4.1). Chaparral was grouped with the woodland category because of the *Ceanothus* spp. tendency to store large amounts of carbon (Gray, 1982) and grow to a treelike form (GAP-USGS 2016). For all land cover classifications except pinyon-juniper, we used a fixed estimate of carbon associated with that land cover type ('stratify and multiply', sensu Goetz et al., 2009; described below in Carbon estimation for other land cover).

4.3.3 Pinyon-juniper percent cover product and validation

Because the Great Basin has little forested area, pinyon-juniper woodlands likely account for the largest portion of aboveground carbon. However, canopy cover of pinyon-juniper varies considerably across the region. Thus, a robust estimate of carbon storage in pinyon-juniper woodland should depend on canopy cover (Rau et al., 2012). Falkowski et al. (2017a) mapped tree canopy cover for the greater sage grouse (*Centrocercus urophasianus*) range, which covers much of the Great Basin. This map of tree canopy cover was based on

identification of individual crowns by applying spatial wavelet analysis to aerial imagery acquired by the National Agriculture Imagery Program (NAIP) between 2011-2013. We aggregated the 1 m presence/absence maps of tree crowns into percent cover estimates at a 30 m resolution, retaining the native UTM projection of the tiled canopy cover maps.

To validate the 30 m resolution data, we used a linear regression to compare pinyon-juniper canopy cover estimates from 265 Sagebrush Steppe Treatment Evaluation Project (SageSTEP) plots (McIver et al., 2014) to the NAIP-based models of canopy cover (Falkowski et al., 2017a). The 265 SageSTEP plots within the modeled canopy cover area were distributed across 14 sites in 5 states and were surveyed in 2006-2008 within a 30 x 33 m square. Field plot corners were georeferenced using a Trimble Juno™ GPS unit with spatial accuracy > 4m (Trimble Inc., Sunnyvale, CA). Crown cover for individual trees in each plot was measured as the longest crown diameter and the diameter perpendicular to the longest crown. Canopy cover at each plot was then calculated based on an ellipsoid with these two dimensions fit to each tree. We retained only the untreated SageSTEP control plots for our comparison to modeled canopy cover, thus cover should not have changed substantively between the time of the survey and the aerial image collection. Although the precise center of the plots does not necessarily align with the mapped pixel, previous comparisons of FIA plots to forest cover data suggest that these small offsets do not affect the overall comparison (Zald et al., 2014).

For areas outside the extent of the pinyon-juniper product generated by Falkowski et al., 2017a (56% of the study area), but designated as pinyon-juniper by LandFire, we developed a canopy cover estimate based on Falkowski et al. 2017b. A stratified random sample of pixels were obtained from the Falkowski et al. 2017a canopy cover map, and predicted tree crown/presence absence was visually assessed against NAIP imagery for these samples. Samples with an accurate representation of the tree canopy were then used to train a random forest

model of canopy cover based on contemporaneous Landsat imagery and topographic indices. Landsat 5, 7, and 8 images from the Tier 1 spectral reflectance product were masked for clouds, cloud shadow, and snow using the provided quality assurance band, which is based on the CFmask algorithm (Foga et al., 2017). Spectral reflectance of the original bands and seasonal medians of Normalized Difference Vegetation Index (NDVI), Normalized Difference Moisture Index (NDMI), Normalized Burn Ratio (NBR) were included as predictors in the random forest model. This model also included topographic predictors derived from the National Elevation Dataset including elevation, slope, and the sine and cosine of aspect. We then predicted pinyon-juniper canopy cover for 2014 Landsat imagery using the random forest model. We used the resulting estimates of canopy cover to calculate aboveground biomass of pinyon-juniper woodlands that were outside of the extents of the high-resolution maps created by Falkowski et al. 2017a.

Any pixel that had >0% pinyon-juniper cover in the Falkowski et al. 2017a product was designated as pinyon-juniper regardless of that LandFire classification in that pixel. Pixels that were designated as pinyon-juniper in LandFire EVT but were not designated as pinyon-juniper by Falkowski et al. (2017a or 2017b) were classified as pinyon-juniper with a percent cover estimate of 0.

4.3.4 Carbon estimation for pinyon-juniper

Total aboveground carbon as a function of tree canopy cover was derived using data from 480 (0.10 ha) field plots measured as part of the Sagebrush Steppe Treatment Evaluation Project (SageSTEP; McIver et al., 2014). Components in the estimate of aboveground carbon included tree biomass, tree litter, shrub biomass, standing herbaceous biomass, down woody debris, and shrub/herbaceous litter. Individual tree carbon was estimated based on crown area

using allometric equations derived from destructively harvesting trees from various size classes (see Tausch, 2009; Rau et al., 2012 for detailed methods). Individual tree estimates were summed to estimate tree carbon at the plot level.

Tree litter carbon was estimated by placing three 0.25 x 0.25 m sampling frames under 6 representative trees in each plot. Sampling frames were placed adjacent to the tree stem, halfway between the stem and the canopy edge, and at the canopy edge. All material inside the frame was cut using a handsaw, collected, dried, and weighed. The carbon content of tree litter was estimated by grinding sub-samples of the dry litter and analyzing for %C via combustion analyzer (Rau et al., 2010; 2012). The total mass of tree litter carbon per plot was estimated by calculating the mass of tree litter carbon per unit area collected and then extrapolating to the total area of litter mat within each plot based on known relationships between tree crown area and litter mat area (Rau et al., 2010; 2012).

Shrub biomass was estimated by measuring the total height, longest crown diameter, and diameter perpendicular to the longest diameter of each shrub intersecting a 2 m wide belt along the 5, 15, and 25 m transects, and then applying species specific allometric equations derived by destructively harvesting shrubs of variable size classes within each species (Reiner et al., 2010). Carbon content of shrubs was estimated by collecting stem, branch, and foliage samples from representative species and obtaining estimates of %C by combustion analyzer (Rau et al., 2010; 2012).

Herbaceous biomass, litter biomass and carbon were estimated in eight total 0.25 x 0.25 m quadrats along two 33 m transects within each plot. Standing herbaceous biomass was clipped at ground level, collected, dried, weighed, and subsamples were analyzed for %C (Rau et al., 2010; 2012). Herbaceous and shrub litter were also collected, dried, weighed, and subsamples were analyzed for %C (Rau et al., 2010; 2012). Down Woody Debris (DWD) biomass

and C were estimated using the planar intercept method on the 5, 15, and 25 m transects, where all woody debris > 0.635cm was inventoried where it intersected each transect (Brown 1974); representative DWD subsamples were analyzed for %C via combustion analyzer (Rau et al., 2010; 2012).

The sum of aboveground carbon per plot was estimated as the sum of Tree C + Shrub C + Standing Herbaceous C + Down Woody Debris C + Tree, Shrub, and Herbaceous Litter C. The mass of total aboveground carbon per plot was then regressed against tree canopy cover using SAS 9.4™ PROC REG (SAS Institute 2009). The best fit model (polynomial) was chosen using adjusted r-squared and AIC.

4.3.5 Carbon estimation in three shrubland landcover types

Total aboveground for each of the three shrubland categories we created a static carbon estimate and applied a stratify and multiply approach to map aboveground carbon (Goetz et al., 2009). These estimates were calculated using data from 455 (0.10 ha) field plots measured as part of the SageSTEP Project (McIver et al., 2014). The vast majority (430) of these plots were categorized as sagebrush steppe (Figure 4.1). These plots all contained basin big sagebrush (*Artemisia tridentata*) or Wyoming sagebrush (*Artemisia tridentata* ssp. *wyomingensis*), but also commonly contained a mix of low sagebrush (*Artemisia arbuscula*), and salt desert scrub (*Atriplex* spp.; *Sarcobatus* spp.). In order to quantify unique communities of low sagebrush and salt desert shrub, we measured 25 supplemental plots (10 low sagebrush, 10 greasewood, 5 saltbrush) adjacent or near the primary SageSTEP plots. All plots were of identical dimensions to the woodland plots described above (30 x 33 m), and all carbon measurements were identical with the exclusion of those associated with trees. The sum of aboveground carbon per plot was estimated as the sum of Shrub C + Standing Herbaceous C + Down Woody Debris C + Shrub and

Herbaceous Litter C. For each unique shrub type the mean aboveground C and standard error were calculated. The mean and standard error were used to create low, medium, and high carbon estimates for each of the three shrubland categories.

4.3.6 Carbon estimation for forest, non-forest, and other

For the other forest/woodland land cover types, we created static estimates using aboveground biomass data from Hudak et al., 2016. These data were created using a two step approach. First, a random forest regression model was created using forest inventory data and co-located lidar measurements to calibrate lidar estimates of aboveground biomass. Second, topography, climate, and Landsat derived spectral indices were used as training data in a second random forest model to predict the lidar-derived aboveground biomass estimates. This model was used to map aboveground biomass in forested land across the Pacific Northwest. Because these data do not cover our entire study area, we created 185 random points in forest land cover within overlapping areas and extracted biomass (Hudak et al., 2016) and land cover (LANDFIRE.US_140EVT GP_N, Rollins, 2009; LANDFIRE, 2014a). We used these values to calculate the average aboveground biomass associated with each LandFire vegetation classification. Because data from Hudak et al., 2016 only encompasses the northern half of our study region, we standardized these values based on the percent total area of each LandFire vegetation group for the entire study region. These estimates refer to total aboveground biomass, so we divided them by 2 to convert them to aboveground carbon (Biomass is roughly 48-50% Carbon). This general conversion is common when converting biomass to carbon (e.g. Saatchi et al., 2011; Kellndorfer et al., 2013). Lastly, pixels that were designated as non-forest or other/excluded were assigned a carbon value of 0.

4.3.7 Comparison to the National Biomass and Carbon Dataset

We compared our results to the National Biomass and Carbon Dataset Version 2 (NBCD; Kellndorfer et al., 2013) which is a national scale, 30 m resolution dataset of aboveground biomass for the U.S. We downloaded the tiles that make up the Great Basin region and mosaicked them using the maximum value in places where these tiles may overlap. We randomly selected 5,000 points within our study area and extracted our carbon values and the NBCD biomass values, which we divided by 2 to estimate carbon. We also extracted our classification of land cover for each point. Because both our carbon estimates and the NBCD carbon estimates on pinyon-juniper are continuous values, we created a linear model using just the randomly selected points associated with the pinyon-juniper land cover type (n=855). For the remaining categories with static carbon estimates, we created boxplots of the NBCD carbon data for each land cover type to compare our estimates.

4.4 Results

4.4.1 Land cover classifications in the Great Basin

We classified seven types of land cover in the Great Basin (Figure 4.1). Of the land cover categories of interest for carbon accounting, sagebrush steppe was the most extensive, making up roughly 27% of our study area, followed by pinyon-juniper woodland (17%), salt desert scrub (12%) and low sagebrush (10%). The other forest and other non-forest categories made up 1.2% and 0.4%, respectively. Roughly one third (~32%) of the Great Basin was excluded from carbon accounting because it was classified as agricultural, introduced grass, barren, developed, or water, which should account for very little aboveground carbon (Figure 4.2).

4.4.2 Validation of the pinyon-juniper percent cover product

Overall, the modeled canopy cover product values ranged from 0-92% cover (mean=15.3%). The 265 SageSTEP control plots encompass a large range of cover from 0-75.7% (mean±SE=14.9± 1.1) and are distributed across the study region. Based on the linear regression comparison to the 30 m tree cover estimates derived from Falkowski et al. (2017a), modeled pinyon-juniper cover from aerial photographs shows a reasonably strong correlation with field-based measurements (R^2 = 0.62; Figure 4.3).

There were 23 data points with a pinyon-juniper cover discrepancy of greater than 20%. SageSTEP field estimates were higher in 17 of these plots (SageSTEP mean±SE= 54.9±2.4; Canopy cover model mean±SE= 22.7±1.2), suggesting that the mapped data may have a tendency to underestimate total pinyon-juniper in areas of high cover. Visual inspection of the 17 underestimated SageSTEP plots in conjunction with the original 1 m resolution data and NAIP imagery also suggest that some tree canopies were omitted in the modeled canopy estimates. The SageSTEP plots that recorded less than 2% cover difference tended to be in areas of relatively low pinyon-juniper cover (n= 139, mean±SE= 3.54±0.74), suggesting that our cover estimates are most accurate in areas of low cover.

4.4.3 Carbon estimates for land cover classes

Based on the SageSTEP field measurements of canopy cover and aboveground biomass C, we calculated the an equation for total aboveground carbon in pixels designated as pinyon-juniper. The equation has high explanatory power and shows a strong positive relationship between percent canopy cover and total aboveground carbon (n=1148, r2=.94, p<0.001; Figure 4.4). Although the equation has a polynomial form, the linear coefficient determines the bulk of

the relationship. The non-zero intercept value of 3,153 kg/ha represents carbon associated with shrubs and herbaceous biomass growing within woodland communities where pinyon-juniper canopy cover is very low or absent.

Mean estimates of total aboveground carbon for the three shrubland categories ranged from 3,056 kg/ha in salt desert scrub to 3,778 kg/ha in low sagebrush, with estimates much more robust in the well-sampled sagebrush steppe. Estimated values for total aboveground carbon for the other forest was 28,122 kg/ha based on aboveground biomass data from Hudak et al. 2017 (Table 4.1). The other non-forest category was assigned a value of 0 kg/ha.

4.4.4 Total Great Basin carbon estimates

Based on our models, we estimated that there was a total of 296.9 Tg of aboveground carbon in the Great Basin when using mean carbon estimates for the three shrubland categories (Table 4.2, Figure 4.5). While the pinyon-juniper land cover type comprises only 16.9% of the Great Basin by total area, it accounted for 43.5% of the total aboveground carbon (Table 4.2). When the three shrubland categories were combined, they account for roughly half of the total land area (49.1%) and contribute 34.2% of the total aboveground carbon estimated for the study area.

4.4.5 Comparison to the National Biomass and Carbon Dataset

The relationship between our estimates of carbon in pinyon-juniper land cover vs. the NBCD data was significant, but weak ($R^2=0.14$, $n=855$; Figure 4.6). While carbon was positively correlated between our estimates and the NBCD (pearson's $r= 0.38$, $n=855$, $p<0.001$) the NBCD dataset estimated zero carbon in 20% of the pixels containing pinyon-juniper woodland. For the

land cover classes that had fixed, rather than continuous, carbon estimates, our carbon estimate was higher in all cases with the exception of the "non-forest' and "other" classifications (Figure 4.7). Total carbon in the Great Basin based on NBCD estimates is 161 Tg, which accounts for only 54.2% of the total carbon in our modeled estimates.

Table 4.1: Carbon per pixel calculated for each land cover type. pinyon-juniper is calculated as a function of canopy cover per pixel (x). The three shrubland categories (low sagebrush, salt desert, and sagebrush steppe) have a mean carbon estimate followed by a low and high estimate based on the standard error.

Land cover Type	Total kg Carbon/ ha
Pinyon-juniper	$1.5x^2 + 564.4x + 3153$
Forest	28122
Sagebrush Steppe	3067 (3011-3122)
Low Sagebrush	3778 (2778-4789)
Salt Desert Scrub	3056 (2500-3622)
Non-Forest	0
Excluded	0

Table 4.2: Total area and teragrams (Tg) of carbon by land cover type using mean estimates for the shrubland categories.

Land cover Type	Total area (%)	Total Carbon (Tg)
Pinyon-Juniper	16.9	129.1
Forest	1.2	66.5
Sagebrush Steppe	27.9	55.0
Low Sagebrush	9.5	23.2
Salt Desert Shrub	11.7	23.1
Non-Forest	0.4	0
Excluded	32.4	0
Total	100	296.9

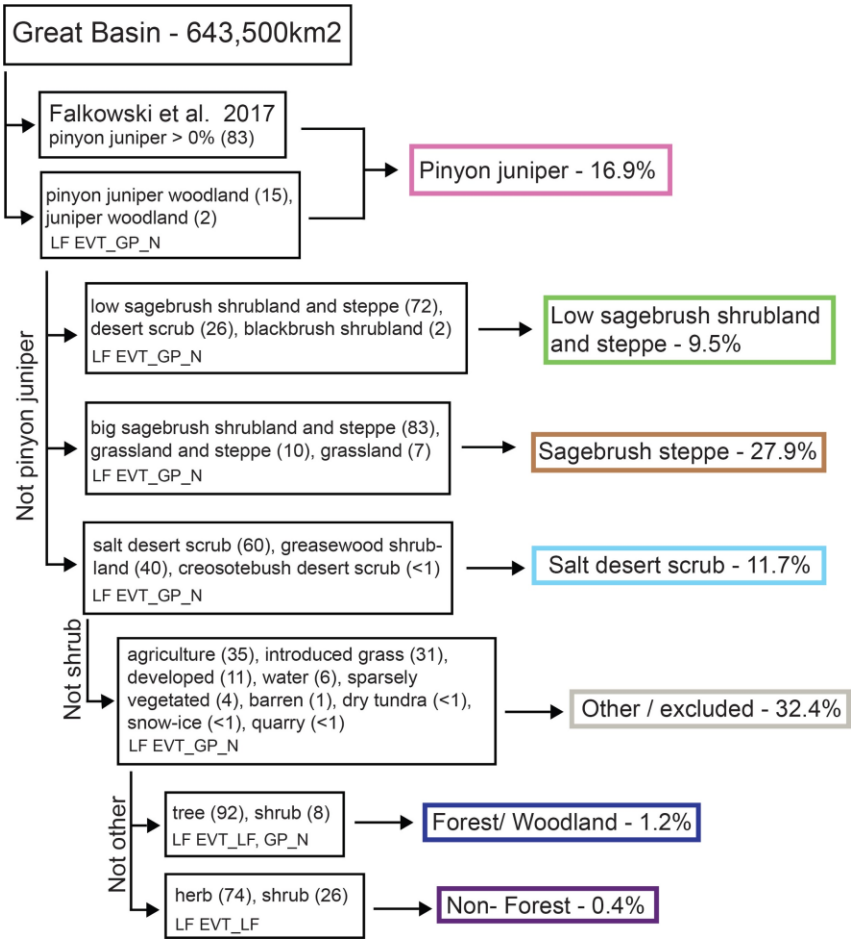

Figure 4.1: Schematic of land cover classification. All pinyon-juniper pixels were classified first. The remaining pixels were reclassified based on their LandFire EVT vegetation group (LF EVT_GP_N) classifications. Non-woodland, non-shrubland pixels were classified based the dominant life form (LF EVT_LF) of that pixel. The vegetation groups within each final classification are listed in order of prevalence within the group, with the percent total in parentheses.

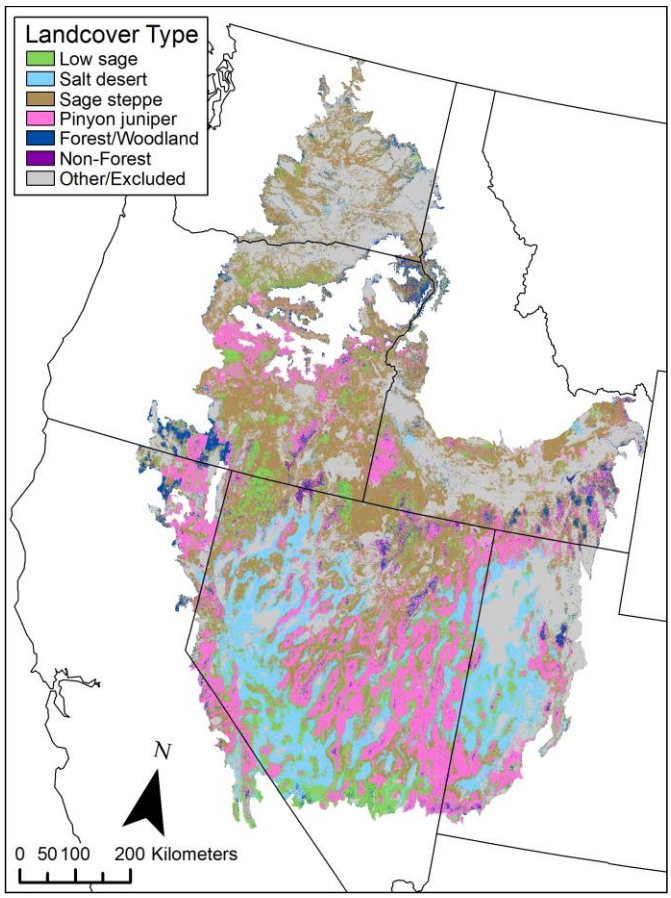

Figure 4.2: Land cover classification for the Great Basin based on a combination of woodland cover from Falkowski et al. 2017a,b and other land cover from LandFire (Rollins, 2009; LANDFIRE, 2014a).

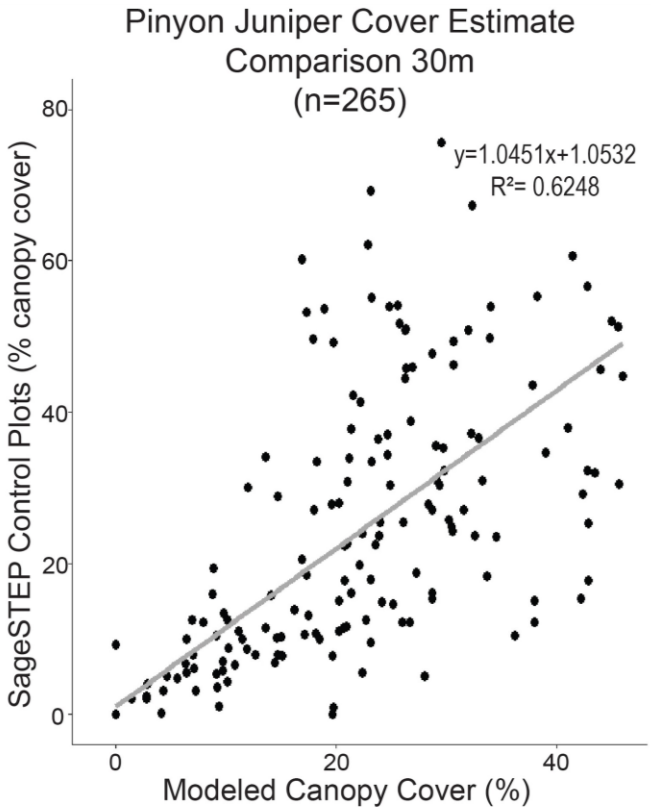

Figure 4.3: Modeled pinyon-juniper canopy cover showed a strong, positive relationship (R2 = 0.62) with SageSTEP field measurements of pinyon-juniper percent cover. Canopy cover estimates were aggregated to a 30 m pixel size, which corresponds to the SageSTEP plot size.

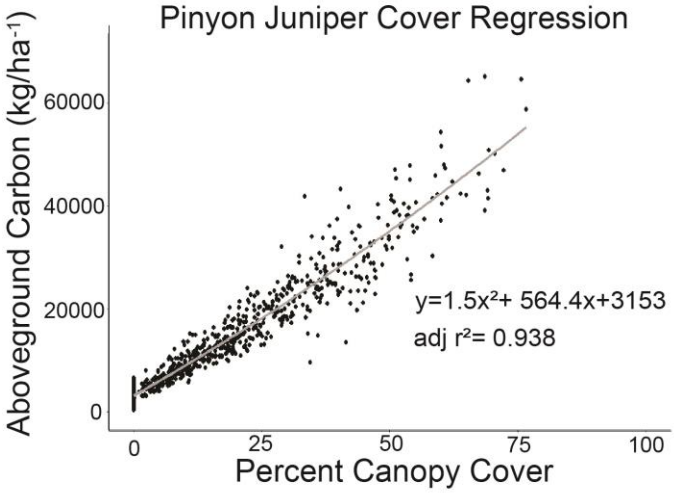

Figure 4.4: Total aboveground carbon in pinyon-juniper is strongly related to canopy cover.

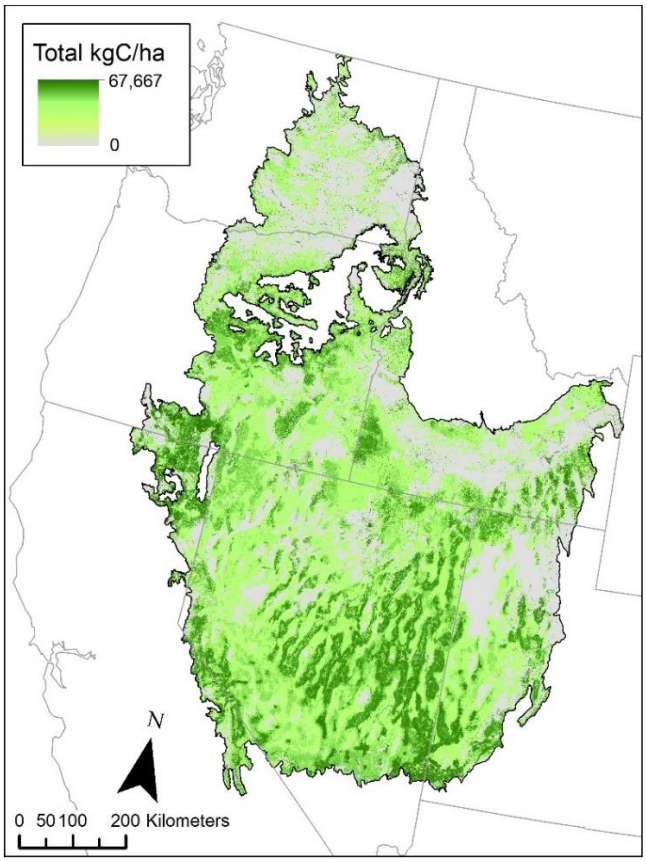

Figure 4.5: Estimated aboveground biomass carbon storage in the Great Basin (kg/ha) using mean estimates for the three shrubland categories.

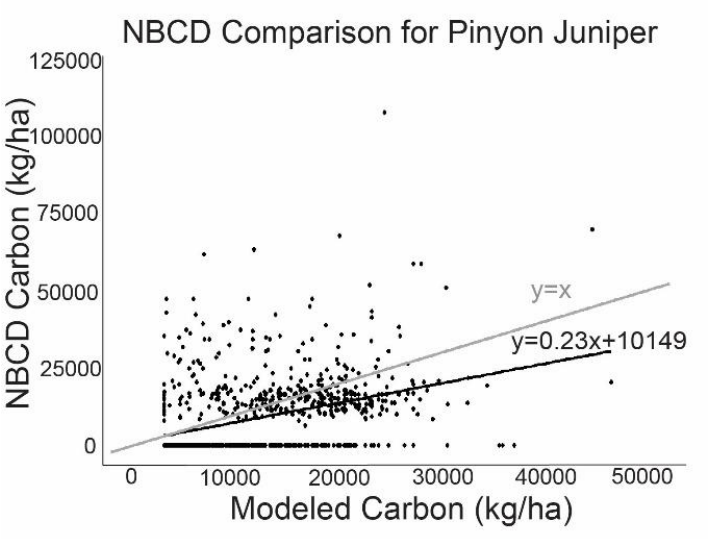

Figure 4.6: Regression of carbon estimates compared to the carbon estimates in the National Biomass and Carbon Dataset for the pinyon-juniper land cover type. There was a weak but significant positive relationship (R2=.147, p<0.01).

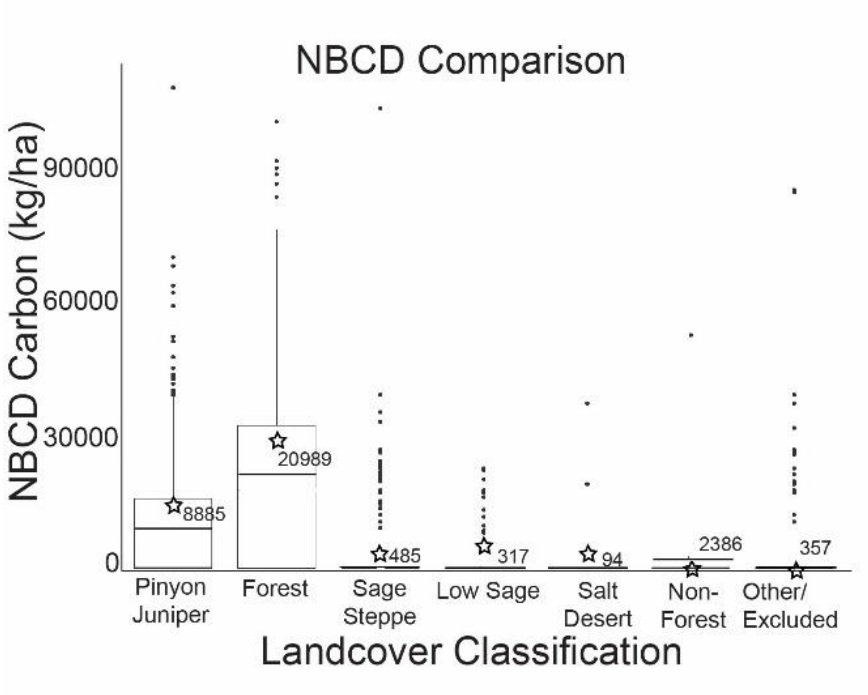

Figure 4.7: For six land cover classes, we provided static carbon estimates (stars; values in Table 4.1). The boxplots show a mean estimate of carbon in the NBCD dataset. Most of the pixels in the associated NBCD dataset for these land cover types had values of 0, with means ranging from 94-20,989 kg/ha. All means (denoted by a line in each boxplot) in the NBCD dataset were lower than the static estimates with the exception of the "other/ excluded" classification. The stars represent the modeled mean for each landcover type. The modeled mean for pinyon-juniper is 12,222 kg/ha and refers to the mean of the 855 pinyon-juniper designated points included in the comparison analysis.

4.5 Discussion

Carbon accounting is increasingly important as we aim to combat climate change by reducing deforestation and degradation in terrestrial ecosystems. To date, aboveground carbon models have largely neglected semi-arid regions and those that have estimated carbon have focused on plot level studies or subsets of ecoregions. Our analysis provides a first comprehensive estimate of aboveground carbon in the Great Basin, a spatially extensive semi-arid region of the western U.S. Our results suggest that Great Basin woodland and shrubland ecosystems contain nearly twice the aboveground carbon estimated by the National Biomass Carbon Dataset. Given that semi-arid ecosystems account for 45% of non-frozen terrestrial lands

globally and are at risk for severe degradation from disturbance and exotic species invasion, this analysis underscores the need to better understand carbon storage in these ubiquitous landscapes. Here we examine factors that may impact our carbon estimates in each landcover type and compare our estimates with previous work in similar regions.

4.5.1 Land cover classifications in the Great Basin

The Great Basin was designated into seven distinct land cover classifications and these general classifications were based on dominant plant functional groups and their potential contributions to aboveground carbon. In the Great Basin, the most widespread of the shrub-steppe communities is the Basin big sagebrush-steppe, and we originally hypothesized that these communities would have higher productivity and carbon storage than the other shrub types. Our results indicate that although highly variable, dependent on local conditions, the salt desert scrub and low sagebrush types can produce similar carbon storage estimates when compared to sagebrush steppe. To better characterize the variance in shrubland carbon estimates additional research may be needed to relate shrub canopy cover and height to biomass and carbon estimates.

4.5.2 Pinyon-juniper carbon

Our results comparing the remotely sensed pinyon-juniper percent cover product (Falkowski et al., 2017) with canopy cover estimates from SageSTEP plots (McIver et al., 2014) are consistent with previous validation work that suggests a tendency of underestimation in high cover areas (Poznanovic et al., 2014; Falkowski et al., 2017a). This was particularly pronounced in areas where SageSTEP plots measured >50% cover. Our estimates of pinyon-juniper canopy cover (mean±SE= 15.1± 0.4, range=0-65.8%, n=855), are similar to remotely

sensed estimates of pinyon-juniper systems in the Colorado Plateau (mean=22%, range= 0-58.9%; Huang et al., 2009) which used a multiscale approach including field measurements, airborne imaging, and Landsat satellite data, suggesting that our estimates are a reasonable representation of canopy cover at regional scales.

Our estimate of total carbon in Great Basin pinyon-juniper systems (~11,870 kg/ha) is also within the range of Huang and colleagues (2009) who estimated a total of 19,240±7,400 kg/ha in pinyon-juniper systems in the Colorado Plateau, and this variation could reflect actual differences in the pinyon-juniper carbon contributions in these different locations. Finally, our estimate of total pinyon-juniper carbon in the Great Basin may also be conservative given the tendency of the canopy cover map to underestimate the high cover field measurements obtained from the SageStep project.

Although our canopy cover model might underestimate aboveground carbon, our land cover map might overestimate the extents of woodland ecosystem. This is because much of our pinyon-juniper classification was based on data from Falkowski et al. (2017a,b) where any pixel with >0% pinyon-juniper cover was designated as pinyon-juniper. These designations superseded cover classifications from LandFire, and therefore, our maps likely represent the maximum land area of pinyon-juniper ecosystems present in the Great Basin. This is illustrated in the high amount of pinyon-juniper area in our land cover map (16.9%) compared to the LANDFIRE map alone (8.2%). In addition, our land cover map estimates 19.7% pinyon-juniper cover compared to 14.6% in the same geographic area in previous work (Bradley and Mustard, 2008.) This overestimation, however, should little impact on the overall carbon estimate in the Great Basin because areas of low pinyon-juniper cover have carbon estimates similar to those in shrubland ecosystems. While classifying all pixels with any pinyon-juniper vegetation as pinyon-juniper is useful for carbon estimates because they are the most significant contributor to

carbon on this landscape, this approach could be problematic if used for mapping habitat for pinyon-juniper specialist species.

4.5.3 Carbon in other land cover

Each of the remaining six land cover classes in the Great Basin was given a static carbon estimate based on field sampling (shrubland) or remotely sensed products (forest). Estimates of aboveground carbon for the low sagebrush and sagebrush steppe shrubland categories are similar to estimates of aboveground biomass for these shrubland ecosystems in previous work (Rickard et al., 1985; Bradley et al., 2006), and salt desert is slightly higher (Driese and Reiners, 1997; Bradley et al., 2006). Because of the high variability in the low sagebrush and salt desert scrub ecosystems partially due to low sample size, we also calculated aboveground carbon estimates using a range of shrubland carbon values. Overall aboveground carbon estimates ranged from 279 Tg to 302 Tg when calculating totals based on low and high shrubland carbon estimates, suggesting that errors in the shrub estimates have minimal effect on the estimate of overall carbon in the Great Basin.

The forest land classification was assigned carbon values using remotely sensed aboveground biomass data (Hudak et al., 2017.), and our estimate for forest aboveground carbon is similar to previous estimates of forest carbon (Kellndorfer et al., 2013; Figure 4.7). While the non-forest land cover category likely has more carbon than the assigned 0 value, it is defined largely by grassland and only accounts for 0.4% of the total study area, suggesting that this land cover category does not have a big impact on the overall carbon storage within the Great Basin region.

While the excluded land cover category made up roughly one third of the Great Basin, we do not expect that this will significantly impact the overall aboveground carbon storage

estimates. Our excluded category included primarily agriculture, introduced grass, development, and water. These vegetation types typically store small amounts of aboveground carbon. For example, in the Great Basin, introduced grassland is primarily cheatgrass which has aboveground carbon typically below 1,000 kgC/ha (Bradley et al., 2006; Diamond et al., 2012; Kessler et al., 2015). While on average, agriculture systems in the U.S. store some carbon, it is typically harvested, resulting in little aboveground carbon storage.

4.5.4 Total Great Basin carbon estimates

Previous work by Kellndorfer et al. 2013 estimated aboveground carbon storage in the Great Basin at 161 Tg, but our regional estimate of carbon is nearly double this amount (296.9 Tg). This is most likely because our estimates include shrubland and woodland aboveground carbon, which collectively make up 66% of the land area (230.4 Tg C) in the Great Basin, while Kellndorfer and colleagues only account for carbon in forest designated pixels of the same region. In addition, Kellndorfer and colleagues reported a strong correlation between modeled carbon and carbon measured in forested FIA plots in the areas included in our Great Basin study map (r=0.44-0.86), however, the relationship we show to aboveground carbon in pinyon-juniper woodland plots is weaker (r=0.38). In fact, 20% of our randomly selected pinyon-juniper pixels were identified as containing 0 kgC by Kellndorfer et al. 2013. As a result, it is likely that national and global scale carbon accounting products focused on forest carbon are poorly suited for estimating carbon in semi-arid ecosystems.

4.5.5 Product applications and management implications

The Great Basin is a region undergoing a high level of land cover change. Aboveground carbon storage in ecosystems is increasingly threatened by fire and conversion to non-native

annual grasslands (Bradley et al., 2006; Balch et al., 2013) and has a history of large-scale alteration of ecosystems due to grazing (Branson, 1953; Hickey, 1961; Mack and Thompson, 1982; Young et al., 1997). Additionally, expansion of woody vegetation, including pinyon-juniper woodland, is common (Miller et al., 2008; Wang et al., 2018). By creating a robust, spatially explicit estimate of aboveground carbon storage in Great Basin ecosystems, this analysis provides an important first step towards measuring and accounting for carbon changes through degradation of this extensive semi-arid region.

BIBLIOGRAPHY

Abatzoglou, J. T., & Kolden, C. A. (2011). Climate change in western US deserts: potential for increased wildfire and invasive annual grasses. *Rangeland Ecology & Management*, *64*(5), 471–478. https://doi.org/10.2111/REM-D-09-00151.1

Abt, K. L., Prestemon, J. P., & Gebert, K. M. (2009). Wildfire suppression cost forecasts for the U.S. Forest Service. *Journal of Forestry*, *107*(4), 173–178.

Ahlström, A., Raupach, M. R., Schurgers, G., Smith, B., Arnet, A., Jung, M., … Zeng, N. (2015). The dominant role of semi-arid ecosystems in the trend and variability of the land CO2 sink Anders. *Science*, *348*(6237), 895–899. https://doi.org/10.1002/2015JA021022

Allen, C. D., Savage, M., Falk, D. A., Suckling, K. F., Thomas, W., Schulke, T., … Jon, T. (2002). Ecological Restoration of Southwestern Ponderosa Pine Ecosystems: A Broad Perspective. *Ecological Applications*, *12*(5), 1418–1433.

Allen, J. M., & Bradley, B. A. (2016). Out of the weeds? Reduced plant invasion risk with climate change in the continental United States. *Biological Conservation*, *203*, 306–312. https://doi.org/10.1016/j.biocon.2016.09.015

Alonso-Canas, I., & Chuvieco, E. (2015). Global burned area mapping from ENVISAT-MERIS and MODIS active fire data. *Remote Sensing of Environment*, *163*, 140–152. https://doi.org/10.1016/j.rse.2015.03.011

Archer, A. J. (2001). Taeniatherum caput-medusae. In: Fire Effects Information System, [Online]. U.S. Department of Agriculture, Forest Service, Rocky Mountain Research Station, Fire Sciences Laboratory (Producer). Available: https://www.fs.fed.us /database/feis/plants/graminoid/taecap/all.html [2018, December 7].

Archibald, S., Nickless, A., Scholes, R. J., & Schulze, R. (2010). Methods to determine the impact of rainfall on fuels and burned area in southern African savannas. *International Journal of Wildland Fire*, *19*(7), 861–878. https://doi.org/10.1071/WF08207

Archibald, S., & Roy, D. P. (2009). Identifying individual fires from satellite-derived burned area data. *International Geoscience and Remote Sensing Symposium (IGARSS)*, *5*, III160-III163. https://doi.org/10.1109/IGARSS.2009.5417974

Archibald, S., Staver, A. C., & Levin, S. A. (2012). Evolution of human-driven fire regimes in Africa. *Proceedings of the National Academy of Sciences*, *109*(3), 847–852. https://doi.org/10.1073/pnas.1118648109

Archibald, S., Roy, D. P., van Wilgen, B. W., & Scholes, R. J. (2008). What limits fire? An examination of drivers of burnt area in Southern Africa. *Global Change Biology*, *15*(3), 613–630. https://doi.org/10.1111/j.1365-2486.2008.01754.x

Argañaraz, J. P., Gavier Pizarro, G., Zak, M., Landi, M. a., & Bellis, L. M. (2015). Human and biophysical drivers of fires in Semiarid Chaco mountains of Central Argentina. *Science of The Total Environment*, *520*(July), 1–12. https://doi.org/10.1016/j.scitotenv.2015.02.081

Baccini, A., Laporte, N., Goetz, S. J., Sun, M., & Dong, H. (2008). A first map of tropical Africa' s above-ground biomass derived from satellite imagery. *Environmental Research Letters*, *3*, 1–9. https://doi.org/10.1088/1748-9326/3/4/045011

Balch, J. K., Bradley, B. A., Abatzoglou, J. T., Nagy, R. C., Fusco, E. J., & Mahood, A. L. (2017). Human-started wildfires expand the fire niche across the United States. *Proceedings of the National Academy of Sciences*, *114*(11), 2946–2951. https://doi.org/10.1073/pnas.1617394114

Balch, J. K., Bradley, B. A., D'Antonio, C. M., & Gómez-Dans, J. (2013). Introduced annual grass increases regional fire activity across the arid western USA (1980-2009). *Global Change Biology*, *19*, 173–183. https://doi.org/10.1111/gcb.12046

Beatley, J. C. (1966). Ecological Status of Introduced Brome Grasses (Bromus Spp .) in Desert Vegetation of Southern Nevada. *Ecology*, *47*(4), 548–554.

Benali, A., Russo, A., Sá, A. C. L., Pinto, R. M. S., Price, O., Koutsias, N., & Pereira, J. M. C. (2016). Determining fire dates and locating ignition points with satellite data. *Remote Sensing*, *8*(4). https://doi.org/10.3390/rs8040326

Biagi, C. J., Cummins, K. L., Kehoe, K. E., & Krider, E. P. (2007). National Lightning Detection Network (NLDN) performance in southern Arizona, Texas, and Oklahoma in 2003-2004. *Journal of Geophysical Research*, *112*(5), 1–17. https://doi.org/10.1029/2006JD007341

Blaisdell, J. P., & Holmgren, R. C. (1984). *Managing intermountain rangelands-salt-desert shrub ranges*. *US Forest Service Intermountain Forest and Range Experiment Station, Ogden UT. General Technical Report*.

Bond, W. J., Woodward, F. I., & Midgley, G. F. (2005). The global distribution of ecosystems in a world without fire. *New Phytologist*, *165*(2), 525–538. https://doi.org/10.1111/j.1469-8137.2004.01252.x

Bond, W. J., & Keeley, J. E. (2005). Fire as a global "herbivore": the ecology and evolution of flammable ecosystems. *Trends in Ecology & Evolution*, *20*(7), 387–94. https://doi.org/10.1016/j.tree.2005.04.025

Boschetti, L., Stehman, S. V., & Roy, D. P. (2016). A stratified random sampling design in space and time for regional to global scale burned area product validation. *Remote Sensing of Environment*, *186*, 465–478. https://doi.org/10.1016/j.rse.2016.09.016

Boshetti L., Roy, D.P., Justice, C.O., Giglio, L. (2010) Global assessment of the temporal reporting accuracy and precision of the MODIS burned area product. *International Journal of Wildland Fire*, *19*, 705-709.

Bowman, D. M. J. S., Balch, J., Artaxo, P., Bond, W. J., Cochrane, M. a, D'Antonio, C. M., … Whittaker, R. (2011). The human dimension of fire regimes on Earth. *Journal of Biogeography*, *38*(12), 2223–2236. https://doi.org/10.1111/j.1365-2699.2011.02595.x

Bowman, D. M. J. S., Balch, J. K., Artaxo, P., Bond, W. J., Carlson, J. M., Cochrane, M. A., … Pyne, S. J. (2009). Fire in the Earth system. *Science (New York, N.Y.)*, *324*(5926), 481–4. https://doi.org/10.1126/science.1163886

Bradley, B. A. (2010). Assessing ecosystem threats from global and regional change: hierarchical modeling of risk to sagebrush ecosystems from climate change, land use and invasive species in Nevada, USA. *Ecography*, *33*(1), 198–208. https://doi.org/10.1111/j.

Bradley, B. A., & Mustard, J. F. (2008). Comparison of phenology trends by land cover class: A case study in the Great Basin, USA. *Global Change Biology*, *14*(2), 334–346. https://doi.org/10.1111/j.1365-2486.2007.01479.x

Bradley, B. A., Houghton, R. A., Mustard, J. F., & Hamburg, S. P. (2006). Invasive grass reduces aboveground carbon stocks in shrublands of the Western US. *Global Change Biology*, *12*(10), 1815–1822. https://doi.org/10.1111/j.1365-2486.2006.01232.x

Bradley, B. A., Early, R., & Sorte, C. J. B. (2015). Space to invade? Comparative range infilling and potential range of invasive and native plants. *Global Ecology and Biogeography*, *24*(3), 348–359. https://doi.org/10.1111/geb.12275/abstract

Bradley, B. A., Curtis, C. A., Fusco, E. J., Abatzoglou, J. T., Balch, J. K., Dadashi, S., & Tuanmu, M. N. (2018). Cheatgrass (Bromus tectorum) distribution in the intermountain Western United States and its relationship to fire frequency, seasonality, and ignitions. *Biological Invasions*, *20*(6), 1493–1506. https://doi.org/10.1007/s10530-017-1641-8

Bradley, B. A., & Mustard, J. F. (2005). Identifying land cover variability distinct from land cover change: Cheatgrass in the Great Basin. *Remote Sensing of Environment*, *94*(2), 204–213. https://doi.org/10.1016/j.rse.2004.08.016

Branson, F. A. (1953). Two new factors affecting resistance of grasses to grazing. *Journal of Range Management*, *6*, 165-171.

Brooks, M. L. (1999). Alien Annual Grasses and Fire in the Mojave Desert. *Madroño*, *46*(1), 13–19.

Brooks, M. L., D'Antonio, C. M., Richardson, D. M., Grace, J. B., Keeley, J. E., DiTomaso, J. M., … Pyke, D. (2004). Effects of Invasive Alien Plants on Fire Regimes. *BioScience*, *54*(7), 677. https://doi.org/10.1641/0006-3568(2004)054[0677:EOIAPO]2.0.CO;2

Brooks, M. L., & Matchett, J. R. (2006). Spatial and temporal patterns of wildfires in the Mojave Desert, 1980-2004. *Journal of Arid Environments*, *67*, 148–164. https://doi.org/10.1016/j.jaridenv.2006.09.027

Brooks, M. L., & Chambers, J. C. (2011). Resistance to Invasion and Resilience to Fire in Desert Shrublands of North America. *Rangeland Ecology & Management*, *64*, 431–438.

Brooks, M.E., Kristensen, K., van Benthem, K. J., Magnusson, A., Berg, C.W., Nielsen, A., Skaug, H.J., Maechler, M., Bolker, B. M. (2017). glmmTMB Balances Speed and Flexibility Among Packages for Zero-inflated Generalized Linear Mixed Modeling. *The R Journal*, *9*(2), 378-400.

Brown, J.K. (1974) Handbook for inventorying downed woody material. *USDA Forest Service General Technical Report.* INT-16. 24p.

Butry, D. T., Mercer, D. E., & Prestemon, J. P. (2001). What is the price of catastrophic wildfire? *Journal of Forestry*, *99*(11), 9–17. Retrieved from http://www.ingentaconnect.com/content/saf/jof/2001/00000099/00000011/art00004

Butry, D. T., & Thomas, D. S. (2017). Underreporting of wildland fires in the US Fire Reporting System NFIRS: California. *International Journal of Wildland Fire*, *26*, 732–743.

Calkin, D. E., Gebert, K. M., Jones, J. G., & Neilson, R. P. (2005). Forest Service large fire area burned and suppression. *Journal of Forestry*, *103*(4), 179–183.

Cardille, J. A., Ventura, S. J., & Turner, M. G. (2001). Environmental and Social Factors Influencing Wildfires in the Upper Midwest , United States. *Ecological Applications*, *11*(1), 111–127.

Cardoso, M. F., Hurtt, G. C., Moore, B., Nobre, C. A., & Bain, H. (2005). Field work and statistical analyses for enhanced interpretation of satellite fire data. *Remote Sensing of Environment*, *96*(2), 212–227. https://doi.org/10.1016/j.rse.2005.02.008

Cartus, O., Kellndorfer, J., Walker, W., Franco, C., Bishop, J., Santos, L., & Fuentes, J. M. M. (2014). A National, Detailed Map of Forest Aboveground Carbon Stocks in Mexico. *Remote Sensing*, *6*, 5559–5588. https://doi.org/10.3390/rs6065559

Chambers, J. C., Bradley, B. A., Brown, C. S., D'Antonio, C., Germino, M. J., Grace, J. B., … Pyke, D. A. (2014). Resilience to stress and disturbance, and resistance to Bromus tectorum L. invasion in cold desert shrublands of western North America. *Ecosystems*, *17*(2), 360–375. https://doi.org/10.1007/s10021-013-9725-5

Chang, D., & Song, Y. (2009). Comparison of L3JRC and MODIS global burned area products from 2000 to 2007. *Journal of Geophysical Research Atmospheres*, *114*(D16106), 1–20. https://doi.org/10.1029/2008JD011361

Chevan, A., & Sutherland, M. (2011). Hierarchical Partitioning. *The American Statistician*, *45*(2), 90–96. https://doi.org/10.2307/2684366

Chojnacky, D. C., Prisley, S. P., & Miller, S. R. (2012). Linking Forest Inventory and Analysis Ground Data to Maps: An Example for Nevada Pinyon–Juniper Forests. *Western Journal of Applied Forestry, 27*(3), 118-127.

Coffman, G. C., Ambrose, R. F., & Rundel, P. W. (2010). Wildfire promotes dominance of invasive giant reed (Arundo donax) in riparian ecosystems. *Biological Invasions*, *12*(8), 2723–2734. https://doi.org/10.1007/s10530-009-9677-z

Commission for Environmental Cooperation Working Group. (1997). Ecological Regions of North America- Toward a Common Perspective. Commission for Environmental Cooperation, Montreal, Canada.

Conklin, F. S., & Fisher, D. E. (1973). *Economic Characteristics of Farms Producing Grass Seed in Oregon ' s Willamette Valley*.

Cross, T., Finn, J. T., & Bradley, B. A. (2017). Frequency of invasive plant occurrence is not a suitable proxy for abundance in the Northeast United States. *Ecosphere*, *8*(5), 1–12. https://doi.org/10.1002/ecs2.1800

Csiszar, I. A., Morisette, J. T., & Giglio, L. (2006). Validation of active fire detection from moderate-resolution satellite sensors: The MODIS example in Northern Eurasia. *IEEE Transactions on Geoscience and Remote Sensing*, *44*(7), 1757–1764. https://doi.org/10.1109/TGRS.2006.875941

Cummins, K. L., & Murphy, M. J. (2009). An overview of lightning locating systems: History, techniques, and data uses, with an in-depth look at the U.S. NLDN. *IEEE Transactions on Electromagnetic Compatibility*, *51*(3 PART 1), 499–518. https://doi.org/10.1109/TEMC.2009.2023450

D'Antonio, C. (1992). Biological Invasions by Exotic Grasses, the Grass Fire Cycle, and Global Change. *Annual Review of Ecology and Systematics*, *23*(1), 63–87. https://doi.org/10.1146/annurev.ecolsys.23.1.63

Dadashi, S. K. (2018). *What is a fire? Identifying individual fire events using the MODIS burned area product*.

Dadashi, S., Balch, J.K., and Bradley, B. A. (2017). "Annual Fire Event Maps for the U.S. (2001-2016) Based on the MODIS Burned Area Product (MCD64A1 Collection 5.1)." *Open Science Framework*, 4 Sept. 2017. Web. [Published dataset] https://osf.io/fmahr/

Davies, K. W., & Svejcar, T. J. (2012). Comparison of Medusahead-Invaded and Noninvaded Wyoming Big Sagebrush Steppe in Southeastern Oregon. *Range*, *61*(6), 623–629.

Dennison, P. E., Brewer, S. C., Arnold, J. D., & Moritx, M. A. (2014). Large wildfire trends in the western United States, 1984-2011. *Geophysical Research Letters*, (41), 1–6. https://doi.org/10.1002/2014GL059576.Received

Diamond, J. M., Call, C. A., & Devoe, N. (2012). Effects of Targeted Grazing and Prescribed Burning on Community and Seed Dynamics of a Downy Brome (Bromus tectorum)–Dominated Landscape. *Invasive Plant Science and Management*, *5*(02), 259–269. https://doi.org/10.1614/IPSM-D-10-00065.1

Dibble, A. C., White, R. H., & Lebow, P. K. (2007). Combustion characteristics of north-eastern USA vegetation tested in the cone calorimeter: Invasive versus non-invasive plants. *International Journal of Wildland Fire*, *16*(4), 426–443. https://doi.org/10.1071/WF05103

Diez, J. M., D'Antonio, C. M., Dukes, J. S., Grosholz, E. D., Olden, J. D., Sorte, C. J. B., … Miller, L. P. (2012). Will extreme climatic events facilitate biological invasions? *Frontiers in Ecology and the Environment*, *10*(5), 249–257. https://doi.org/10.1890/110137

Driese, K. L., & Reiners, W. A. (1997). Aerodynamic roughness parameters for semi-arid natural shrub communities of Wyoming, USA. *Agricultural and Forest Meteorology*, *88*, 1–14. https://doi.org/10.1016/S0168-1923(97)00055-5

Dukes, J. S., & Mooney, H. A. (1999). Does global change increase the success of biological invaders? *Trends in Ecology and Evolution*, *14*(4), 135–139. https://doi.org/10.1016/S0169-5347(98)01554-7

EDDMapS, Early Detection and Distribution Mapping System. (2018). The University of Georgia - Center for Invasive Species and Ecosystem Health Accessed July 9, 2018.

Eidenshink, J., Schwind, B., Brewer, K., Zhu, Z., Quayle, B., & Howard, S. (2007). A Project for Monitoring Trends in Burn Severity. *Fire Ecology*, *3*(1), 3–21.

Fairman, T. A., Bennett, L. T., & Nitschke, C. R. (2019). Short-interval wildfires increase likelihood of resprouting failure in fire-tolerant trees. *Journal of Environmental Management*, *231*, 59–65. https://doi.org/10.1016/j.jenvman.2018.10.021

Falkowski, M. J., Evans, J. S., Naugle, D. E., Hagen, C. A., Carleton, S. A., Maestas, J. D., … Lawrence, A. J. (2017). Mapping tree canopy cover in support of proactive prairie grouse conservation in western North America. *Rangeland Ecology and Management*, *70*(1), 15–24. https://doi.org/10.1016/j.rama.2016.08.002

Falkowski, M. J., Hudak, A. T., Filippelli, S. K., & Fekety, P.A. (2017b). Developing a Carbon Monitoring System For Pinyon-juniper Forests and Woodlands. *Presented at the American Geophysical Union, Fall Meeting*, New Orleans, LA. Retrieved from https://agu.confex.com/agu/fm17/meetingapp.cgi/Paper/295240

Federal Geographic Data Committee. (2008). The National Vegetation Classification Standard, Version 2. FGDC Vegetation Subcommittee. FGDC-STD-005-2008 (Version 2). pp. 126.

Flannigan, M. D., Krawchuk, M. A., de Groot, W. J., Wotton, B. M., & Gowman, L. M. (2009). Implications of changing climate for global wildland fire. *International Journal of Wildland Fire*, *18*(5), 483–507. https://doi.org/10.1071/WF08187

Flory, S. L., Clay, K., Emery, S. M., Robb, J. R., & Winters, B. (2015). Fire and non-native grass invasion interact to suppress tree regeneration in temperate deciduous forests. *Journal of Applied Ecology*, *52*(4), 992–1000. https://doi.org/10.1111/1365-2664.12437

Foga, S., Scaramuzza, P. L., Guo, S., Zhu, Z., Dilley, R. D., Beckmann, T., ... & Laue, B. (2017). Cloud detection algorithm comparison and validation for operational Landsat data products. *Remote Sensing of Environment, 194*, 379-390.

Fornacca, D., Ren, G., & Xiao, W. (2017). Performance of Three MODIS fire products (MCD45A1, MCD64A1, MCD14ML), and ESA Fire_CCI in a mountainous area of Northwest Yunnan, China, characterized by frequent small fires. *Remote Sensing*, *9*, 1–20. https://doi.org/10.3390/rs9111131

Fox, J., & Monette, G. (1992). Generalized Collinearity Diagnostics. *Journal of the American Statistical Association*, *87*(417), 178–183. https://doi.org/10.1080/01621459.1992.10475190

Franklin, J. (2010). *Mapping Species Distributions: Spatial Inference and Prediction*. *Cambridge University Press*. https://doi.org/10.1017/CBO9780511810602

Fryer, J. L. (2011). Microstegium vimineum. In: Fire Effects Information System, [Online]. U.S. Department of Agriculture, Forest Service, Rocky Mountain Research Station, Fire Sciences Laboratory (Producer). Available: https://www.fs.fed.us /database/feis/plants/graminoid/micvim/all.html [2018, December 7].

Fusco, E. J., Abatzoglou, J. T., Balch, J. K., Finn, J. T., & Bradley, B. A. (2016). Quantifying the human influence on fire ignition across the western USA. *Ecological Applications*, *26*(8), 2390–2401. https://doi.org/10.1002/eap.1395

GAP/USGS. (2016). *LANDFIRE / GAP Land Cover Map Unit Descriptions*.

GeoMac (2017). Geospatial Multi-Agency Coordination Group (GeoMAC) Wildland Fire Support: Interagency Website: http://www.geomac.gov/index.shtml

Giglio, L., Csiszar, I., & Justice, C. O. (2006). Global distribution and seasonality of active fires as observed with the Terra and Aqua Moderate Resolution Imaging Spectroradiometer (MODIS) sensors. *Journal of Geophysical Research*, *111*, 1–12. https://doi.org/10.1029/2005JG000142

Giglio, L., Descloitres, J., Justice, C. O., & Kaufman, Y. J. (2003). An enhanced contextual fire detection algorithm for MODIS. *Remote Sensing of Environment*, *87*, 273–282. https://doi.org/10.1016/S0034-4257(03)00184-6

Giglio, L., Loboda, T., Roy, D. P., Quayle, B., & Justice, C. O. (2009). An active-fire based burned area mapping algorithm for the MODIS sensor. *Remote Sensing of Environment*, *113*(2), 408–420. https://doi.org/10.1016/j.rse.2008.10.006

Giglio, L., Randerson, J. T., & van der Werf, G. R. (2013). Analysis of daily, monthly, and annual burned area using the fourth-generation global fire emissions database (GFED4). *Journal of Geophysical Research: Biogeosciences*, *118*(1), 317–328. https://doi.org/10.1002/jgrg.20042

Gillespie, T. W., Chu, J., Frankenberg, E., & Thomas, D. (2007). Assessment and Prediction of Natural Hazards from Satellite Imagery. *Progress in Physical Geography*, *31*(5), 459–470. https://doi.org/10.1177/0309133307083296.Assessment

Goetz, S. J., Baccini, A., Laporte, N. T., Johns, T., Walker, W., Kellndorfer, J., … Sun, M. (2009). Mapping and monitoring carbon stocks with satellite observations: a comparison of methods. *Carbon Balance and Management*, *4*(2), 1–7. https://doi.org/10.1186/1750-0680-4-2

Gray, J. T. (1982). Community Structure and Productivity in Ceanothus Chaparral and Coastal Sage Scrub of Southern California. *Ecological Monographs*, *52*(4), 415–435.

Greenall, J. A. (1995). First-year regrowth of three marsh plant communities after fall and spring fires in the Delta Marsh, Manitoba. *Masters Thesis*, *University*(Department of Botany), 1–135.

Gucker, C. L. (2008). Phragmites australis. In: Fire Effects Information System, [Online]. U.S. Department of Agriculture, Forest Service, Rocky Mountain Research Station, Fire Sciences Laboratory (Producer). Available: https://www.fs.fed.us /database/feis/plants/graminoid/phraus/all.html [2018, December 7].

Guyette, R. P., Muzika, R. M., & Dey, D. C. (2002). Dynamics of an Anthropogenic Fire Regime. *Ecosystems*, *5*, 472–486. https://doi.org/10.1007/s10021-002-0115-7

Hantson, S., Padilla, M., Corti, D., & Chuvieco, E. (2013). Strengths and weaknesses of MODIS hotspots to characterize global fire occurrence. *Remote Sensing of Environment*, *131*, 152–159. https://doi.org/10.1016/j.rse.2012.12.004

Hantson, S., Pueyo, S., & Chuvieco, E. (2015). Global fire size distribution is driven by human impact and climate. *Global Ecology and Biogeography*, *24*(1), 77–86. https://doi.org/10.1111/geb.12246

Hardison, J. R. (1980). Role of Fire for Disease Control in Grass Seed Production. *Plant Disease*, *64*, 641–645.

Harrington, J.B., Donnelly, R.E. (1978). Fire probabilities in Ontario's boreal forest. In Proceedings of the Fifth Join Conference on Fire and Forest Meteorology. 1-4. *American Meteorological Society*, Boston, Massachusetts, USA.

Hauser, A. S. (2008). Pennisetum ciliare. In: Fire Effects Information System, [Online]. U.S. Department of Agriculture, Forest Service, Rocky Mountain Research Station, Fire Sciences Laboratory (Producer). Available: https://www.fs.fed.us /database/feis/plants/graminoid/pencil/all.html [2018, December 7].

Haverd, V., Ahlström, A., Smith, B., & Canadell, J. G. (2017). Carbon cycle responses of semi-arid ecosystems to positive asymmetry in rainfall. *Global Change Biology*, *23*(2), 793–800. https://doi.org/10.1111/gcb.13412

Hawbaker, T. J., Radeloff, V. C., Syphard, A. D., Zhu, Z., & Stewart, S. I. (2008). Detection rates of the MODIS active fire product in the United States. *Remote Sensing of Environment*, *112*, 2656–2664. https://doi.org/10.1016/j.rse.2007.12.008

Hawbaker, T. J., Vanderhoof, M. K., Beal, Y. J., Takacs, J. D., Schmidt, G. L., Falgout, J. T., … Dwyer, J. L. (2017). Mapping burned areas using dense time-series of Landsat data. *Remote Sensing of Environment*, *198*(September), 504–522. https://doi.org/10.1016/j.rse.2017.06.027

Hawbaker, T. J., Radeloff, V. C., Stewart, S. I., Hammer, R. B., Keuler, N. S., & Clayton, M. K. (2013). Human and biophysical influence on fire occurrence in the United States. *Ecological Applications*, *23*(3), 565–582. https://doi.org/10.1890/12-1816.1

Hickey, W. C. (1961). Growth form of crested wheatgrass as affected by site and grazing. *Ecology, 42*:173-176.

Houghton, R. A. (2007). Balancing the Global Carbon Budget. *Annual Review of Earth and Planetary Sciences*, *35*(1), 313–347. https://doi.org/10.1146/annurev.earth.35.031306.140057

Howard, J. L. (2005). Imperata brasiliensis, I. cylindrica. In: Fire Effects Information System, [Online]. U.S. Department of Agriculture, Forest Service, Rocky Mountain Research Station, Fire Sciences Laboratory (Producer). Available: https://www.fs.fed.us /database/feis/plants/graminoid/impspp/all.html [2018, December 7].

Hu, X., Yu, C., Tian, D., Ruminski, M., Robertson, K., Waller, L. A., & Liu, Y. (2016). Comparison of the hazard mapping system (HMS) fire product to ground-based fire records in Georgia, USA. *Journal of Geophysical Research*, *121*(6), 2901–2910. https://doi.org/10.1002/2015JD024448

Huang, C.-Y., Asner, G. P., Martin, R. E., Barger, N. N., & Neff, J. C. (2009). Multiscale Analysis of Tree Cover and Aboveground Carbon Stocks in Pinyon-Juniper Woodlands. *Ecological Applications*, *19*(3), 668–681.

Hudak, A. T., Fekety, P.A., Falkowski, M. J., Kennedy, R. E., Crookston, N. L., Smith, A. M., ... Woodall, C. W. (2016, December). Multi-Scale Mapping of Vegetation Biomass. Presented at the American Geophysical Union, Fall Meeting, San Francisco, CA. Retrieved from https://agu.confex.com/agu/fm16/meetingapp.cgi/Paper/126817

Invasive Plant Atlas of the United States. (2018). Invasive plant atlas of the United States - database of plants invading natural areas. URL: http://www.invasiveplantatlas.org/. (Accessed June, 2018)

Jørgensen, U. (2011). Benefits versus risks of growing biofuel crops: The case of Miscanthus. *Current Opinion in Environmental Sustainability*, *3*, 24–30. https://doi.org/10.1016/j.cosust.2010.12.003

Justice, C. O., Giglio, L., Korontzi, S., Owens, J., Morisette, J., Roy, D., … Kaufman, Y. (2002). The MODIS fire products. *Remote Sensing of Environment*, *83*, 244–262. https://doi.org/10.1016/S0034-4257(02)00076-7

Kauffman, J. B., & Uhl, C. (1990). Interactions of anthropogenic activities, fire, and rian forests in the Amazon Basin: Fire in the Tropical Biota. *Fire in the Tropical Biota*, *84*, 117–134. https://doi.org/10.1360/zd-2013-43-6-1064

Keane, R. E., Agee, J. K., Fulé, P., Keeley, J. E., Key, C., Kitchen, S. G., … Schulte, L. A. (2008). Ecological effects of large fires on US landscapes: benefit or catastrophe? *International Journal of Wildland Fire*, *17*(6), 696–712. https://doi.org/10.1071/WF071484

Kellndorfer, J., W. Walker, K. Kirsch, G. Fiske, J. Bishop, L. Lapoint, M. Hoppus, and J. Westfall. (2013). NACP Aboveground Biomass and Carbon Baseline Data, V.2 (NBCD 2000), U.S.A., 2000. ORNL DAAC, Oak Ridge, Tennessee, USA. https://doi.org/10.3334/ORNLDAAC/1161

Kessler, K. C., Nissen, S. J., Meiman, P. J., & Beck, K. G. (2015). Litter Reduction by Prescribed Burning Can Extend Downy Brome Control. *Rangeland Ecology and Management*, *68*(4), 367–374. https://doi.org/10.1016/j.rama.2015.05.006

Knapp, P. A. (1996). Cheatgrass (Bromus tectorum L.) dominance in the Great Basin Desert: History, persistence, and influences to human activities. *Global Environmental Change*, *6*, 37–52.

Knapp, P. A. (1998). Spatio-temporal patterns of large grassland fires in the Intermountain West, U.S.A. *Global Ecology and Biogeography Letters*, *7*(1998), 259–273.

Knorr, W., Kaminski, T., Arneth, a., & Weber, U. (2014). Impact of human population density on fire frequency at the global scale. *Biogeosciences*, *11*(4), 1085–1102. https://doi.org/10.5194/bg-11-1085-2014

Korontzi, S., McCarty, J., Loboda, T., Kumar, S., & Justice, C. (2006). Global distribution of agricultural fires in croplands from 3 years of Moderate Resolution Imaging Spectroradiometer (MODIS) data. *Global Biogeochemical Cycles*, *20*(2), 1–15. https://doi.org/10.1029/2005GB002529

Korontzi, S., Roy, D. P., Justice, C. O., & Ward, D. E. (2004). Modeling and sensitivity analysis of fire emissions in southern Africa during SAFARI 2000. *Remote Sensing of Environment*, *92*, 255–275. https://doi.org/10.1016/j.rse.2004.06.010

Krawchuk, M. A., Moritz, M. A., Parisien, M.-A., Van Dorn, J., & Hayhoe, K. (2009). Global pyrogeography: The current and future distribution of wildfire. *PLoS ONE*, *4*(4). https://doi.org/10.1371/journal.pone.0005102

Lal, R. (2004). Carbon Sequestration in Dryland Ecosystems. *Environmental Management*, *33*(4), 528–544. https://doi.org/10.1007/978-3-319-92318-5

Lambert, A. M., D'Antonio, C. M., & Dudley, T. L. (2010). Invasive species and fire in California ecosystems. *Fremontia*, *38*. Retrieved from http://www.cnps.org/cnps/publications/fremontia/Fremontia_Vol38-No2-3.pdf#page=31

LANDFIRE. (2008). Existing Vegetation Type Layer. LANDFIRE 1.1.0 U.S. *Department of the Interior, Geological Survey*. Accessed April 2014 at http//landfire.cr.usgs.gov/viewer/

LANDFIRE. (2012a). Existing Vegetation Type Layer, LANDFIRE 1.3.0, U.S. Department of the Interior, Geological Survey. Accessed 30 January 2017 at https://www.landfire.gov/version_comparison.php?mosaic=Y.

LANDFIRE. (2012b). Disturbance (year) Layers, LANDFIRE 1.3.0, U.S. Department of the Interior, Geological Survey. Accessed 30 March 2017 at https://www.landfire.gov/version_comparison.php?mosaic=Y.

LANDFIRE. (2014a). Existing Vegetation Type Layer, LANDFIRE 1.4.0, U.S. Department of the Interior, Geological Survey. Accessed 9 January 2018 at https://www.landfire.gov/version_comparison.php?mosaic=Y.

LANDFIRE. (2014b) Biophysical Setting, LANDFIRE 1.4.0, U.S. Department of the Interior, Geological Survey. Accessed 30 April 2018 at https://www.landfire.gov/version_comparison.php?mosaic=Y.

Langmann, B., Duncan, B., Textor, C., Trentmann, J., & van der Werf, G. R. (2009). Vegetation fire emissions and their impact on air pollution and climate. *Atmospheric Environment*, *43*, 107–116. https://doi.org/10.1016/j.atmosenv.2008.09.047

Leu, M., Hanser, S. E., & Knick, S. T. (2008). The Human Footprint in the West: A Large-Scale Analysis of Anthropogenic Impacts. *Ecological Applications*, *18*(5), 1119–1139. Retrieved from http://www.ncbi.nlm.nih.gov/pubmed/18686576

Liang, S. & Xiao, Z. (2012). Global Land Surface Products: Leaf Area Index Product Data Collection (1985-2010). http://www.dx.doi.org/10.6050/glass863.3004.db (Beijing Normal University). Accessed 8 May 2018

Lippincott, C. L. (2000). Effects of Imperata cylindrica (L.) Beauv. (Cogongrass) Invasion on Fire Regime in Florida Sandhill (USA). *Natural Areas Journal*, *20*(2), 140–149.

Littell, J. S., McKenzie, D., Peterson, D. L., & Westerling, A. L. (2009). Climate and wildfire area burned in western U . S . ecoprovinces, 1916-2003. *Ecological Applications*, *19*(4), 1003–1021.

Liu, Y., Stanturf, J., & Goodrick, S. (2010). Trends in global wildfire potential in a changing climate. *Forest Ecology and Management*, *259*(4), 685–697. https://doi.org/10.1016/j.foreco.2009.09.002

Loepfe, L., Lloret, F., & Román-Cuesta, R. M. (2012). Comparison of burnt area estimates derived from satellite products and national statistics in Europe. *International Journal of Remote Sensing*, *33*(12), 3653–3671. https://doi.org/10.1080/01431161.2011.631950

Mack, R. N. (1981). Invasion of Bromus Tectorum L. Into Western North America: An Ecological Chronicle. *Agro-Ecosystems*, *7*, 145–165.

Magnusson, A., Skaug, H.J., Nielsen, A., Berg, C.W., Kristensen, K., Maechler, M., van Benthem, K.J., Bolker, B.M., Brooks, M.E. (2017). glmmTMB: Generalized Linear Mixed Models using Template Model Builder. R package version 0.1.3. https://github.com/glmmTMB

Marks, M., Lapin, B., & Randall, J. (1994). Phragmites australis (P. communis): Threats, Management, and Monitoring. *Natural Areas Journal*, *14*(4), 285–294.

Marlon, J. R., Bartlein, P. J., Gavin, D. G., Long, C. J., Anderson, R. S., Briles, C. E., … Walsh, M. K. (2012). PNAS Plus: Long-term perspective on wildfires in the western USA. *Proceedings of the National Academy of Sciences*, *109*(9), E535–E543. https://doi.org/10.1073/pnas.1112839109

Marlon, J. R., Bartlein, P. J., Carcaillet, C., Gavin, D. G., Harrison, S. P., Higuera, P. E., … Prentice, I. C. (2008). Climate and human influences on global biomass burning over the past two millennia. *Nature Geoscience*, *1*(10), 697–702. https://doi.org/10.1038/ngeo468

Marvin, D. C., Bradley, B. A., & Wilcove, D. S. (2009). A Novel, Web-Based, Ecosystem Mapping Tool Using Expert Opinion. *Natural Areas Journal*, *29*(3), 281–292.

McArthur, E. D., & Taylor, J. R. (2004). Artemisia arbuscula Nutt. low sagebrush. Wildland Shrubs of the United States and Its Territories: Thamnic Descriptions: Volume, 47.

McCarty, J. L., Justice, C. O., & Korontzi, S. (2007). Agricultural burning in the Southeastern United States detected by MODIS. *Remote Sensing of Environment*, *108*, 151–162. https://doi.org/10.1016/j.rse.2006.03.020

McDonald, C. J., & McPherson, G. R. (2013). Creating hotter fires in the Sonoran Desert: Buffelgrass produces copious fuels and high fire temperatures. *Fire Ecology*, *9*(2), 26–39. https://doi.org/10.4996/fireecology.0902026

McIver, J., Brunson, M., Bunting, S., Chambers, J., Doescher, P., Grace, J., Hulet, A., Johnson, D., Knick, S., Miller, R., Pellant, M., Pierson, F., Pyke, D., Rau, B., Rollins, K., Roundy, B., Schupp, E., Tausch, R., Williams, J. (2014). A Synopsis of Short-Term Response to Alternative Restoration Treatments in Sagebrush-Steppe: The SageSTEP Project. *Rangeland Ecology and Management*. *67*, 584–598. doi:10.2111/REM-D-14-00084.1

McWilliams, J. (2004). Arundo donax. In: Fire Effects Information System, [Online]. U.S. Department of Agriculture, Forest Service, Rocky Mountain Research Station, Fire Sciences Laboratory (Producer). Available: https://www.fs.fed.us /database/feis/plants/graminoid/arudon/all.html [2018, December 7].

Miller, R. F., Tausch, R. J., McArthur, E. D., Johnson, D. D., & Sanderson, S. C. (2008). *Age structure and expansion of pinyon-juniper woodlands: a regional perspective in the Intermountain West. Rocky Mountain Research Station Research Paper RMRS-RP-69*. https://doi.org/10.1016/j.apmr.2010.08.011.Accelerometry

Moore, M. M., Covington, W. W., & Fule, P. Z. (1999). Reference Conditions and Ecological Restoration : A Southwestern Ponderosa Pine Perspective. *Ecological Applications*, *9*(4), 1266–1277.

Morisette, J. T., Giglio, L., Csiszar, I., & Justice, C. O. (2005). Validation of the MODIS active fire product over Southern Africa with ASTER data. *International Journal of Remote Sensing*, *26*(19), 4239–4264. https://doi.org/10.1080/01431160500113526

Nagy, R. C., Fusco, E., Bradley, B., Abatzoglou, J. T., & Balch, J. (2018). Human-Related Ignitions Increase the Number of Large Wildfires across U . S . Ecoregions. *Fire*, *1*(1), 1–14. https://doi.org/10.3390/fire1010004

National Wildfire Coordinating Group. NWCG. (2005). *Wildfire Origin & Cause Determination Handbook*.

Omernik, J.M. (1987). Ecoregions of the conterminous United States. *Annals of the Association of American Geographers*, *77*, 118-125.

Oom, D., Silva, P. C., Bistinas, I., & Pereira, J. M. C. (2016). Highlighting biome-specific sensitivity of fire size distributions to time-gap parameter using a new algorithm for fire event individuation. *Remote Sensing*, *8*, 1–15. https://doi.org/10.3390/rs8080663

Padilla, M., Stehman, S. V., Ramo, R., Corti, D., Hantson, S., Oliva, P., … Chuvieco, E. (2015). Comparing the accuracies of remote sensing global burned area products using stratified random sampling and estimation. *Remote Sensing of Environment*, *160*, 114–121. https://doi.org/10.1016/j.rse.2015.01.005

Parisien, M. A., Snetsinger, S., Greenberg, J. A., Nelson, C. R., Schoennagel, T., Dobrowski, S. Z., & Moritz, M. A. (2012). Spatial variability in wildfire probability across the western United States. *International Journal of Wildland Fire*, *21*(4), 313–327. https://doi.org/10.1071/WF11044

Pausas, J. G., & Ribeiro, E. (2013). The global fire-productivity relationship. *Global Ecology and Biogeography*, *22*(6), 728–736. https://doi.org/10.1111/geb.12043

Pechony, O., & Shindell, D. T. (2009). Fire parameterization on a global scale. *Journal of Geophysical Research*, *114*(D16), D16115. https://doi.org/10.1029/2009JD011927

Platt, W. J., & Gottschalk, M. (2001). Effects of exotic grasses on potential fine fuel loads in the groundcover of south Florida slash pine savannas. *International Journal of Wildland Fire*, *10*, 155–159.

Pouliot, G., Rao, V., McCarty, J. L., & Soja, A. (2017). Development of the crop residue and rangeland burning in the 2014 National Emissions Inventory using information from multiple sources. *Journal of the Air and Waste Management Association*, *67*(5), 613–622. https://doi.org/10.1080/10962247.2016.1268982

Poulter, B., Frank, D., Ciais, P., Myneni, R. B., Andela, N., Bi, J., … Van Der Werf, G. R. (2014). Contribution of semi-arid ecosystems to interannual variability of the global carbon cycle. *Nature*, *509*, 600–603. https://doi.org/10.1038/nature13376

Poznanovic, A. J., Falkowski, M. J., Maclean, A. L., Smith, A. M. S., & Evans, J. S. (2014). An Accuracy Assessment of Tree Detection Algorithms in Juniper Woodlands. *Photogrammetric Engineering & Remote Sensing*, *80*(5), 627–637. https://doi.org/10.14358/PERS.80.7.627

Pyne, S. J. (1982). Fire in America. A cultural history of wildland and rural fire. Princeton University Press.

R Studio Team. (2015). RStudio: Integrated Development for R. RStudio, Inc., Boston, MA URL http://www.rstudio.com/.

Radeloff, V. C., Hammer, R. B., Stewart, S. I., Fried, J. S., Holcomb, S. S., & Mckeefry, J. F. (2005). the Wildland – Urban Interface in the United States. *Ecological Applications*, *15*(3), 799–805. https://doi.org/10.1890/04-1413

Rau, B. M., Tausch, R., Reiner, A., Johnson, D. W., Chambers, J. C., & Blank, R. R. (2012). Developing a model framework for predicting effects of woody expansion and fire on ecosystem carbon and nitrogen in a pinyon-juniper woodland. *Journal of Arid Environments*, *76*(1), 97–104. https://doi.org/10.1016/j.jaridenv.2011.06.005

Rau, B. M., Tausch, R., Reiner, A., Johnson, D. W., Jeanne, C., Blank, R. R., & Lucchesi, A. (2010). Influence of Prescribed Fire on Ecosystem Biomass, Carbon, and Nitrogen in a Pinyon Juniper Woodland. *Rangeland Ecology & Management*, *63*, 197–202.

Reichard, S. H., & White, P. (2001). Horticulture as a Pathway of Invasive Plant Introductions in the United States. *BioScience*, *51*(2), 103–113. https://doi.org/http://dx.doi.org/10.1641/0006-3568(2001)051[0103:HAAPOI]2.0.CO;2

Reiner, A.L., Tausch, R.J., & Walker, R.F. (2010). Estimation procedures for understory biomass and fuel loads in sagebrush steppe invaded by woodlands. *Western North American Naturalist: 70*(3):312-322.

Rickard, W. H. (1985). Biomass and shoot production in an undisturbed sagebrush-bunchgrass community. *Northwest Science*, *59*(2), 126–133. https://doi.org/10.1016/B978-0-12-214674-9.50003-5

Rollins, M. G. (2009). LANDFIRE: A nationally consistent vegetation, wildland fire, and fuel assessment. *International Journal of Wildland Fire*, *18*(3), 235–249. https://doi.org/10.1071/WF08088

Romme, W. H. (1980). *Proceedings of the Fire History Workshop: Fire history terminology: report of the ad hoc committee*. *USDA- General Technical Report RM-81, Eds. Stokes and J.H. Dieterich, Rocky Mountain Research Station*.

Roy, D. P., Boschetti, L., Justice, C. O., & Ju, J. (2008). The collection 5 MODIS burned area product — Global evaluation by comparison with the MODIS active fire product. *Remote Sensing of Environment*, *112*(9), 3690–3707. https://doi.org/10.1016/j.rse.2008.05.013

Roy, D. P., Jin, Y., Lewis, P. E., & Justice, C. O. (2005). Prototyping a global algorithm for systematic fire-affected area mapping using MODIS time series data. *Remote Sensing of the Environment*, *97*(2), 137–162. https://doi.org/10.1016/j.rse.2005.04.007

Roy, D.P., Lewis, P.E., & Justice, C.O. (2002). Burned area mapping using multi-temporal moderate spatial resolution data—A bi-directional reflectance model-based expectation approach. *Remote Sensing of Environment*, *83*, 263-286.

Saatchi, S. S., Harris, N. L., Brown, S., Lefsky, M., Mitchard, E. T. A., Salas, W., … Morel, A. (2011). Benchmark map of forest carbon stocks in tropical regions across three continents. *Proceedings of the National Academy of Sciences*, *108*(24), 9899–9904. https://doi.org/10.1073/pnas.1019576108

Sanderson, E. W., Jaiteh, M., Levy, M. A., Redford, K. H., Wannebo, A. V., & Woolmer, G. (2002). The Human Footprint and the Last of the Wild. *BioScience*, *52*(10), 891–904. https://doi.org/10.1641/0006-3568(2002)052[0891:THFATL]2.0.CO;2

Sankey, T., Shrestha, R., Sankey, J. B., Hardegree, S., & Strand, E. (2013). Lidar-derived estimate and uncertainty of carbon sink in successional phases of woody encroachment. *Journal of Geophysical Research: Biogeosciences*, *118*(3), 1144–1155. https://doi.org/10.1002/jgrg.20088

SAS Institute Copyright ©. (2009). SAS Institute Inc., Cary, NC

Schoennagel, T., Veblen, T. T., & Romme, W. H. (2004). The Interaction of Fire, Fuels, and Climate across Rocky Mountain Forests. *BioScience*, *54*(7), 661–676. https://doi.org/10.1641/0006-3568(2004)054

Schroeder, W., Ellicott, E., Ichoku, C., Ellison, L., Dickinson, M. B., Ottmar, R. D., … Kremens, R. (2014). Integrated active fire retrievals and biomass burning emissions using complementary near-coincident ground, airborne and spaceborne sensor data. *Remote Sensing of Environment*, *140*, 719–730. https://doi.org/10.1016/j.rse.2013.10.010

Schroeder, W., Prins, E., Giglio, L., Csiszar, I., Schmidt, C., Morisette, J., & Morton, D. (2008). Validation of GOES and MODIS active fire detection products using ASTER and ETM+ data. *Remote Sensing of Environment*, *112*(5), 2711–2726. https://doi.org/10.1016/j.rse.2008.01.005

Short, K. C. (2014). A spatial database of wildfires in the United States, 1992-2011. *Earth System Science Data*, *6*(1), 1–27. https://doi.org/10.5194/essd-6-1-2014

Short, K.C. (2015a). Spatial wildfire occurrence data for the United States, 1992-2013 [FPA_FOD_20150323]. 3rd Edition. Fort Collins, CO: Forest Service Research Data Archive. https://doi.org/10.2737/RDS-2013-0009.3

Short, K. C. (2015b). Sources and implications of bias and uncertainty in a century of US wildfire activity data. *International Journal of Wildland Fire*, *24*(7), 883–891. https://doi.org/10.1071/WF14190

Short, K. C. (2017). Spatial wildfire occurrence data for the United States, 1992-2015 [FPA_FOD_20170508]. 4th Edition. Fort Collins, CO: Forest Service Research Data Archive. DOI:10.2737/RDS-2013-0009.4

Siljander, M. (2009). Predictive fire occurrence modelling to improve burned area estimation at a regional scale: A case study in East Caprivi, Namibia. *International Journal of Applied Earth Observation and Geoinformation*, *11*(6), 380–393. https://doi.org/10.1016/j.jag.2009.06.004

Simonin, K. A. (2001). Bromus madritensis, Bromus rubens. In: U.S. Department of Agriculture, Forest Service, Rocky Mountain Research Station, Fire Sciences Laboratory (Producer). Available: https://www.fs.fed.us /database/feis/plants/graminoid/brospp/all.html [2018, December 7].

Stephens, S.L. (2005). Forest fire causes and extent on United States Forest Service lands. *International Journal of Wildland Fire*, *14*, 213-222.

Stone, K. R. (2010). Neyraudia reynaudiana. In: Fire Effects Information System, [Online]. U.S. Department of Agriculture, Forest Service, Rocky Mountain Research Station, Fire Sciences Laboratory (Producer). Available: https://www.fs.fed.us /database/feis/plants/graminoid/neyrey/all.html [2018, December 7].

Strand, E. K., Vierling, L. A., Smith, A., & Bunting, S.C. (2008). "Net changes in aboveground woody carbon stock in western juniper woodlands, 1946–1998." *Journal of Geophysical Research: Biogeosciences, 113*(G1).

Syphard, A. D., Radeloff, V. C., Keeley, J. E., Hawbaker, T. J., Clayton, M. K., Stewart, S. I., & Hammer, R. B. (2007). Human influence on California fire regimes. *Ecological Applications*, *17*(5), 1388–1402.

Syphard, A. D., Radeloff, V. C., Hawbaker, T. J., & Stewart, S. I. (2009). Conservation threats due to human-caused increases in fire frequency in mediterranean-climate ecosystems. *Conservation Biology*, *23*(3), 758–769. https://doi.org/10.1111/j.1523-1739.2009.01223.x

Tausch, R. J. (2009). A structurally based analytic model for estimation of biomass and fuel loads of woodland trees. *Natural Resource Modeling*, *22*(4), 463–488. https://doi.org/10.1111/j.1939-7445.2009.00045.x

Theobald, D. M., & Romme, W. H. (2007). Expansion of the US wildland–urban interface. *Landscape and Urban Planning*, *83*(4), 340–354. https://doi.org/10.1016/j.landurbplan.2007.06.002

TIGER/Line Shapefiles. (2016). Machine readable data files / prepared by the U.S. Census Bureau.

Torell, P. J., Erickson, L. C., & Haas, R. H. (1961). The Medusahead Problem in Idaho. *Weeds*, *9*(1), 124–131.

Tse, S. D., & Fernandez-Pello, A. C. (1998). On the flight paths of metal particles and embers generated by power lines in high winds—a potential source of wildland fires. *Fire Safety Journal*, *30*(4), 333–356. https://doi.org/10.1016/S0379-7112(97)00050-7

Tsela, P., Wessels, K., Botai, J., Archibald, S., Swanepoel, D., Steenkamp, K., & Frost, P. (2014). Validation of the two standard MODIS satellite burned-area products and an empirically-derived merged product in South Africa. *Remote Sensing*, *6*, 1275–1293. https://doi.org/10.3390/rs6021275

Tueller, P. T. (1989). Vegetation and land use in Nevada. *Rangelands, 11*(5), 204-210.

U.S. Department of Agriculture, Forest Service, Rocky Mountain Research Station, Missoula Fire Sciences Laboratory (Producer). (2018). *Fire Effects Information System (FEIS)*, [Online]. Available: www.feis-crs.org/feis/#

U.S. Department of Agriculture Forest Service Fire and Aviation Management and Department of the Interior Office of Wildland Fire, Washington, D. (2015). Quadrennial Fire Review (2015) 2014 Quadrennial Fire Review: Final Report.

U.S. Environmental Protection Agency. (2013). Level IV Ecoregions of the Conterminous United States. U.S. EPA Office of Research & Development (ORD) - National Health and Environmental Effects Research Laboratory (NHEERL). ftp://ftp.epa.gov/wed/ecoregions/us/us_eco_l4.zip, http://edg.epa.gov

US Geological Survey (USGS) Gap Analysis Program (GAP). (2015). Protected Areas Database of the United States (PAD-US). Edition 1.4. https://gapanalysis.usgs.gov/PADUS

van der Werf, G.R., Randerson, J.T., Collatz, G.J., Giglio, L. (2003). Carbon emissions from fires in tropical and subtropical ecosystems. *Global Change Biology, 9*: 547–562. doi:10.1046/j.1365-2486.2003.00604.x

van der Werf, G. R., Randerson, J. T., Giglio, L., Collatz, G. J., Mu, M., Kasibhatla, P. S., … Van Leeuwen, T. T. (2010). Global fire emissions and the contribution of deforestation,

savanna, forest, agricultural, and peat fires (1997-2009). *Atmospheric Chemistry and Physics*, *10*(23), 11707–11735. https://doi.org/10.5194/acp-10-11707-2010

van der Werf, G. R., Randerson, J. T., Giglio, L., Gobron, N., & Dolman, A. J. (2008). Climate controls on the variability of fires in the tropics and subtropics. *Global Biogeochemical Cycles*, *22*(3), 1–13. https://doi.org/10.1029/2007GB003122

VanDerWal, J., Shoo, L. P., Graham, C., & Williams, S. E. (2009). Selecting pseudo-absence data for presence-only distribution modeling: How far should you stray from what you know? *Ecological Modelling*, *220*(4), 589–594. https://doi.org/10.1016/j.ecolmodel.2008.11.010

Vega-Garcia, C., Woodard, P. M., Titus, S. J., Adamowicz, W. L., & Lee, B. S. (1995). A Logit Model for Predicting the Daily Occurrence of Human Caused Forest-Fires. *International Journal of Wildland Fire*, *5*(2), 101–111. https://doi.org/10.1071/WF9950101

Waggy, M. A. (2011). Miscanthus sinensis. In: Fire Effects Information System, [Online]. U.S. Department of Agriculture, Forest Service, Rocky Mountain Research Station, Fire Sciences Laboratory (Producer). Available: https://www.fs.fed.us /database/feis/plants/graminoid/missin/all.html [2018, December 7].

Wagner, S. A., & Fraterrigo, J. M. (2015). Positive feedbacks between fire and non-native grass invasion in temperate deciduous forests. *Forest Ecology and Management*, *354*, 170–176. https://doi.org/10.1016/j.foreco.2015.06.024

Walsh, C., & MacNally, R. (2003). Hierarchical partitioning. R project for statistical computing.

Wang, J., Xiao, X., Qin, Y., Doughty, R. B., Dong, J., & Zou, Z. (2018). Characterizing the encroachment of juniper forests into sub-humid and semi-arid prairies from 1984 to 2010 using PALSAR and Landsat data. *Remote Sensing of Environment*, *205*, 166–179. https://doi.org/10.1016/j.rse.2017.11.019

Westerling, A. L., Hidalgo, H. G., Cayan, D. R., & Swetnam, T. W. (2006). Warming and Earlier Spring Increase Western U.S. Forest Wildfire Activity. *Science*, *313*, 940–943. https://doi.org/10.1126/science.1128834

Westerling, A. L. (2016). Increasing western US forest wildfire activity: sensitivity to changes in the timing of spring. *Philosophical Transactions of the Royal Society B*, *371*, 1–10. https://doi.org/http://dx.doi.org/10.1098/rstb.2015.0178

Westerling, A., Gershunov, A., Brown, T. J., Cayan, D. R., & Dettinger, M. . (2003). Climate and wildfire in the western united states. *Bulletin of the American Meteorological Society*, *84*(5), 595–604. https://doi.org/10.1175/BAMS-84-5-595

Whisenant, S. G. (1989). Changing Fire Frequencies on Idaho's Snake River Plains: Ecological and Management Implications. *Pages 4-10 in E. D. McArthur, E. M. Romney, S. D. Smith, and P. T. Tueller, Editors. Symposium on Cheatgrass Invasion, Shrub Die-off, and Other Aspects of*

Shrub Biology and Management. Intermountain Research Station, Ogden, UT, Las Vegas, NV 20, 4–10.

Wickham, H. (2009). ggplot2: Elegant Graphics for Data Analysis. Springer-Verlag New York.

Wilson, A.M., Jetz, W. (2016). Remotely Sensed High-Resolution Global Cloud Dynamics for Predicting Ecosystem and Biodiversity Distributions. *PLoS Biology 14*(3): e1002415. doi:10.1371/journal. pbio.1002415

Wood, S. N. (2011). Fast stable restricted maximum likelihood and marginal likelihood estimation of semiparametric generalized linear models. *Journal of the Royal Statistical Society, Series B (Statistical Methodology)*, *73*(1), 3–36.

Wu, Z., He, H. S., Yang, J., Liu, Z., & Liang, Y. (2014). Relative effects of climatic and local factors on fire occurrence in boreal forest landscapes of northeastern China. *Science of The Total Environment*, *493*, 472–480. https://doi.org/10.1016/j.scitotenv.2014.06.011

Xiao, Z., Liang, S., Wang, J., Chen, P., Yin, X., Zhang, L., & Song, J. (2014). Use of general regression neural networks for generating the GLASS leaf area index product from time-series MODIS surface reflectance. *IEEE Transactions on Geoscience and Remote Sensing*, *52*(1), 209–223. https://doi.org/10.1109/TGRS.2013.2237780

Yang, J., He, H. S., Shifley, S. R., & Gustafson, E. J. (2007). Spatial Patterns of Modern Period Human-Caused Fire Occurrence in the Missouri Ozark Highlands. *Forest Science*, *53*(1), 1–15.

Young, J. A., Evans, R.A., & Kay, B. L. (1987). Cheatgrass. *Rangelands*, *9*, 266-270.

Zald, H. S. J., Ohmann, J. L., Roberts, H. M., Gregory, M. J., Henderson, E. B., & Braaten, J. (2014). Influence of lidar, Landsat imagery, disturbance history, plot location accuracy, and plot size on accuracy of imputation maps of forest composition and structure. *Remote Sensing of Environment, 14*, 26–38. http://doi.org/10.1016/j.rse.2013.12.013

Zhu, C., Kobayashi, H., Kanaya, Y., & Saito, M. (2017). Size-dependent validation of MODIS MCD64A1 burned area over six vegetation types in boreal Eurasia: Large underestimation in croplands. *Scientific Reports*, *7*(1), 1–9. https://doi.org/10.1038/s41598-017-03739-0

Zouhar, K. (2003). Bromus tectorum. In: Fire Effects Information System, [Online]. U.S. Department of Agriculture, Forest Service, Rocky Mountain Research Station, Fire Sciences Laboratory (Producer). Available: https://www.fs.fed.us /database/feis/plants/graminoid/brotec/all.html [2018, December 7].

Zuur, A. F., Ieno, E. N., Walker, N. J., Saveliev, A. A., & Smith, G. M. (2009). GLM and GAM for count data. In *Mixed effects models and extensions in ecology with R* (pp. 209-243). Springer, New York, NY.

Zuur, A.F., & Ieno, E.N. (2016). Beginner's Guide to Zero-Inflated Models with R. Highland Statistics Ltd, Newburgh, United Kingdom. highstat@statat.com.

Zuur, A. F., Ieno, E. N., Walker, N., Saveliev, A. A., & Smith, G. M. (2009). *Mixed effects models and extensions in ecology with R, Statistics for Biology and Health*. Springer Science + Business Media LLC. https://doi.org/10.1007/978-0-387-87458-6